Baryon modelling in a two-flavour Nambu–Jona-Lasinio model

Master-Thesis

Theory Center of the Institute for Nuclear Physics

TECHNISCHE UNIVERSITÄT DARMSTADT

Kraatz, Dominic

Darmstadt, September 2016

Baryon modelling in a two-flavour Nambu–Jona-Lasinio model
Baryonen im zwei flavour Nambu–Jona-Lasinio Modell

Vorgelegte Master-Thesis von Dominic Kraatz

1. Gutachter: Priv. Doz. Dr. Michael Buballa
2. Gutachter: Prof. Dr. Jochen Wambach

Tag der Einreichung:

Erklärung zur Master-Thesis

Hiermit versichere ich, die vorliegende Master-Thesis ohne Hilfe Dritter, nur mit den angegebenen Quellen und Hilfsmitteln angefertigt zu haben. Alle Stellen, die aus Quellen entnommen wurden, sind als solche kenntlich gemacht.

Darmstadt, den 09. September 2016

Dominic Kraatz

Zusammenfassung

In dieser Arbeit modellieren wir Baryonen als gebundene Zustände der Diquark-Quark Streuung mit Hilfe des Zwei-Flavour Nambu–Jona-Lasinio Modells. Hierzu ist es notwendig die auftretenden Diquarks, ähnlich wie die Mesonen, durch eine Bethe-Salpeter Gleichung in Random-Phase Näherung zu beschreiben. Dabei werden wichtige Eigenschaften der Diquarks, wie deren Farbstruktur und effektive Kopplungskonstante mit den Quarks extrahiert, welche zur Darstellung der Baryonen notwendig sind. Basierend auf der Dyson-Gleichung für den Baryonenpropagator lässt sich im Anschluss eine Bethe-Salpeter Gleichung für die Diquark-Quark Streuung motivieren. Durch eine Analyse der Vertexstruktur und Anwendung der statischen Näherung ist es möglich, die Bethe-Salpeter Gleichung in einen Ausdruck umzuschreiben, welcher große Ähnlichkeit zur Dirac-Gleichung aufweist.

Neben den Vakuumeigenschaften, wie der Masse oder der spontanen Brechung der chiralen Symmetrie, werden weitere Effekte für endliche Temperatur und chemisches Potential der Hadronen und Quarks untersucht. Von besonderem Interesse ist hierbei, die Schmelztemperatur der Diquarks und Nukleonen im Rahmen des Modells zu bestimmen und mit den Ergebnissen bereits vorhandener Arbeiten zu vergleichen. Darüber hinaus studieren wir das grundlegende Verhalten der Pionen, Diquarks und Nukleon für endliches chemisches Potential bei kleiner Temperatur.

Abstract

In this thesis, we model baryons as diquark-quark bound states within the framework of the two-flavour Nambu-Jona–Lasinio model. Therefore, the diquarks are described as bound states of two quarks, which can be evaluated in a similar way as for the mesons. This analysis leads to important properties of diquarks, i.e. their colour structure and effective coupling constant to the quarks, which are necessary for the further discussion. As the following step, a Bethe-Salpeter-like equation is motivated through a Dyson equation to obtain the scattering matrix for diquark-quark scattering. After a detailed description of the vertex structure, the static approximation is used to simplify the Bethe-Salpeter equation, which leads to a less computationally intensive Dirac-like equation.

Besides the vacuum properties of those particles, including the mass or spontaneously broken chiral symmetry, effects of finite temperature and chemical potential are studied. Especially, the melting temperature of the diquark and nucleon within the model are calculated in order to compare the results to other theoretical investigations. Moreover, we study the basic behaviour of the pion, diquark and nucleon for low temperature and non-vanishing chemical potential.

Contents

Chapter 1

Introduction

More than two thousand years ago the ancient Greeks had the idea that matter does consist of indestructible sub-particles which they called atom. This concept was rediscovered in the 18th century by scientists in order to explain new chemical observations within a particle model of matter in an elegant way. Around 200 years later, Ernest Rutherford presented his model in which an atom has an assumed solid core, the nucleus, surrounded by an electron cloud. He was able to prove the model suggestions with the well-known scattering experiment where he shot alpha particles on a thin gold layer. Moreover, Rutherford showed in later experiments that the nucleus is not as solid as he had thought. The nucleus is composed of protons, which he could detect experimentally, and a theoretical particle, which was later called neutron. It took sixty more years, until deep inelastic electron scattering led to the proof that the constituent nucleons, i.e. proton and neutron, do have constituents as well. Nevertheless, the theoretical physicist Murray Gell-Mann claimed the existence of such particles some years before [1], which he has called quarks and received the Nobel price in physics for this work in 1969.

With the description of strongly interacting matter based on quantum field theoretical methods in 1973, quarks and their properties became of particular interest in science. Thereby, the widely accepted quantum field theory for strongly interacting matter is the theory of quantum chromodynamics (QCD), which describes the interaction of colour-charged quarks and gluons [2]. More precisely, QCD is a non-abelian $SU(3)$ Yang-Mills theory, where the eight gluons are the massless gauge bosons. From the Lagrangian

$$\mathcal{L}_{\text{QCD}} = -\frac{1}{4}\mathcal{F}^a_{\mu\nu}\mathcal{F}^{\mu\nu}_a + \bar{\psi}\left(i\slashed{D} - m\right)\psi, \tag{1.1}$$

containing the covariant derivative

$$(D_\mu)_{c'c} = \delta_{cc'}\partial_\mu - ig\frac{1}{2}(\lambda_a)_{cc'}A^a_\mu \tag{1.2}$$

and the gluon field strength tensor

$$\mathcal{F}^a_{\mu\nu} = \partial_\mu A^a_\nu - \partial_\nu A^a_\mu + g f^a_{bc} A^b_\mu A^c_\nu, \tag{1.3}$$

one can already see that the gluons carry colour, which is one of the differences between QCD and quantum electrodynamics (QED). In the latter one the gauge bosons, namely the photons, do not carry a charge. In the above Lagrangian, g is the strong coupling constant, while ψ denotes the quark fields of the six quarks up, down, strange, charm, bottom and top. The structure constants of $SU_{\mathrm{colour}}(3)$ are denoted by f_{abc}. The non-abelian character of QCD leads to a running coupling, which is strong for small momenta (or large distances) and decreases for large momenta (or small distances), respectively. As a result, some interesting features emerge in this theory, from which we specifically want to mention confinement [3] and asymptotic freedom [4, 5]. The latter describes the weak interaction of quarks and gluons in the high-energy regime. It follows that quarks can be treated as nearly free particles within this regime, which allows to use perturbation techniques. The confinement meanwhile arises due to the strong coupling of the QCD in the low-energy regime. Therefore, strongly interacting particles are always bound into colourless states within this regime. To be more precise, these colourless states have to be colour-singlets, which are called hadrons. Hadrons are physical particles that consist either of a quark-antiquark pair (mesons) or three quarks (baryons) as valence quarks. Until now, no mathematical proof has been found for confinement, although some lattice QCD calculations indicate it [6].

Another interesting discussion follows by leaving the vacuum and entering a medium description, i.e. finite temperature and chemical potential, of the QCD. Due to high energy collider experiments at RHIC at Brookhaven Nation Lab or LHC at CERN, physicists are able to study the QCD phase diagram experimentally. Therefore, it becomes possible to draw conclusions for hot dense states of matter, which were present in the very early universe where neither mesons nor baryons existed. One interesting phenomenon in this discussion is the understanding of the emerging deconfined state of matter, the so-called quark-gluon plasma (QGP) [7]. With increasing temperature and/or pressure a phase transition is expected, where the quarks and gluons are no longer confined in hadrons and hence become the proper degrees of freedom. Since this state of matter can not be observed directly, the particle yields and energy spectra after the QGP state where quarks and gluons are confined within hadrons again, are the only possibility to understand the physics of the QGP. Moreover, these and later experimental set-ups may be able to confirm the predictions of QCD about the phase diagram and hence test the theory itself. Therefore, certain aspects of hadrons in hot dense matter have to be studied theoretically and proven in experiments as well. Especially, the composition of hadrons and mesons as well as their medium properties are of particular interest.

Besides the confinement and asymptotic freedom properties of QCD, the non-abelian character makes it very complicated to solve the full QCD for systems in both, vacuum and the medium, states. Due to the sign problem in lattice QCD approaches [8], one has to restrict oneself to certain regimes and models, which may include non-observable properties. While in the low-energy regime, perturbative techniques are no longer suitable because of the running coupling constant of QCD, other approaches, such as effective models, can be used to simulate the dynamics of strongly interacting matter. As a simple assumption, the mass of the gluon can be assumed to be infinitely large with the consequence that the Lagrangian reduces to a local point-like interaction. Nevertheless, these models can be used to investigate some of the aspects that are not yet reachable from the full QCD treatments. The model used in this work, the so called Nambu–Jona-Lasinio-model [9, 10], was originally developed to describe elementary nucleons, and was later reinterpreted as a low-energy effective model of QCD [11, 12, 13]. Beside the quarks, a bound state of two quarks represents a non-observable particle within this model, due to its non-vanishing colour structure and thus has to be treated with care. However, this bound state, which is called diquark, will be valuable in the modelling of the baryons to simplify the non-trivial three-body problem.

The goal of this work is to model baryons within the NJL model in a two-flavour case and discuss certain aspects in vacuum and hot dense matter. Since this discussion is based on a three-body problem, we will introduce proper approximations and assumptions to simplify the modelling by transformation into a two-body problem. Before we can start with the baryons, we give an overview of the NJL model in the second chapter and discuss certain properties of it, e.g. spontaneous symmetry breaking and vertex structure. This discussion leads to the Fierz transformation, which is used to separate the particle-particle channel from the particle-antiparticle channel. With the latter, we are able to model the mesons in chapter three and fit the free parameters of the NJL model to the pion mass and the pion decay constant. In the fourth chapter, we use the particle-particle channel to model the diquarks and discuss their structure in colour and flavour space. Finally, in the fifth chapter, our results from the previous discussions are used to motivate the structure of the baryons in the NJL model as bound states of a diquark-quark scattering process. This leads to a Bethe-Salpeter-like equation for the introduced static approximation. Besides the vacuum investigation, the emerging bound state is discussed in the medium as well. Thereupon, in the last chapter a short summary is given and followed by an outlook on possible extensions.

Chapter 2

The Nambu–Jona-Lasinio model

In this chapter, we will give an overview of the NJL model, which is used in this work to describe physical particles, like mesons and baryons. Originally the NJL model was designed by Y. Nambu and G. Jona-Lasinio in 1961, to explain the high nucleon mass in accordance with the partially conserved axial current in the pre-QCD era [9, 10]. Later, it was reinterpreted for QCD calculations in the low-energy regime, where gluon degrees of freedom are supposed to be frozen-out, by reducing the complex structure of strong interactions in the full QCD Lagrangian to a point like local interaction. Due to the non-renormalizable character of the NJL model, an additional cutoff parameter appears, which has to be included to handle the upcoming divergent integrals.

In particular, the NJL model shares the same global symmetries with QCD and in this way can describe the chiral symmetry and its spontaneous breaking in the vacuum as well. It also allows to study the thermodynamic aspects of QCD like the restoration of the chiral symmetry for high temperatures and densities in the QCD phase diagram [14, 15]. Besides the non-renormalizable character of the NJL model, another drawback is the lack of confinement due to the missing gluonic interactions. Nonetheless, the NJL model can be used to study strongly interacting matter in a more computationally friendly way than solving the complex QCD.

An NJL-type Lagrangian can be separated into two parts: The first one is the interaction-free part including the Dirac equation, which describes the kinematic of the system, while the second one represents the interaction in the model, which has in our case the form of a local four-point one:

$$\mathcal{L}^{\text{NJL}} = \mathcal{L}^{\text{free}} + \mathcal{L}^{\text{int}} \tag{2.1}$$

$$= \bar{\psi}\left(i\slashed{\partial} - m\right)\psi + \sum_I g_I(\bar{\psi}\Gamma^I\psi)^2 \tag{2.2}$$

Here ψ is a Dirac spinor, representing a quark field. Additional indices for the colour and flavour space are for now omitted. The mass m denotes a diagonal matrix of dimension N_f (number of flavours) containing the different current (or bare) masses

of the quarks. In the so-called chiral limit, the masses will be neglected, such that m vanishes. In this case, the Lagrangian does not explicitly break the chiral symmetry any more, cf. section 2.2. For the interaction term we have made the general ansatz

$$\mathcal{L}^{\text{int}} = \sum_I g_I (\bar{\psi}\Gamma^I\psi)^2 \,, \tag{2.3}$$

where Γ^I is an operator corresponding to a certain interaction channel with specific coupling constant g_I. The interaction channel Γ^I is a tensor product of operators acting in Dirac, colour and flavour space:

$$\Gamma^I = \Gamma^{H,f,c} = \underbrace{\Delta^H}_{\text{Dirac}} \otimes \underbrace{\Gamma^c}_{\text{Colour}} \otimes \underbrace{\Gamma^f}_{\text{Flavour}} \,, \tag{2.4}$$

where the index H denotes a certain hadronic spin channel, i.e. spin channels for mesons or diquarks. At this point, it is valuable to introduce the Fierz transformation to separate the particle-antiparticle from the particle-particle channel. The latter will lead to the description of the diquarks, which we need to model baryons within the NJL model as a bound state of the diquark-quark scattering process.

2.1. Fierz transformation

A general ansatz for an NJL-type interaction Lagrangian is given by (2.3). We can rewrite this equation without loosing any information by using the anticommutation rules for fermions [14]:

$$\mathcal{L}_{\text{int}} = g_I (\bar{\psi}\Gamma^I\psi)^2 = g_I \Gamma^I_{ij}\Gamma^I_{kl} \bar{\psi}_{\bar{\imath}}\psi_j \bar{\psi}_{\bar{k}}\psi_l \tag{2.5}$$

$$= -g_I \Gamma^I_{ij}\Gamma^I_{kl} \bar{\psi}_{\bar{\imath}}\psi_l \bar{\psi}_{\bar{k}}\psi_j \tag{2.6}$$

$$= g_I \Gamma^I_{ij}\Gamma^I_{kl} \bar{\psi}_{\bar{\imath}}\bar{\psi}_{\bar{k}}\psi_l \psi_j \tag{2.7}$$

where the bared indices are related to the complex conjugated quark fields. For simplicity, we restrict ourself to Hartree-type approximations, where the first and second as well as the third and fourth field are contracted. It follows that equation (2.6) and (2.7) are no longer equivalent. This leads, for equation (2.6), to the exchange diagrams or Fock terms, used to describe the mesons and are represented by the Lagrangian

$$\mathcal{L}_{\text{ex}} := -g_I \Gamma^I_{\bar{\imath}j}\Gamma^I_{\bar{k}l} \bar{\psi}_{\bar{\imath}}\psi_l \bar{\psi}_{\bar{k}}\psi_j \,. \tag{2.8}$$

Meanwhile equation (2.7) yields the particle-particle contribution, which is connected to the description of diquarks with the corresponding Lagrangian

$$\mathcal{L}_{\psi\psi} := g_I \Gamma^I_{\bar{\imath}j}\Gamma^I_{\bar{k}l} \bar{\psi}_{\bar{\imath}}\bar{\psi}_{\bar{k}}\psi_l \psi_j \,. \tag{2.9}$$

Now it would be useful to rewrite the operators $\Gamma^I_{\bar{i}j}\Gamma^I_{\bar{k}l}$ as

$$\Gamma^I_{\bar{i}j}\Gamma^I_{\bar{k}l} = \sum_M c^I_M \Gamma^M_{\bar{i}l}\Gamma^M_{\bar{k}j} \tag{2.10}$$

to obtain the exchange term

$$\mathcal{L}_{\text{ex}} = -g_I \sum_M c^I_M (\bar{\psi}\Gamma^M\psi)^2\,. \tag{2.11}$$

Here M denotes the corresponding meson (spin) channel, i.e. scalar (S), pseudoscalar (P), vector (V), axial (A), tensor (T) as well as the flavour and colour channels. Combining this with the original term $\mathcal{L}_{\text{dir}} := \mathcal{L}_{\text{int}}$ representing the direct interaction, we get the full effective particle-antiparticle contribution

$$\mathcal{L}_{\bar{\psi}\psi} = \mathcal{L}_{\text{dir}} + \mathcal{L}_{\text{ex}} = \sum_M g_M (\bar{\psi}\Gamma^M\psi)^2 \tag{2.12}$$

with

$$g_M = \begin{cases} -c^I_M g_I & \text{for } M \neq I \\ (1 - c^I_I)g_I & \text{for } M = I \end{cases} \tag{2.13}$$

For the particle-particle channel, a similar expression can be found using the charge conjugation operator $C = i\gamma_2\gamma_0$ [14]. It has the following properties:

$$C^2 = -\mathbb{1} \Rightarrow C^{-1} = -C \tag{2.14}$$

$$C^T = C^\dagger = -C^* = C^{-1} = -C \tag{2.15}$$

Performing this on the different channels in Dirac space, one finds for the transposed Δ^H

$$(\Delta^H)^T = -S^{(N)}C\Delta^H C \tag{2.16}$$

with

$$S^{(S)} = S^{(P)} = S^{(A)} = 1 \tag{2.17}$$

$$S^{(V)} = S^{(T)} = -1. \tag{2.18}$$

Overall, we find for the particle-particle channel in Dirac space:

$$\Gamma^{(a)}_{\bar{i}j}\Gamma^{(a)}_{\bar{k}l} = -S^{(a)}\sum_b (\Gamma^b C)_{\bar{i}k}(C\Gamma^b)_{lj} \tag{2.19}$$

We can use (2.19) to get the particle-particle contribution of the original Lagrangian

$$\mathcal{L}_{\psi\psi} = \sum_D d^I_D g_I (\bar{\psi}\Gamma^D C\bar{\psi}^T)(\psi^T C\Gamma^D\psi) \tag{2.20}$$

$$= \sum_D h_D (\bar{\psi}\Gamma^D C\bar{\psi}^T)(\psi^T C\Gamma^D\psi)\,, \tag{2.21}$$

where a redefined coupling constant h_D for the different particle-particle channels has been included. Up to this point, we do not distinguish between the spaces such that the above discussion holds in each space separately. For the full transformation, the matrices c_M^I and d_D^I have to be calculated in Dirac, flavour and colour space. A more detailed calculation of these matrices can be found in appendix B.

2.2. Global symmetries of the NJL model

In order to study certain QCD aspects, an NJL model Lagrangian has to have the same global symmetries as the QCD Lagrangian. Typically, the symmetries of a certain NJL model Lagrangian are [16]

$$SU(2)_\text{V} \otimes SU(2)_\text{A} \otimes U(1)_\text{V} \tag{2.22}$$

for two considered flavours up and down. The related transformations read:

- $SU(2)_\text{V}$

$$\psi \mapsto \exp(-i\vec{\tau}\vec{\theta}/2)\psi\,, \tag{2.23}$$

- $SU(2)_\text{A}$

$$\psi \mapsto \exp(-i\gamma_5\vec{\tau}\vec{\theta}/2)\psi\,, \tag{2.24}$$

- $SU(1)_\text{V}$

$$\psi \mapsto \exp(-i\alpha)\psi\,, \tag{2.25}$$

with $\theta \in \mathbb{R}^3$, $\alpha \in \mathbb{R}$ and $\vec{\tau}$ the vector containing the three Pauli matrices. The Noetherian current of the $U(1)_\text{V}$ symmetry, which is always satisfied, corresponds to the conservation of baryon number. However, while the $SU(2)_\text{V}$ vector symmetry is already satisfied in the isospin limit with equal bare masses, the Lagrangian is only invariant under a $SU(2)_\text{A}$-rotation for vanishing bare quark masses.

In the chiral limit, an important phenomenon appears with increasing coupling constant when the $SU(2)_\text{A}$ is broken spontaneously by the chiral condensate. According to the Goldstone theorem, the three broken generators of the $SU(2)_\text{A}$ symmetry correspond to three massless Goldstone bosons. Indeed, we will see that the masses of the three pions are equal to zero in the chiral limit. For non-zero, but small bare

quark masses, the $SU(2)_A$ symmetry is explicitly broken, thus the pion masses do not vanish. In this case, the pions are called pseudo Goldstone bosons, since their mass is small compared to other mesons [14]. In general, the $SU(2)_V \otimes SU(2)_A$ symmetry is written by the isomorphic chiral symmetry, represented by independent $SU(2)$ transformations of the left- and right-handed quark fields.

2.3. NJL Lagrangian

After the general discussions of the NJL model in the previous sections, we want to determine a local four-point interaction Lagrangian, based on the colour-current Lagrangian

$$\mathcal{L}^{\text{int}} = -g(\bar{\psi}\gamma^\mu\lambda^a\psi)^2. \tag{2.26}$$

This Lagrangian can be directly motivated from the QCD Lagrangian as a massive gluon exchange, which leads to the point like interaction term above. After performing a Fierz transformation of Lagrangian (2.26), cf. detail Appendix B.3, it can be separated into a particle-particle and particle-antiparticle contribution. The resulting particle-antiparticle Lagrangian, which is related to the mesonic spectrum, reads

$$\mathcal{L}_{\bar{\psi}\psi} = 2g\frac{N_c^2-1}{N_c^2}\Big[(\bar{\psi}\psi)^2 + (\bar{\psi}i\gamma_5\psi)^2 + (\bar{\psi}\tau_m\psi)^2 + (\bar{\psi}i\gamma_5\tau_m\psi)^2$$
$$- \frac{1}{2}(\bar{\psi}\gamma^\mu\psi)^2 - \frac{1}{2}(\bar{\psi}\gamma^\mu\gamma_5\psi)^2 - \frac{1}{2}(\bar{\psi}\gamma^\mu\tau_m\psi)^2 - \frac{1}{2}(\bar{\psi}\gamma^\mu\gamma_5\tau_m\psi)^2\Big]. \tag{2.27}$$

Since the physical mesons are in a colour singlet state, we have omitted terms proportional to the colour-octet, i.e. λ_a. To simplify the notation, we define

$$g_s := 2g\frac{N_c^2-1}{N_c^2}, \tag{2.28}$$

as a new coupling constant for the scalar channel. Moreover, we will restrict ourselves to the scalar mesons and neglect the vector terms, i.e. terms which include γ^μ.
The term $(\bar{\psi}\psi)^2$ is connected to the (scalar) sigma meson, while the term $(\bar{\psi}i\gamma_5\tau_m\psi)^2$ describes the pseudoscalar pions. Since these terms can be transformed into each other by a chiral rotation, they are often called "chiral partners". Note that this Lagrangian is invariant under a $U(1)_A$ rotation due to the remaining terms $(\bar{\psi}i\gamma_5\psi)^2$ and $(\bar{\psi}\tau_m\psi)^2$. This symmetry can be explicitly broken by including an additional instanton-induced interaction term, that comes with the same coupling constant g_s,[1] which exhibits chiral

---

[1]This condition is not necessary, but simplifies the Lagrangian.

symmetry, but violates the $U(1)_A$ symmetry [14]. Overall, the used NJL Lagrangian for the mesonic spectrum reads

$$\mathcal{L}_{\bar\psi\psi} = g_s \left[(\bar\psi\psi)^2 + (\bar\psi i\gamma_5\vec\tau\psi)^2 \right] . \tag{2.29}$$

For the particle-particle channel, we find after performing a Fierz transformation of the Lagrangian (2.26)

$$\begin{aligned}
\mathcal{L}_{\psi\psi} = 2g \Bigg\{ &\frac{N_c+1}{2N_c} \Big[(\bar\psi C\tau_A\lambda_{A'}\bar\psi^T)(\psi^T C\tau_A\lambda_{A'}\psi) + (\bar\psi i\gamma_5 C\tau_A\lambda_{A'}\bar\psi^T)(\psi^T Ci\gamma_5\tau_A\lambda_{A'}\psi) \\
&- \frac{1}{2}(\bar\psi\gamma^\mu\gamma_5 C\tau_A\lambda_{A'}\bar\psi^T)(\psi^T C\gamma_5\gamma_\mu\tau_A\lambda_{A'}\psi) \\
&- \frac{1}{2}(\bar\psi\gamma^\mu C\tau_S\lambda_{A'}\bar\psi^T)(\psi^T C\gamma_\mu\tau_S\lambda_{A'}\psi) \Big] \\
&- \frac{N_c-1}{2N_c} \Big[(\bar\psi C\tau_A\lambda_{S'}\bar\psi^T)(\psi^T C\tau_A\lambda_{S'}\psi) + (\bar\psi i\gamma_5 C\tau_A\lambda_{S'}\bar\psi^T)(\psi^T Ci\gamma_5\tau_A\lambda_{S'}\psi) \\
&- \frac{1}{2}(\bar\psi\gamma^\mu C\tau_A\lambda_{S'}\bar\psi^T)(\psi^T C\gamma_\mu\tau_A\lambda_{S'}\psi) \\
&- \frac{1}{2}(\bar\psi\gamma^\mu\gamma_5 C\tau_A\lambda_{S'}\bar\psi^T)(\psi^T C\gamma_\mu\gamma_5\tau_A\lambda_{S'}\psi) \Big] \Bigg\} .
\end{aligned} \tag{2.30}$$

Due to the fact that diquarks are a system of two bound fermions and hence have to fulfil Pauli's principle, the restriction in the Lagrangian (2.30) to totally antisymmetric terms is appropriate.

For the vector and axial-vector channel, i.e. $\Delta^D \in \{\gamma^\mu, \gamma_5\gamma^\mu\}$, the corresponding polarisation loop in the BS equation of the diquarks would have a transversal and longitudinal contribution, similar to the discussion of vector mesons in [17]. Therefore, in order to simplify the modelling of baryons, we will only consider the scalar and neglect the vector diquarks. Moreover, the second term with pre-factor $-\frac{N_c-1}{2N_c}$ is related to the colour sextet, which cannot be combined with a third quark to obtain a colourless state and thus will be neglected too. It follows that the considered interaction Lagrangian for the particle-particle channel is given by

$$\mathcal{L}_{\psi\psi} = h_s \left[(\bar\psi C\tau_A\lambda_{A'}\bar\psi^T)(\psi^T C\tau_A\lambda_{A'}\psi) + (\bar\psi i\gamma_5 C\tau_A\lambda_{A'}\bar\psi^T)(\psi Ci\gamma_5\tau_A\lambda_{A'}\psi) \right] ,$$

where

$$h_s := 2g \frac{N_c+1}{2N_c} \tag{2.31}$$

is the corresponding coupling constant. This Lagrangian satisfies the same global symmetries as the mesonic Lagrangian given in equation (2.29).

Summarizing the above discussion the considered NJL Lagrangian used in this work reads

$$
\begin{aligned}
\mathcal{L}_{\mathrm{NJL}} =& \bar{\psi} \left(i \slashed{\partial} - m \right) \psi \\
& + g_s \left[(\bar{\psi}\psi)^2 + (\bar{\psi}i\gamma_5\vec{\tau}\psi)^2 \right] \\
& + h_s \left[(\bar{\psi}C\tau_A\lambda_{A'}\bar{\psi}^T)(\psi^T C\tau_A\lambda_{A'}\psi) + (\bar{\psi}i\gamma_5 C\tau_A\lambda_{A'}\bar{\psi}^T)(\psi Ci\gamma_5\tau_A\lambda_{A'}\psi) \right] .
\end{aligned}
\tag{2.32}
$$

Since the choice of Lagrangian (2.26) is not unique, one can imagine other possible interaction terms which share the same global symmetries with QCD. Therefore, the coupling constants can be redefined in any way. At the end, the parameter g_s as well as h_s, and other free parameters of the model, have to be fitted to certain physical observable values, which will be discussed later.

2.4. Gap equation and constituent quarks

In this section, we want to describe the self interaction of the quarks in the so-called Hartree- or mean-field approximation, where a quark propagates in the averaged potential of all other quarks. The corresponding self-energy leads to an effective mass, the so-called constituent mass, that is larger than the bare quark mass included in the Lagrangian. As mentioned in the previous section, the vertices of the NJL Lagrangian are point-like with four external (anti)fermions fields. The dressed quark propagator can be defined via the Dyson equation, which is diagrammatically depicted in figure 2.1, where only direct terms are included. Due to the local four-point
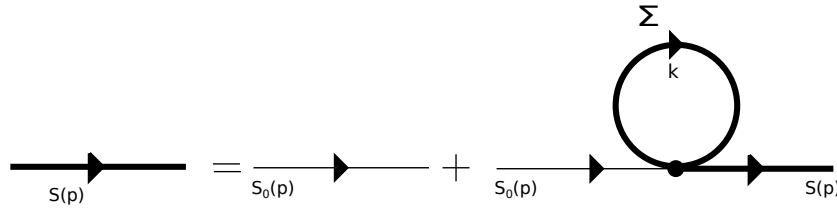

Figure 2.1. Gap equation in Hartree approximation.

character of the interaction, the exchange terms can always be transformed by a Fierz transformation into direct-like ones. In this sense the Hartree approximation is equivalent to the more general Hartree-Fock approximation up to a redefinition of the coupling constants in the Lagrangian. For the left-hand side of figure 2.1, we claim that the new dressed quark propagator for a certain flavour f (bold lines) can

be written as a Feynman propagator with modified dressed quark mass M_f

$$iS^f(p) = i(\not{p} - M_f + i\epsilon)^{-1}. \tag{2.33}$$

With the bare quark propagator

$$iS_0^f(p) = i(\not{p} - m_f + i\epsilon)^{-1} \tag{2.34}$$

and the self-energy Σ, the self-consistent equation of picture 2.1 has to be solved to obtain the constituent mass M:

$$iS^f(p) = iS_0^f(p) + iS_0^f(p)(-i\Sigma)iS^f(p) \tag{2.35}$$

$$= \left((S_0^f(p))^{-1} - i\Sigma\right)^{-1} \tag{2.36}$$

The self-energy in Hartree approximation is given by

$$-i\Sigma := -i\sum_I \Sigma_I = -2i\sum_I g_I \Gamma^I \int \frac{\mathrm{d}^4k}{(2\pi)^4} \mathrm{Tr}(\Gamma^I iS(k)), \tag{2.37}$$

where we used, that for closed fermion loops we have to take the trace over all spaces and integrate over the internal four-momentum k with an additional negative sign. In Hartree approximation with quark propagator (2.33), there are only contributions from the particle-antiparticle channel in the Lagrangian, i.e. we only have to consider terms in the sum of equation (2.37) where $I = M$ holds, such that (2.29) will be used. In the Lagrangian, the self-energy can be associated with a linearisation of the expression $\mathcal{L}_{\mathrm{int}}$ in terms of the condensate $\langle\bar{\psi}\Gamma^M\psi\rangle$

$$(\bar{\psi}\Gamma^M\psi)^2 \approx 2\bar{\psi}\Gamma^M\psi\langle\bar{\psi}\Gamma^M\psi\rangle - \langle\bar{\psi}\Gamma^M\psi\rangle^2 + \mathcal{O}(\delta_{\bar{\psi}\psi}^2), \tag{2.38}$$

and neglecting higher order terms. Since the quadratic term in the upper expression only shifts the Lagrangian it can be also neglected in the context of this work. After inserting (2.38) into the Lagrangian (2.32) and comparing the result with the Dyson equation (2.35), one obtains immediately that the chiral condensate is given by

$$\langle\bar{\psi}\Gamma^M\psi\rangle = -i\int \frac{\mathrm{d}^4k}{(2\pi)^4} \mathrm{Tr}(\Gamma^M S(k)). \tag{2.39}$$

Due to the trace in relation (2.37) and (2.39), only vertices and condensates will survive, which do not contain terms proportional to γ_5 or one of the Pauli matrices, since these matrices are traceless. The remaining condensate related to $\Gamma^M = \mathbb{1}$ is the so called chiral condensate.

However, comparing both sides of equation (2.35), yields

$$M_f = m_f + \Sigma(M_f) \tag{2.40}$$

$$= m_f + 2i \sum_M g_s \Gamma^M \int \frac{\mathrm{d}^4 k}{(2\pi)^4} \, \mathrm{Tr}(\Gamma^M S(k)) \tag{2.41}$$

$$= m_f + 2g_s \mathbb{1} i \int \frac{\mathrm{d}^4 k}{(2\pi)^4} \, \mathrm{Tr}(\mathbb{1} S(k)) \tag{2.42}$$

$$= m_f + 8 N_c g_s i \int \frac{\mathrm{d}^4 k}{(2\pi)^4} \sum_{f'} \frac{M_{f'}}{k^2 - M_{f'}^2 + i\epsilon} \,. \tag{2.43}$$

which simplifies in case of the isospin limit ($m_u = m_d$) for two quark flavours to

$$M = m + 16 M N_c g_s i \int \frac{\mathrm{d}^4 k}{(2\pi)^4} \frac{1}{k^2 - M^2 + i\epsilon} \,. \tag{2.44}$$

The emerging divergent integral will be labelled as

$$i I_1 := i \int \frac{\mathrm{d}^4 k}{(2\pi)^4} \frac{1}{k^2 - M^2 + i\epsilon} \tag{2.45}$$

and has to be regularised in a proper way, which will be discussed later.
Within the chiral limit, equation (2.44) has always the trivial solution $M = 0$. For increasing coupling constant g_s also non-trivial solutions will appear, that lead to the spontaneously broken $SU(2)_A$ symmetry. For sufficiently small couplings meanwhile, the $SU(2)_A$ symmetry is not broken in the chiral limit, whereas it explicitly broken for a non-vanishing bare quark mass. This behaviour is shown in figure 2.2 which makes use of parameter set [E] introduced in chapter 3.3 and the cutoff parameter Λ discussed in the following section. Typically, the chiral condensate is used as the order parameter for the spontaneously broken chiral symmetry. Figure 2.3 demonstrates the behaviour of the condensate in dependence of the inverse coupling constant. Keeping in mind that the introduced coupling constants and bare quark masses are treated as free parameters of the model, we have to fix them on physical observables like the pion mass and the pion decay constant. Beside these free parameters, the cutoff Λ, emerging from the regularisation scheme, is another free parameter of the model and will be formally introduced in the following section.

2.5. Regularisation

The description of mesons and other physical quantities contains divergent integrals like I_1 in equation (2.44), which have to be regularised in a proper way. In this
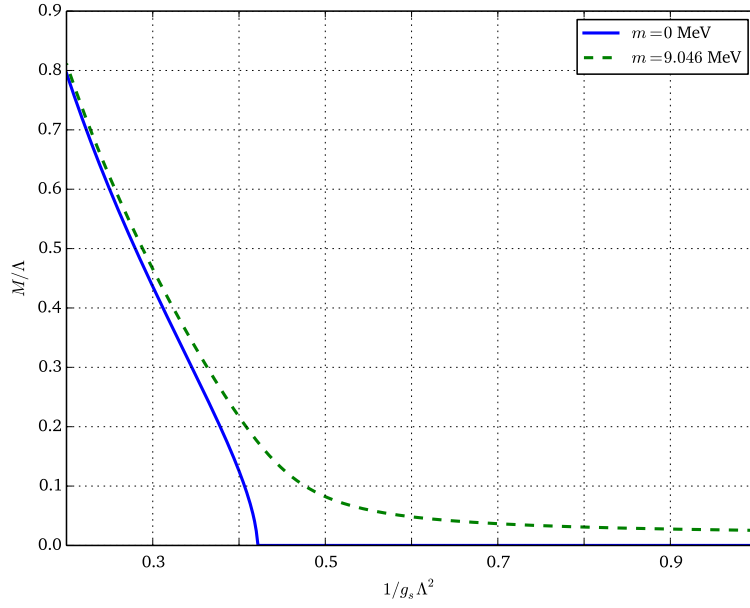
Figure 2.2. Solutions of the gap equation for certain bare quark masses. The constituent mass M breaks the $SU(2)_A$ symmetry spontaneously, since the quarks obtain a non-vanishing constituent mass. Here parameter set [E], cf. chapter 3.3, has been used.

work, we will use Pauli-Villars (PV) regularisation, since it preserves the Lorentz invariance in contrast to the other commonly used three-momentum cutoff. While this method uses a sharp cutoff to determine the divergent integrals, PV regularisation subtracts additional terms that behave like the integrand itself for large momenta, but only have a small contribution for small momenta [17]. Therefore, the number of additional terms depends on the degree of divergence of the considered integral. In this context, another advantage of PV regularisation compared to hard-cutoff methods is the possibility to make any substitutions within the integrand without taking care of the domain.

Overall, one replaces the original integrand by a weighted sum over new masses, i.e.

$$\int \frac{\mathrm{d}^4 k}{(2\pi)^4} f(M,k) \longrightarrow \int \frac{\mathrm{d}^4 k}{(2\pi)^4} \sum_{j=0}^{N} c_j f(M_j,k). \tag{2.46}$$

Of course with coefficient $c_0 = 1$ and $M_0 = M$. In order to regularise the integral I_1, which exhibits the highest order of divergence in this work, we find for the upper
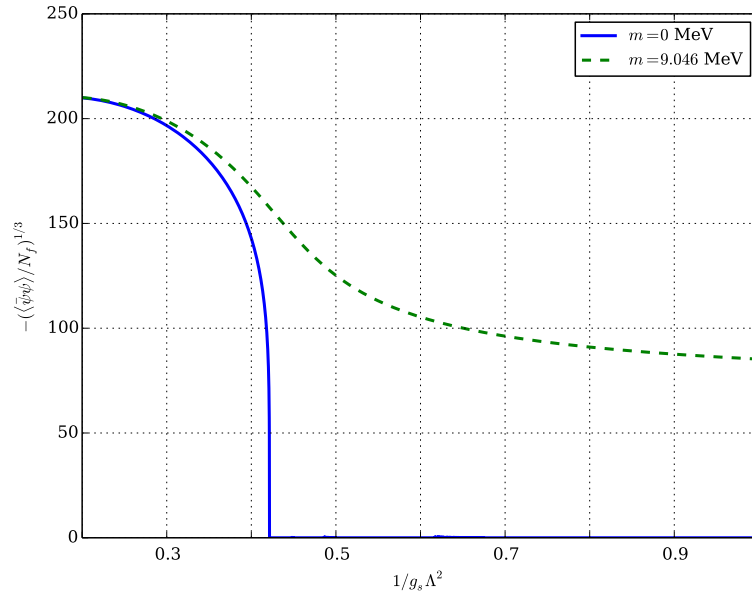
13

Figure 2.3. Chiral condensate (per flavour) as order parameter for the spontaneously broken chiral symmetry, with parameter set [E].

substitution

$$
iI_1(M) = i \int \frac{\mathrm{d}^4 k}{(2\pi)^4} \frac{1}{k^2 - M^2 + i\epsilon}
$$

$$
\rightarrow i \int \frac{\mathrm{d}^4 k}{(2\pi)^4} \left(c_0 \frac{1}{k^2 - M^2 + i\epsilon} + c_1 \frac{1}{k^2 - (M^2 + \Lambda^2) + i\epsilon} + c_2 \frac{1}{k^2 - (M^2 + 2\Lambda^2) + i\epsilon} \right),
$$

$$(2.47)$$

where the ansatz

$$
M_j^2 = M^2 + j \cdot \Lambda^2 \tag{2.48}
$$

for the masses M_j has been made. The (soft) cutoff Λ in equation (2.48) enters the model as a new free parameter. Since the original integral diverges quadratically, which can be directly seen by counting the powers of k in the denominator a minimum of two regulators have to be used. To ensure that all divergences are treated, the coefficients c_j for the three terms in equation (2.47) have to fulfil

$$
\sum_j c_j = 0 \tag{2.49}
$$

$$
\sum_j c_j \cdot M_j^2 = 0, \tag{2.50}
$$

14

which leads to $c_0 = c_2 = 1$, $c_1 = -2$.

Now the k_0 integration can be separated in each term from the $\vec{k}$ one, by using

$$\int \frac{\mathrm{d}^4 k}{(2\pi)^4} \frac{1}{k^2 - M^2 + i\epsilon} = \int \frac{\mathrm{d}^3 k}{(2\pi)^3} \int \frac{\mathrm{d}k_0}{2\pi} \frac{1}{k_0 + E_{\vec{k}} - i\epsilon} \cdot \frac{1}{k_0 - E_{\vec{k}} + i\epsilon} \tag{2.51}$$

and

$$E_{\vec{k}} = \sqrt{k^2 + M^2} \,. \tag{2.52}$$

After application of the residue theorem, the k_0 integration can be carried out. The remaining three-momentum integration can be solved analytically. Finally, the integral I_1 take the analytical form

$$iI_1(M, \Lambda) = \frac{1}{16\pi^2} \left(M^2 \log \left(\frac{M^2}{M^2 + \Lambda^2} \right) + (M^2 + 2\Lambda^2) \log \left(\frac{M^2 + 2\Lambda^2}{M^2 + \Lambda^2} \right) \right). \tag{2.53}$$

As already mentioned, the integral I_1 has the highest order of divergence in this work. In order to be consistent, all other encountered integrals will be regularised in the same way. This means, always two additional terms with coefficients $c_1 = -2$, $c_2 = 1$ will be added.

2.6. Quarks in the medium

So far, we have studied quarks for zero temperature and vanishing chemical potential. However, in order to study hadrons in dense hot matter, we have to transform our results in the context of finite temperature field theory. Hereby, the Matsubara formalism will be used, where we have to replace the energy integration by a sum over discrete Matsubara frequencies

$$i \int \frac{\mathrm{d}^4 k}{(2\pi)^4} f(k) \mapsto -T \sum_{\{i\omega\}} \int \frac{\mathrm{d}^3 k}{(2\pi)^3} f(i\omega + \mu, \vec{k}) \,. \tag{2.54}$$

In case of the gap equation, $i\omega$ is related to fermionic Matsubara frequencies defined as $i\omega_F := i\nu = (2n+1)\pi i T$, with $n \in \mathbb{Z}$.

We find that the gap equation (2.44) is formally equal to the vacuum case, up to a redefinition of the emerging integral. The gap equation thus reads

$$M = m + 16 M N_c g_s L_1 \,, \tag{2.55}$$

with

$$L_1(M, T, \mu) := iI_1(M, T, \mu) = -T \sum_{\{i\nu\}} \int \frac{\mathrm{d}^3 k}{(2\pi)^3} \frac{1}{(i\nu + \mu)^2 - E_k^2} \,. \tag{2.56}$$

The new integral L_1 now depends on temperature T and chemical potential μ as well. A detailed discussion of the techniques to calculate this kind of integral can be found in appendix C.
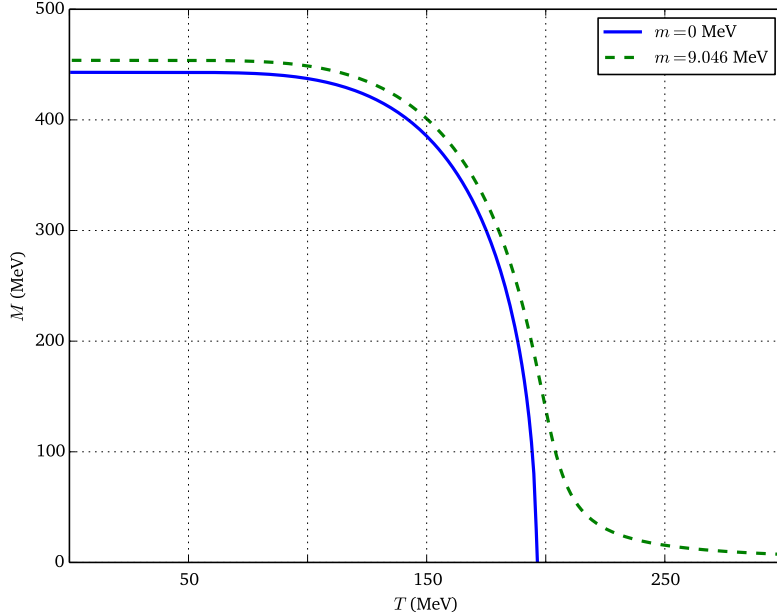

Figure 2.4. Solution of the gap equation for varying temperature and zero chemical potential.

We have already seen that the chiral symmetry is explicitly broken for non-vanishing bare quark mass m in vacuum. Furthermore, the quarks obtain a mass higher than the actual bare quark mass due to the spontaneously broken chiral symmetry. Under a variation of the temperature with vanishing chemical potential, cf. figure 2.4, the quarks obtain the constituent mass as for the vacuum case, until a temperature of approximately $T \approx 100$ MeV has been reached. Increasing the temperature further, leads to a smoothly decreasing constituent mass until it reaches nearly the value of the bare quark mass. This behaviour is related to an restoration of the chiral symmetry. While for non-vanishing mass the transition to the chirally restored phase is smooth and is associated with a crossover, it is more abrupt in the chiral limit. This can be identified with a second order phase transition. Due to $m = 0$ MeV, the chiral symmetry will be fully restored for temperatures higher than $T_c \approx 195$ MeV.

A slightly different behaviour shows for a variation of the chemical potential as shown in figure 2.5. For a fixed temperature $T = 1$ MeV constituent mass stays constant in the chiral limit and for non-vanishing bare quark mass as well. However, a certain quark does not feel any restraints for appropriate low chemical potential and behaves like it is in the vacuum and hence obtain the vacuum mass in accordance with the
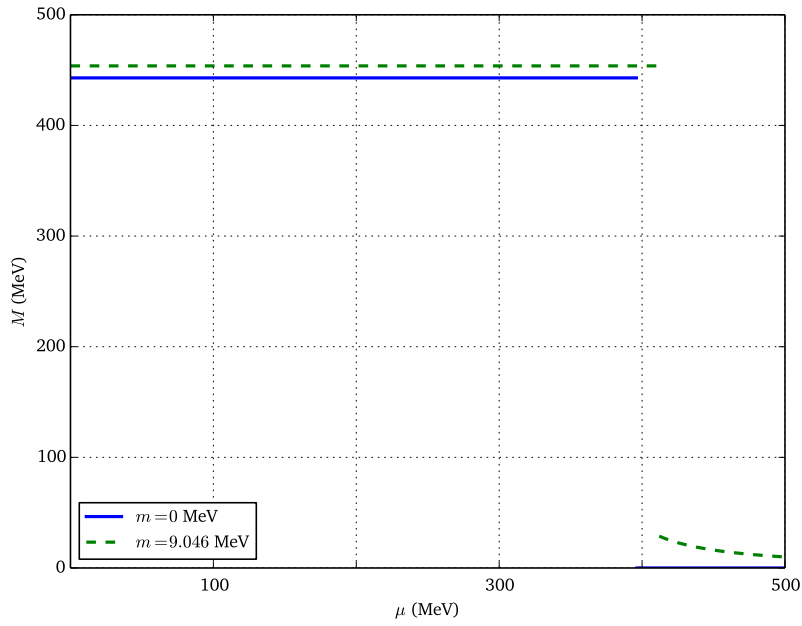
Figure 2.5. Solution of the gap equation for varying chemical potential and $T = 1$ MeV.

silver-blaze property. This property is expected to be valid for zero temperature or approximately satisfied for appropriate low temperatures.[2] The statement of this property can be summarised to the fact that all observables, and therefore the mass of a particle as well, should not depend on the chemical potential up to a critical value of μ at zero temperature [18]. Especially in the case of $T = 1$ MeV we will see for mesons as physical particles that the prediction of the silver-blaze property will be fulfilled. Meanwhile, for the quarks, we obtain a first order phase transition at $\mu_c \approx 400$ MeV. The quark mass jumps down instantly to zero in the chiral limit or to a certain value for non-vanishing bare quark mass and runs towards zero for high values of μ.

An other possible situation can be found for chemical potentials larger than M_{vac}. Hereby, the mass will decrease at $\mu = M_{\text{vac}}$ before it jumps down. In our discussion we obtain the first case in which the constituent mass falls down without decreasing smoothly first.

---

[2]We will use $T = 1$ MeV for all following discussions to investigate the behaviour of vanishing temperature.

Chapter 3

Mesonic spectrum

In the following chapter, we will continue with the description of mesons in the NJL model for two quark flavours, to obtain expressions for the meson masses and pion decay constant. In order to generate a set of parameters for the bare quark mass m_q, cutoff Λ, coupling constant g_s and constituent mass M, the pion mass and pion decay constant will be fixed to the experimental values. Then, the equation for the pion mass and decay constant, as well as the gap-equation represents a coupled system of equations, which can be simultaneously solved.

Mesons are physical particles built of a quark and an antiquark. Since mesons are observable in nature, their colour structure has to be a singlet state. In flavour space, we can identify a scalar singlet and a pseudoscalar triplet state for two assumed flavours, where the latter can be identified with the three pions. In accordance with the almost degenerate mass of the three pions in nature, the study of the pions can be performed in the isospin limit which is a convenient simplification for the expressions. The singlet state in flavour space meanwhile is typically identified with the sigma meson. We will later discuss the fact that the sigma meson is not a well defined particle and hence is not important for our goal to model baryons.

The particles in this chapter will be described by a quark-antiquark scattering process as a collective excitation in the theoretical framework of a Bethe-Salpeter (BS) equation in random-phase approximation (RPA). Hereby, the BS equation describes the bound state of a two-body system and can be motivated directly from the Dyson equation corresponding to the two-body Greens-function or S-matrix, respectively. After cutting off external fermion fields, one arrives at the BS equation.

However, before we can solve the BS equation, the scattering kernel and the meson polarisation loop need to be discussed.

In the previous chapter, we have already seen that a Fierz transformation of the colour-current interaction Lagrangian (2.26) leads to the already introduced Lagrangian for

the mesonic channel

$$\mathcal{L} = \mathcal{L}^{\text{free}} + \mathcal{L}_{\bar{\psi}\psi} \tag{3.1}$$

$$= \bar{\psi}\left(i\slashed{\partial} - m\right)\psi + g_s\left[(\bar{\psi}\psi)^2 + (\bar{\psi}i\gamma_5\vec{\tau}\psi)^2\right] . \tag{3.2}$$

To proceed with the derivation of the pions, it is convenient to transform the interaction part of the Lagrangian (3.2) into the form

$$\mathcal{L}_{\bar{\psi}\psi} = g_s\left[(\bar{\psi}\psi)^2 + (\bar{\psi}i\gamma_5\vec{\tau}\psi)^2\right] \tag{3.3}$$

$$= g_s\sum_M\left[\left(\bar{\psi}_{\bar{i}}\Gamma^M_{\bar{i}j}\psi_j\right)\left(\bar{\psi}_{\bar{k}}\Gamma^M_{\bar{k}l}\psi_l\right)\right] , \tag{3.4}$$

that is similar to the one shown in the discussion of the Fierz transformation. Here, the vertex functions Γ^M denotes the different mesonic channels and can be extracted directly from the Lagrangian (3.3). For the sigma meson the corresponding vertex structure reads

$$\Gamma^\sigma = \mathbb{1} \otimes \mathbb{1}_c \otimes \mathbb{1}_f \tag{3.5}$$

while for the pion

$$\Gamma^{\pi,f} = i\gamma_5 \otimes \mathbb{1}_c \otimes \tau^f \tag{3.6}$$

holds. To obtain an expression for the meson propagator, and thus for the masses, the Bethe-Salpeter equation in random-phase approximation, diagrammatically represented in figure 3.1 will be investigated. The left-hand side of the Bethe-Salpeter
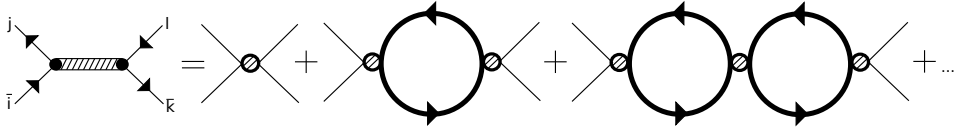

Figure 3.1. Bethe-Salpeter equation in random-phase approximation (RPA) as an infinite sum over polarisation loops.

equation is the scattering matrix (T-matrix) with the desired propagator having a pole at the mass of the corresponding meson. The two bold dots denote the quark-meson vertices which, at this point, are allowed to be different from the vertices included in the scattering kernel (cross-hatched dots). In random-phase approximation, where only quark-antiquark polarisation loops are included, the right-hand side of the Bethe-Salpeter equation is the sum over all these loops. The leading order term therefore is the scattering kernel itself. Evaluating figure 3.1, the scattering matrix $i\mathcal{T}$ has the (simplified) form

$$i\mathcal{T} = i\mathcal{K} + i\mathcal{K}(-i\Pi)i\mathcal{K} + i\mathcal{K}(-i\Pi)i\mathcal{K}(-i\Pi)i\mathcal{K} + \dots \tag{3.7}$$
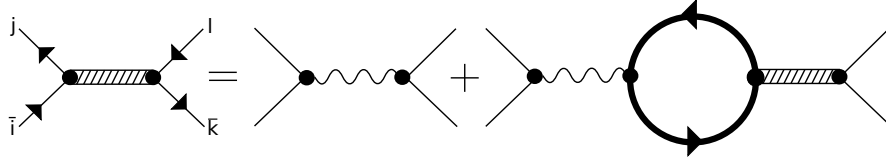
Figure 3.2. Self-consistent expression for the Bethe-Salpeter equation in RPA.

where $i\mathcal{K}$ and $i\Pi$ denote the scattering kernel and the polarisation loop, respectively. Both quantities, in general, are matrices which do not have to be diagonal at all. Reinserting the full scattering matrix into the right-hand side finally leads to the self-consistent expression

$$i\mathcal{T}(q) = i\mathcal{K} + i\mathcal{K}(-i\Pi)i\mathcal{T}(q) \tag{3.8}$$

with diagrammatic interpretation shown in figure 3.2. In accordance with the Lagrangian (3.2), the scattering kernel $i\mathcal{K}$ with all indices reads

$$= i\mathcal{K}_{j\bar{i},\bar{k}l} = 2ig_s \sum_M (\Gamma^M_{j\bar{i}} \Gamma^M_{\bar{k}l}), \tag{3.9}$$

which can also be written as [17]

$$i\mathcal{K}_{j\bar{i},\bar{k}l} = 2ig_s \sum_M (\Gamma^M_{j\bar{i}} \Gamma^M_{\bar{k}l}) = 2ig_s \sum_{M,M'} \delta^{MM'} (\Gamma^M_{j\bar{i}} \Gamma^{M'}_{\bar{k}l}) \tag{3.10}$$

with the factor of two entering the kernel as a result of the Feynman rules when applying Wick's theorem. In flavour space, the vertex structure of the scattering kernel (3.10) for the three pions can be rewritten, which yields

$$\sum_f \Gamma^f \Gamma^f = \sum_f \tau^f \otimes \tau^f \tag{3.11}$$

$$= \tau^1 \otimes \tau^1 + \tau^2 \otimes \tau^2 + \tau^3 \otimes \tau^3 \tag{3.12}$$

$$= \frac{1}{2}(\tau^1 + i\tau^2) \otimes (\tau^1 - i\tau^2) + \frac{1}{2}(\tau^1 - i\tau^2) \otimes (\tau^1 + i\tau^2) + \tau^3 \otimes \tau^3. \tag{3.13}$$

Hence, the three pions can be distinguished from each other through the corresponding representation in flavour space. We find that the vertex structure related to the first term leads to the π^+, cf. the l.h.s. of figure 3.1 with an intermediate π^+ state between the two vertices. The second term corresponds to π^-, while the last one yields π^0. The vertex structures for the three pions have been summarised in table 3.1.

Table 3.1. Representation for the three different pions.

pion	state (flavour space)	vertex structure in flavour space
$\lvert \pi^+ \rangle$	$\lvert \bar{d}u \rangle$	$\frac{1}{\sqrt{2}}(\tau^1 + i\tau^2) \otimes \frac{1}{\sqrt{2}}(\tau^1 - i\tau^2)$
$\lvert \pi^- \rangle$	$\lvert \bar{u}d \rangle$	$\frac{1}{\sqrt{2}}(\tau^1 - i\tau^2) \otimes \frac{1}{\sqrt{2}}(\tau^1 + i\tau^2)$
$\lvert \pi^0 \rangle$	$\frac{1}{\sqrt{2}}\left(\lvert \bar{u}u \rangle - \lvert \bar{d}d \rangle\right)$	$\tau^3 \otimes \tau^3$

We have already noted in the introduction that the three pion masses are approximately equal in nature. Hence, we will make use of the isospin limit, such that the pions are degenerate in flavour space. Therefore, only one mass occurs within our investigations.
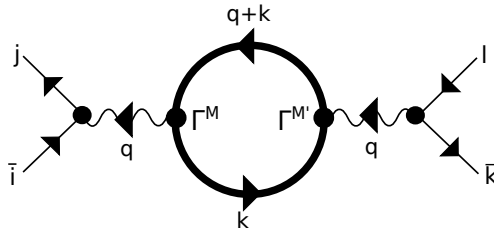
Figure 3.3.   Second order diagram in the BS equation for the scalar meson channel.

We now go back to the BS equation. In order to obtain an expression for scattering matrix, we have to evaluate the second order diagram of the BS equation, depicted in figure 3.3, which contains the so called polarisation loop. After a carefull evaluation of this diagram under virtue of the Feynman rule for closed fermion loops, we find

$$i\mathcal{K}(-i\Pi)i\mathcal{K} = -4i^2 g_s^2 \sum_{M,M'} \Gamma_{j\bar{i}}^M \int \frac{\mathrm{d}^4 k}{(2\pi)^4}\, \Gamma_{k'l'}^M iS_{l'j'}(q+k)\Gamma_{j'\bar{i}'}^{M'} iS_{\bar{i}'\bar{k}'}(k)\Gamma_{\bar{k}l}^{M'}. \tag{3.14}$$

The propagators of the quark, and antiquark, in this equation are defined in (2.33). One can now insert expression (2.33) for the propagators S of the quark and antiquark,

21

to obtain the polarisation loop

$$-i\Pi^{M,M'}(q) :=$$

$$(3.15)$$

$$:= -\int \frac{d^4k}{(2\pi)^4} \Gamma^M_{\bar{k}'l'} iS_{l'j'}(q+k)\Gamma^{M'}_{j'\bar{i}'} iS_{\bar{i}'\bar{k}'}(k) = -\int \frac{d^4k}{(2\pi)^4} \text{Tr}\left(\Gamma^M iS_q(q+k)\Gamma^{M'} iS_{\bar{q}}(k)\right),$$

$$(3.16)$$

for the mesonic channel. A detailed evaluation of the pion polarisation loop can be found in appendix D.1. Considering the Lagrangian (3.4), we find that the polarisation loop only gives a non-vanshing result for $M = M'$. Hence, the polarisation loop is diagonal in all spaces just like the scattering kernel.

Back to the BS equation (3.7), and taking into account the above expressions finally leads to the result that the scattering matrix itself is diagonal. As a consequence, the different spin channels are fully separated from each other, such that the pion and sigma meson do not mix. The scattering matrix for a certain meson thus reads

$$i\mathcal{T}^M = i\mathcal{K} + i\mathcal{K}(-i\Pi)i\mathcal{T}(q) \tag{3.17}$$

$$=: \Gamma^M t_M \Gamma^M, \tag{3.18}$$

with the scalar function

$$it_M(q) := 2ig_s + 2ig_s 2ig_s i\Pi^M(q)\dots \tag{3.19}$$

$$= 2ig_s + 2ig_s i\Pi^M(q)it_M(q), \tag{3.20}$$

which represents a self-consistent equation itself and can be interpreted as the propagator of a meson M. More precisely, it is the amputated BS equation, such that the left-hand side of figure 3.2 defines the meson propagator, where the meson-quark vertex is included. Later, we will discuss the meson-quark vertex in pole-approximation to obtain an effective meson-quark coupling constant (cf. section 3.1). Nevertheless, we will call the function defined in (3.19) meson propagator, but keep the included vertex structure in mind.

Near the pole the propagator (3.20) is expected to behave like a free boson, which propagator reads

$$D_M(q) = \frac{1}{q^2 - m_M^2}. \tag{3.21}$$

Hence, at $q^2 = m_M^2$ a pole emerges and can be used to define the mass m_M. In order to fit the free parameters of our model to the experimentally well known pion mass, we have to evaluate the corresponding propagtor (3.20) for $M = \pi$, at its pole. We can rewrite expression (3.20) into

$$it_\pi(q) = (1 - 2g_s\Pi_\pi(q))^{-1}2ig_s \tag{3.22}$$

For the on-shell condition, i.e $q^2 = m_\pi^2$, the inverse propagator has to be zero. Therefore, the mass determination reduces to a search for roots of the denominator in the above equation in consideration of the on-shell condition $q^2 = m_\pi^2$. After inserting the pion polarisation loop

$$-i\Pi^\pi(q) = 8N_c \int \frac{\mathrm{d}^4k}{(2\pi)^4} \frac{1}{k^2 - M^2} - 8N_c \frac{q^2}{2} \int \frac{\mathrm{d}^4k}{(2\pi)^4} \frac{1}{[(q+k)^2 - M^2] \cdot [k^2 - M^2]} \tag{3.23}$$

$$= 8N_c iI_1 - 4N_c q^2 iI_2(q^2) \, , \tag{3.24}$$

in the denominator, we have to solve

$$D_\pi^{-1}(q) := 1 - 2g_s \left(8N_c iI_1 - 4N_c q^2 iI_2(q) \right) |_{q^2=m_\pi^2} = 0 \, , \tag{3.25}$$

with

$$iI_2(q) := i \int \frac{\mathrm{d}^4k}{(2\pi)^4} \frac{1}{[(q+k)^2 - M^2 + i\epsilon] \cdot [k^2 - M^2 + i\epsilon]} \, . \tag{3.26}$$

A detailed investigation of this integral can be found in appendix D.1.1. Note that the upper relations always contain a general four-momentum for the pion. It is convenient to investigate the emerging expression in the rest frame of the corresponding particle, which means using $\vec{q} = 0$. Then, the dependency of D_π^{-1} is only given by q_0 rather than q. The inverse propagator (3.25) as a function of q_0 is shown in figure 3.4.

In the chiral limit, the inverse pion propagator (3.25) simplifies under virtue of gap-equation (2.44) for $m = 0$ MeV to

$$D_\pi^{-1}(q) = 8N_c q^2 iI_2(q^2)) |_{q^2=m_\pi^2} = 0 \, , \tag{3.27}$$

which yields a vanishing pion mass in accordance with the Goldstone theorem. Thus, the pion(s) become the Goldstone bosons for the spontaneously broken $SU(2)_A$ symmetry.

It turns out that the behaviour of iI_2 in the above equation is related to another drawback of the NJL model due to its lack of confinement: For meson masses higher than the sum of two quark masses, the polarisation loop, or to be more precise the integral iI_2, receives a non-vanishing imaginary part. This imaginary part can be
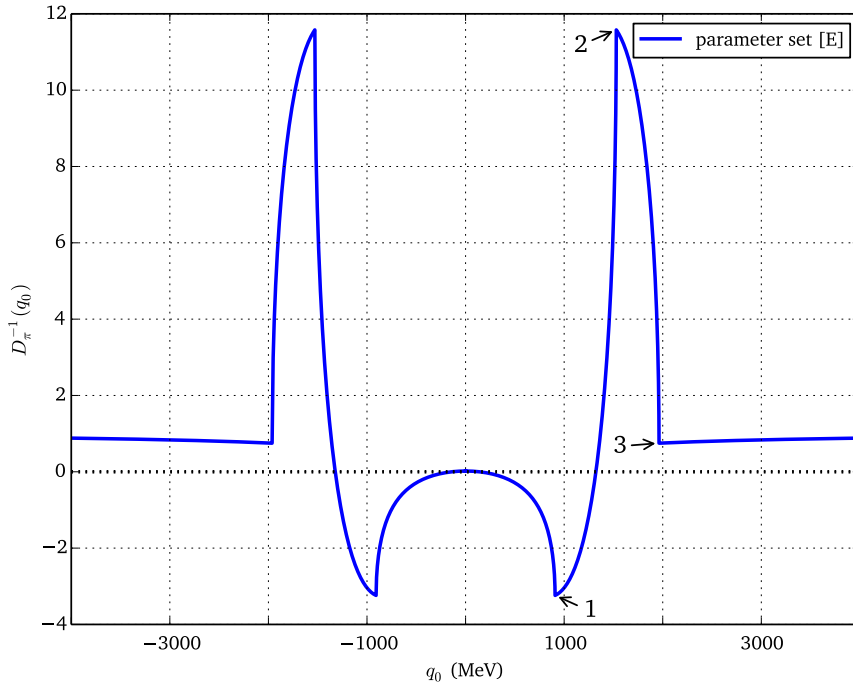
Figure 3.4. Inverse pion propagator for parameter set [E], cf. section 3.3

identified with a finite decay width and is related to a decay of a meson into a quark–antiquark pair.

The other possible particle described by the Lagrangian (2.12), the sigma meson, is sometimes discussed controversially due to its large mass. Experimental investigations have shown that the corresponding decay width has the magnitude of the mass itself [19], such that this particle is not well-defined. Even though this does not hold for the NJL model analysis with the random-phase approximation, the sigma meson will not be part of the further discussion as already noted.

Nevertheless, we have to take care of the emerging imaginary part of iI_2 for the pion as well. To obtain physically relevant masses for the pions only the real part of the propagator will be used. An opening imaginary part then shows up as a kink in the propagator denoted with "1" in figure 3.4. Hence, roots related to values of q_0 after these kinks correspond to pions which are allowed to decay into an quark-antiquark pair. The other two kinks, namely "2" and "3", emerge due to the PV regularisation scheme, where the two regulators become active.

3.1. Effective Pion-quark coupling constant

In the previous section, we have discussed the amputated BS equation and have identified its solution with the pion propagator given in equation (3.22). Diagrammatically, this propagator includes the quark-meson vertices and therefore the pion-quark coupling constant. To obtain an expression for this effective coupling constant, which in general will depend on the momentum q, we make the ansatz

$$t_\pi(q_0) = -\frac{g^2_{\pi qq}}{q_0^2 - m_\pi^2} \, , \tag{3.28}$$

where, we use the rest frame of the pion, i.e. $\vec{q} = 0$ in order to simplify the discussion. Equation (3.28) is based on the assumption, that near the pole the dependence of the coupling $g_{\pi qq}$ on q is weak, such that it can be treated as a constant. The so-called pole approximation utilizes this by expanding the denominator of (3.28) around zero. We can apply the pole approximation to equation (3.22), which leads to

$$1 - 2g_s\Pi_\pi(q_0^2) \approx \underbrace{1 - 2g_s\Pi^\pi(q_0^2)\big|_{q_0^2=m_\pi^2}}_{=0} - 2g_s\left.\frac{\partial\Pi^\pi(q_0^2)}{\partial q_0^2}\right|_{q_0^2=m_\pi^2}(q_0^2 - m_\pi^2)$$

$$+ \mathcal{O}((q_0^2 - m_\pi^2)^2) \, . \tag{3.29}$$

Comparing the pole expansion of (3.28) with (3.29), we find that the coupling constant can be expressed as

$$g_{\pi\bar{q}q}^{-2} = \left.\frac{\partial\Pi^\pi(q_0^2)}{\partial q_0^2}\right|_{q_0^2=m_\pi^2} \, . \tag{3.30}$$

We will see in following discussions that it is better suited to take the derivative with respect to q_0 instead of q_0^2. This yields

$$g_{\pi\bar{q}q}^{-2} = \left.\frac{\frac{\partial\Pi^\pi(q_0^2)}{\partial q_0}}{2q_0}\right|_{q_0=m_\pi} \, , \tag{3.31}$$

which for sure leads to the same results as equations (3.30).

3.2. Pion decay

The observed weak decay of the charged pions into a muon and a muon-neutrino can be described as the transition probability that a pion decays into the hadronic

25

vacuum [20]. Although the electromagnetic decay of π^0 into two photons is favoured, the weak decay constant will be calculated for simplicity with the vertex structure of the uncharged pion.

Due to parity conservation, the pion is only allowed to decay through the axial current. It follows that the decay constant f_π, determining the strength of the chiral symmetry breaking [21], can be defined through

$$\langle 0|A_\mu^a(x)|\pi^b(q)\rangle = if_\pi q_\mu \delta^{ab} e^{iqx} , \tag{3.32}$$

with the corresponding Feynman diagram shown in figure 3.5. After an evaluation of
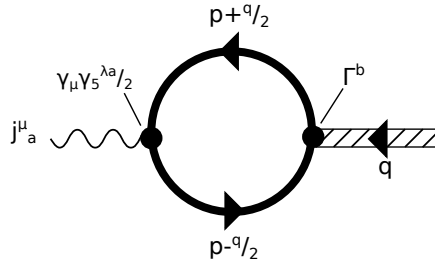

Figure 3.5. Pion decay Feynman diagram: The pion-decay constant is a result of the coupling between the pion (right-hand side) and the axial current.

the diagram in figure 3.5, one finds for the pion decay constant

$$f_\pi = -4N_c g_{\pi qq} M i I_2(q^2)\big|_{q^2=m_\pi^2} . \tag{3.33}$$

3.3. Parameter set and chiral theorems

We are now able to compute a set of parameters, which will be used in the further studies. The pion mass, pion decay constant and the gap equation are solved simultaneously with fixed values for the pion mass $m_\pi = 140$ MeV and the pion decay constant $f_\pi = 92.21$ MeV [19]. The results are given in the table 3.2 by varying the constituent mass parameter M. In addition the chiral condensate (per flavour) and the pion-quark coupling constant are displayed.

Typically, one uses a variation of the chiral condensate $(\langle \bar{q}q \rangle / N_f)^{\frac{1}{3}}$ to obtain different parameter sets of the NJL model, due to the fact that it is not known quite well. Since we want to fit the free parameters later on to the well known nucleon mass, the chiral condensate can be ignored. Nevertheless, the value of the condensate has been given for completeness. Moreover, we will see in the discussion of the inverse nucleon

propagator that the modelling of the baryons requires a relatively high mass M.
In order to verify our parameter sets, the Goldberger-Treiman relation can be used,

Table 3.2. Computed set of parameters for fixed values of $m_\pi = 140$ MeV and $f_\pi = 92.21$ MeV.

	[A]	[B]	[C]	[D]	[E]
M [MeV]	300	350	400	450	453.811
m [MeV]	7.57	8.46	8.89	9.04	9.05
$g_S \Lambda^2$	3.23	3.651	4.095	4.555	4.589
Λ [MeV]	696.676	647.491	624.828	615.359	615
$g_{\pi\bar{q}q}$	3.179	3.72	4.263	4.808	4.848
$(\langle\bar{\psi}\psi\rangle/N_f)^{\frac{1}{3}}$ [MeV]	-222.3	-214.04	-210.459	-209.29	-209.267

which connects the pion decay constant to the quark-pion coupling constant [16, 22]

$$g_{\pi qq} f_\pi = M + \mathcal{O}(m). \tag{3.34}$$

It is one of a couple of chiral theorems that should be satisfied independently from a certain regularisation scheme. In addition to the Goldberger-Treiman relation, the Gell-Mann-Oakes-Renner relation [16]

$$m_\pi^2 = -\frac{m\langle\bar{\psi}\psi\rangle}{f_\pi^2} + \mathcal{O}(m^2) \tag{3.35}$$

gives the correlation between the pion mass and the bare quark mass. In the discussion of the inverse pion propagator, we have already noted, that a non-vanishing bare quark mass leads to a physical pion mass, while for massless quarks the pion becomes the (massless) Goldstone boson. One can directly obtain from (3.35) that the Gell-Mann-Oaks-Renner relation also leads to a massless pion for a vanishing bare quark mass. In table 3.3 and 3.4 the Goldberger-Treiman and Gell-Mann-Oakes-Renner realtion respectively have been evaluated for the different parameter sets. Note that

Table 3.3. Goldberger-Treiman results used for the parameter sets [A]-[E]

	[A]	[B]	[C]	[D]	[E]
M [MeV]	300	350	400	450	453
$g_{\pi\bar{q}q}$	3.179	3.72	4.263	4.808	4.848
$g_{\pi qq} f_\pi$ [MeV]	293.174	343.067	393.086	443.351	447.068

the condensate per flavour has been changed to the (full) condensate, which is simply the sum over the two equal flavour condensates. It turns out that all parameter sets are in accordance with both relations.

Table 3.4. Gell-Mann-Oakes-Renner relation results for the parameter sets [A]-[E] with constant $m_\pi = 140$ MeV and $f_\pi = 92.21$ MeV.

	[A]	[B]	[C]	[D]	[E]
m [MeV]	7.57	8.46	8.89	9.04	9.05
$\langle \bar{\psi}\psi \rangle^{\frac{1}{3}}$ [MeV]	-280.081	-269.674	-265.162	-263.689	-263.66
$\sqrt{-\frac{m\langle \bar{\psi}\psi \rangle}{f_\pi^2}}$ [MeV]	139.823	139.687	139.642	139.638	139.639

However, parameter set [E] leads to best result when recalculating the pion mass as well as the pion decay constant and hence will be used in following discussion of pions in the medium and in the modelling of diquarks.

3.4. Mesons in the medium

In this section, we want to investigate the behaviour of pions in the medium. We find that the formal derivation of mesons with the BS equation is equal to the vacuum case. Therefore, the propagator is given by

$$it_\pi(i\omega, \vec{q}) = \frac{2ig_s}{1 - 2g_s \, \Pi^\pi(i\omega, \vec{q})|_{q^2 = m_\pi^2}} \, , \tag{3.36}$$

where $i\omega$ is a bosonic Matsubara frequency, related to q_0. The only thing one has to take care of, is the modification of the polarisation loop. The medium polarisation loop within the Matsubara formalism for the pion reads

$$\Pi^\pi(i\omega, \vec{q}) = -T \sum_{\{iv\}} \int \frac{\mathrm{d}^3 k}{(2\pi)^3} \mathrm{Tr} \left[\Gamma^\pi S(i\omega + iv + \mu, \vec{q} + \vec{k}) \Gamma^\pi S(iv + \mu, \vec{k}) \right] . \tag{3.37}$$

Here, iv is a fermionic Matsubara frequency related to the zero-component of the quark momentum k. After a straight forward evaluation of the traces for the different spaces and the fact that the sum of a bosonic and fermionic Matsubara frequencies is fermionic again, we find that the pion polarisation loop reads

$$\Pi^\pi(i\omega, \vec{q}) = 8N_c L_1(M, T, \mu) - ((i\omega)^2 - \vec{q}^2) 4N_c L_2(i\omega, \vec{q}) \, , \tag{3.38}$$

where the medium integral L_1 from the discussion of the quarks in the medium, cf. section 2.6, has been used. The integral L_2 is defined as

$$L_2(i\omega, \vec{q}) := -T \sum_{\{iv\}} \int \frac{\mathrm{d}^3 k}{(2\pi)^3} \frac{1}{(i\omega + iv + \mu)^2 - E_{q+k}^2} \frac{1}{(iv + \mu)^2 - E_k^2} \, , \tag{3.39}$$

and is basically the medium version of iI_2. The integral has been evaluated in detail for vanishing three-momentum $\vec{q}$ in appendix D.2.1. As for the medium version of iI_1 one can separate the vacuum and medium part of the upper expression. The medium contribution reads

$$L_2^{\text{med}}(q_0, \vec{q} = 0; T, \mu) = -\int \frac{d^3k}{(2\pi)^3} \frac{1}{E_k} \frac{1}{q_0^2 - 4E_k^2 + \text{sign}(q_0)i\epsilon} \left(n_f(E_k - \mu) + n_f(E_k + \mu) \right),$$
(3.40)

while the vacuum part is given by

$$L_2^{\text{vac}}(q_0, \vec{q} = 0; T, \mu) = \int \frac{d^3k}{(2\pi)^3} \frac{1}{E_k} \frac{1}{q_0^2 - 4E_k^2 + \text{sign}(q_0)i\epsilon}.$$
(3.41)

Here, we have used the analytical continuation $i\omega \mapsto q_0 + i\epsilon$ to obtain a dependence on real momenta within the propagator. Further more, the additional (small) positive imaginary part is related to the retarded version of the integral and hence the propagator itself for $\epsilon \longrightarrow 0$. Beside, it would be possible to use the advanced or the Feynman propagator as well. The retarded, advanced and Feynman propagator only differs in the choice of how (mass) poles are encircled. While for the retarded propagator the contour goes clockwise around both poles, the poles of an advanced propagator are encircled anticlockwise. The contour for the Feynman propagator, which has been used in the vacuum discussion, goes anticlockwise around the left and clockwise around the right pole.

Compared to the vacuum case the polarisation loop and hence the inverse propagator itself, depends on q_0 and $\vec{q}$ directly. Therefore, the inverse pion propagator, as well as all other propagators in dense matter which we will discuss, have to be treated as functions of q_0 and $\vec{q}$.

Note that the vacuum propagator depends only on $q^2 = q_0^2 - \vec{q}^2$ (with Minkowski metric) due to Lorentz invariance. Thus, one can choose the rest frame of the particle, i.e. $\vec{q} = 0$ in order to simplify the expressions. In the medium case this is much more difficult, since the Lorentz invariance is broken and the medium itself defines a preferred frame. In fact, it makes a physical difference if a certain particle moves relatively to this frame or not. Hence, the squared mass of a particle is equal to the square of the four-momentum q with, in general, non-vanishing three-momentum $\vec{q}$. Nevertheless, it has been shown in reference [23] that within a Pauli-Villar regularisation scheme the contribution of the external momentum $\vec{q}$ is relatively small for the pion propagator for not too high values of $\vec{q}$. In addition, one has to choose an arbitrarily $\vec{q}$ in order to perform any calculations. Further discussions thus will be performed for vanishing three-momentum $\vec{q}$, which will simplify the expressions significantly.
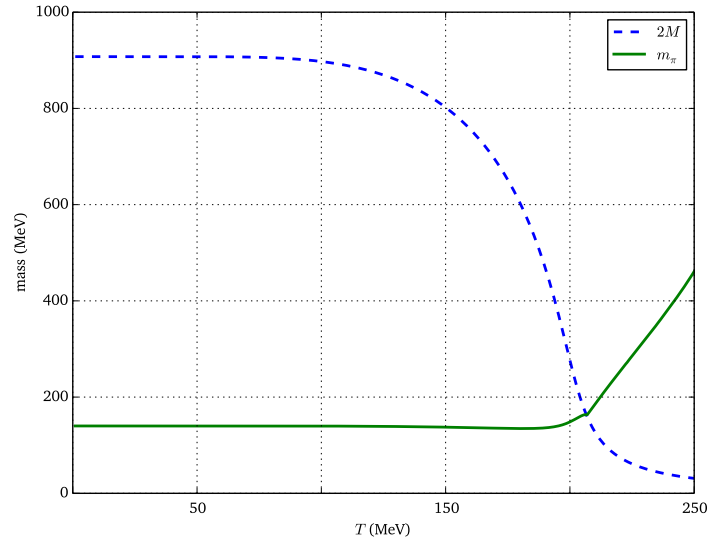
Figure 3.6. Temperature dependency of the pion mass compared to the (double) constituent mass.
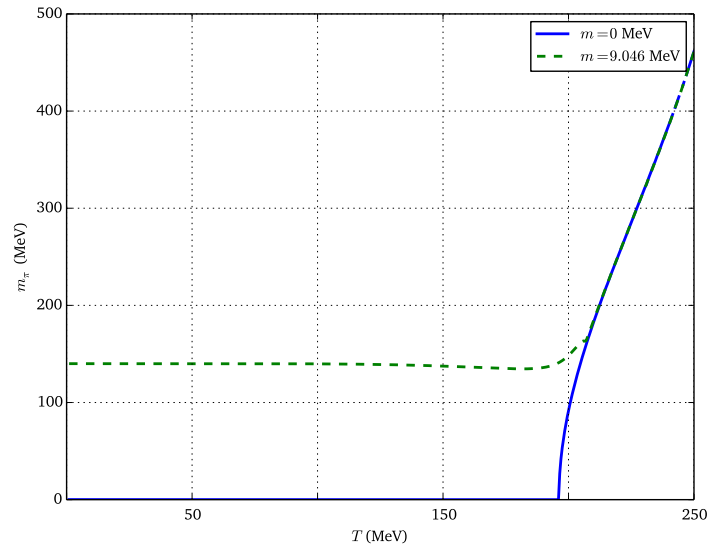

Figure 3.7. Temperature dependency of the pion mass in the chiral limit and non-vanishing bare quark mass.

In figure 3.7 the pion mass for varying temperature and fixed chemical potential $\mu = 0$ MeV is shown. Again, we distinguish between the chiral limit and a finite value of the bare quark mass. In case of a non-vanishing mass the pion mass stays approximately constant at its vacuum value until two times the constituent quark mass becomes lower than the vacuum mass of the pion, cf. figure 3.6. As already

discussed in the beginning of this chapter the polarisation loop, and therefore the inverse propagator, becomes complex, i.e. a non-zero imaginary part emerges. Note that the kink in the pion mass at $T \approx 220$ MeV within the upper figure is related to this opening imaginary part. Hence, the pion is allowed to decay into its constituents and obtains a higher mass.

In the chiral limit meanwhile the pion is the Goldstone boson for the spontaneously broken $SU(2)_A$ symmetry and thus is massless. For a temperature $T_c = 195$ MeV, at which the constituent quark mass becomes zero and hence the chirally restored phase begins, the pion obtains a non-vanishing mass.

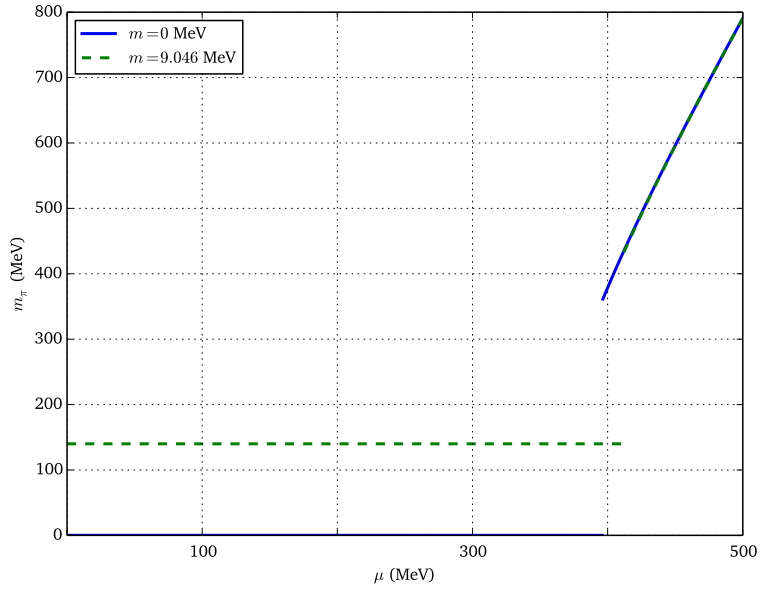For vanishing temperature and varying chemical potential the pion mass also stays

Figure 3.8. Pion mass for parameter set [E] with vanishing and non-vanishing bare quark mass as a function of the chemical potential μ with fixed value of $T = 1$ MeV.

constant at its vacuum value, cf. figure 3.8, in accordance with the silver-blaze property. For higher values of μ the first order phase transition leads to a non-vanishing imaginary part of the propagator due to the abruptly decreasing constituent quark mass. Compared to the temperature behaviour, the constituent quark mass is not a smooth function of T but jumps at $\mu_c \approx 400$ MeV to a significantly lower value instead. Hence, we obtain an analogous behaviour of the pion mass, except for the fact that it jumps to a higher value.

For completeness the temperature and chemical potential dependency of the effective pion-quark coupling $g_{\pi qq}$ is shown in figure 3.9 and 3.10. We will later discuss in detail the effective pion-quark coupling in section 4.3 in order to compare it with the
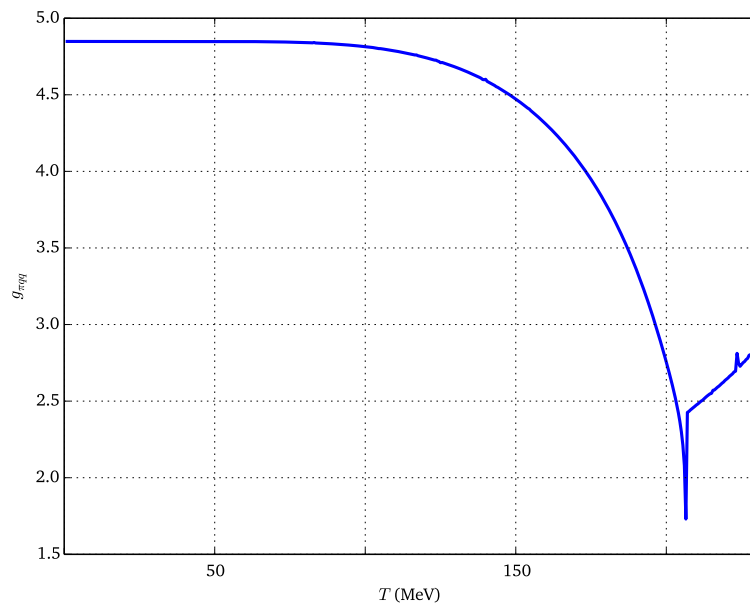
diquark-quark coupling.

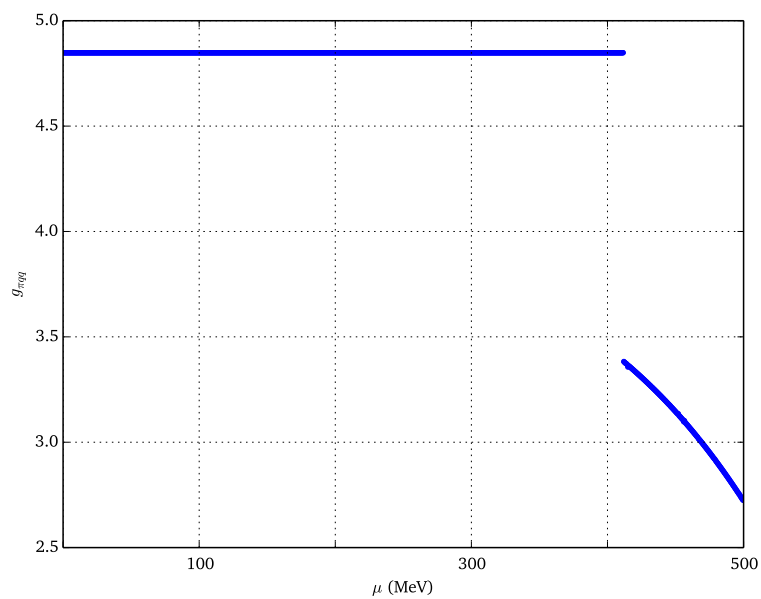**Figure 3.9.** Pion-quark coupling as function of T with vanishing chemical potential.

Figure 3.10. Pion-quark coupling as function of μ with $T = 1$ MeV.

Chapter 4

Diquark modelling

As mentioned in section 2.3, we consider the interaction Lagrangian

$$\mathcal{L}_{\psi\psi} = h_s \left[(\bar{\psi} C \tau_A \lambda_{A'} \bar{\psi}^T)(\psi^T C \tau_A \lambda_{A'} \psi) + (\bar{\psi} i \gamma_5 C \tau_A \lambda_{A'} \bar{\psi}^T)(\psi C i \gamma_5 \tau_A \lambda_{A'} \psi) \right] \quad (4.1)$$

for the particle-particle channel. Diquarks are non-observable bound states of two quarks, which cannot be found in nature due to confinement. However, the NJL model does not contain any confinement and thus we can view them as physical particles which can be described by a BS equation. In accordance with the $SU(3)$ addition rule for three different colours, diquarks can occur in a sextet and an antitriplet state [24]. Unlike the mesons composed of a quark and antiquark, we can thus identify particles which will be antisymmetric in flavour and colour indices. In particular, the particles antisymmetric in colour space can be coupled with a single quark to obtain a colourless object and thus can be used to model the baryons as a colour-singlet state.[1] Hence, the emerging sextet in colour space will not be considered in the further discussion, which has already been implemented in the Lagrangian (4.1).

In flavour space, we can identify a triplet and a singlet state. Due to Pauli's principle, the overall wave function for a certain diquark has to be totally antisymmetric, which leads to a restriction of allowed combinations for the different spaces. A certain representation for the two-flavour case, including vector contributions for completeness, can be found in the table 4.1, adapted from reference [25]. The lower indices denote whether the state is symmetric or antisymmetric in the considered space. Hereby the scalar and pseudoscalar, as well as the vector and axial-vector, channel have switched the representation in Dirac space compared to the mesonic spectrum. This is related to the charge conjugation operator entering the Lagrangian (4.1), cf. section 2.1.

---

[1]Like the mesons, baryons are physically observable in nature, thus they are in a colour singlet state, which is invariant under an $SU(3)$ colour rotation.

Table 4.1. Possible diquark structure in colour and flavour space [25].

	Flavour	Colour	Δ_D^μ	J^P
scalar	1_A	3_A	$i\gamma_5$	0^+
pseudoscalar	1_A	3_A	$\mathbb{1}$	0^-
axial	3_S	3_A	γ^μ	1^+
vector	1_A	3_A	$\gamma_5\gamma^\mu$	1^-

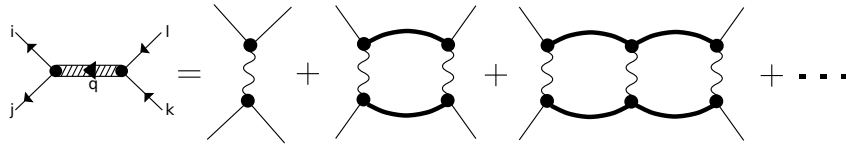## 4.1. Bethe-Salpeter equation for diquarks

In this section, we want to introduce the BS equation for diquarks and determine expressions for the corresponding scattering kernel and polarisation loop. The interaction Lagrangian in the quark-quark channel (4.1) can be expressed as

$$\mathcal{L}_{\psi\psi} = h_s \sum_D (\bar{\psi}\Gamma^D C \bar{\psi}^T)(\psi^T C \Gamma^D \psi) \,, \tag{4.2}$$

in accordance with the discussion of section 2.1. Therefore, the scattering kernel of a particular particle-particle channel Γ^D reads

$$i\mathcal{K}_{ij,kl}^D := \quad \text{} \quad = 2ih_s(\Gamma^D C)_{ij}(C\Gamma^D)_{kl} \,, \tag{4.3}$$

where we have simplified the notation to increase overview. Note that we assumed for the moment distinguishable quarks. Nevertheless, the BS equation can be used to obtain the bound state within this channel and is schematically shown in figure 4.1. Compared to the mesons, or more general, the particle-antiparticle channel, the second order diagram in the BS equation does not contain a closed fermion loop. Therefore, the derivation of the related polarisation loop will be more complicated. However, the polarisation loop can be brought into an form similar to the mesonic channel, as

Figure 4.1. Diquark Bethe-Salpeter equation for the quark-quark scattering.

34

shown in appendix E.1. For the scalar channel, we find

$$\Pi^D(q) = -i \int \frac{d^4k}{(2\pi)^4} \, \text{Tr} \left(\Gamma^D S_q(k+q) \Gamma^D S_q(k) \right) \tag{4.4}$$

$$= -i \text{tr}_c \left(\lambda^c \lambda^{c'} \right) \tau^f_{k'i'} \tau^{f'}_{i'k'} \int \frac{d^4k}{(2\pi)^4} \, \text{tr}_D \left(\Delta_D S_q(k+q) \Delta_D S_q(k) \right) . \tag{4.5}$$

Here, the trace performed in colour space is related to a conservation of the colour during the propagation of a diquark [25].

From a phenomenological point of view, we could expect this transformation, since mesons are described through the propagation of a quark and an antiquark. Due to the charge conjugation operator C the antiquark in some way has been transformed into a particle with quantum numbers of a quark, leading in the scattering process to a diquark. Furthermore, the interaction kernel for the particle-particle channel looks like the exchange diagram in the mesonic spectrum, up to the kind of incoming and outgoing particles. Within the particle-antiparticle channel, the exchange diagram has been transformed by a Fierz transformation into a direct-like diagram.

It follows, that the diquark scattering matrix iT^D reads

$$i\tilde{\mathcal{T}}^D_{ij,kl} = i\mathcal{K}^D_{ij,kl} + i\mathcal{K}^D_{ij,mn} \left(-i\Pi^D(q) \right) i\tilde{\mathcal{T}}^D_{nm,kl} \tag{4.6}$$

$$= \bar{\Omega}_{ij} i\tilde{t}^D(q) \Omega_{kl} \tag{4.7}$$

with

$$\tilde{t}_D(q) := 2h_D + 2h_D \Pi^D(q) \tilde{t}_D(q) , \tag{4.8}$$

$$\bar{\Omega}_{ij} := (\Gamma^D C)_{ij} , \tag{4.9}$$

as the diquark propagator and vertex, respectively. The diagrammatic representation of expression (4.6) is shown in figure 4.2 and is similar to the scattering matrix of the mesons in 3.2 except for the different coupling constants and vertex functions. To distinguish between the mesonic and diquark scattering matrices, we keep the non-closed form of the polarisation loop.
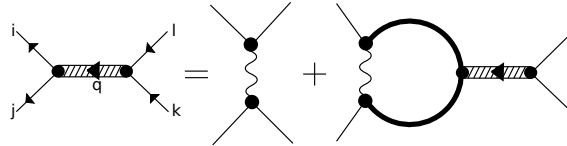

Figure 4.2.   BS equation for the diquarks reduced to a mesonic description.

Another possible scattering kernel of the particle-particle channel, is given by the exchange of the outgoing quarks, cf. figure (4.3). This scattering kernel is related to
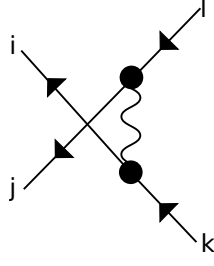
Figure 4.3. Diquark scattering kernel with exchanged outgoing particles.

the fact, that quarks are indistinguishable fermions. Therefore, we have to include this kind of scattering process to obtain a description for indistinguishable particles. Using this kernel, the scattering matrix differs only on the external outgoing quark indices on the left-hand side of figure 4.1. To obtain the full scattering matrix, both contributions have to be summed

$$iT^D_{ij,kl}(q) = i\tilde{T}^D_{ij,kl} - i\tilde{T}^D_{ji,kl} \, , \tag{4.10}$$

where the minus sign in front of the second term is a result of the fermion exchange. Hence, we are now treating the quarks as indistinguishable. Taking into account the general vertex structure given by in the Lagrangian (4.2), we find

$$iT^D_{ij,kl}(q) = \left(\bar{\Omega}_{ij} - \bar{\Omega}_{ji}\right) it_D(q)\Omega_{kl} \tag{4.11}$$

$$= \begin{cases} 0 & \text{for } \bar{\Omega}_{ij} = (\Gamma^D C)_{ij} \text{ totally symmetric} \\ 2i\tilde{T}^D_{ij,kl}(q) & \text{for } \bar{\Omega}_{ij} = (\Gamma^D C)_{ij} \text{ totally antisymmetric} \end{cases} . \tag{4.12}$$

Here, we notice, that only totally antisymmetric interaction channels will survive, in accordance with Pauli's principle.

As already mentioned, equation (4.8) will be interpreted as a propagator for the scalar diquarks, similarly to the mesons, and thus its pole contains the diquark mass. Therefore, the self-consistent equation for the scalar diquark propagator t_{sad} under virtue of the factor of two in equation (4.12), reads

$$t_{sad}(q) = \frac{4h_s}{1 - 2h_s\Pi^{sad}(q)} \, , \tag{4.13}$$

where the polarisation loop for the scalar diquarks is given by

$$\Pi^{sad}(q) = 16iI_1 - 8q^2iI_2(q) \tag{4.14}$$

$$= \frac{2}{N_c}\Pi^\pi(q) \, . \tag{4.15}$$

This shows that within the vacuum case the polarisation loop of the scalar diquark can be related to the polarisation loop of pseudoscalar meson channel. A detailed

derivation of the diquark polarisation loop can be found in appendix E.1. The general behaviour of the inverse propagator within the rest frame ($\vec{q} = 0$) for parameter set [E] is shown in figure 4.4. As in the discussion of the mesons, the coupling constant
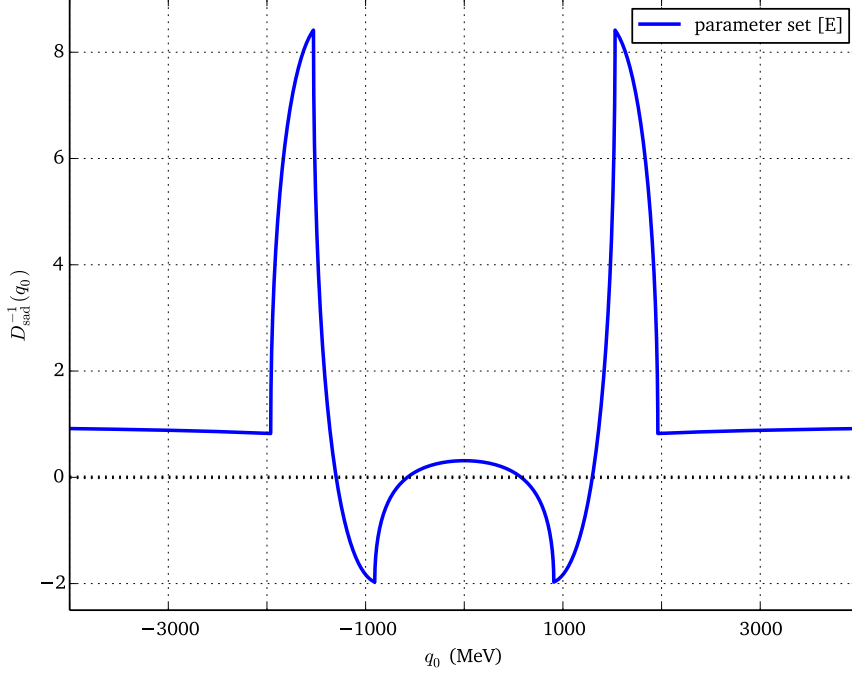

Figure 4.4. Inverse propagator for the scalar diquark as function of q_0. Here we set $h_s = 1.169 g_s$.

of the diquark channel h_s will be treated as a free parameter. Nevertheless, with the transformation matrices given in appendix B for the colour-current interaction, the two coupling constants h_s and g_s are related to each other by

$$\frac{g_s}{h_s} = 2\frac{N_c - 1}{N_c}, \tag{4.16}$$

which, with three assumed colours, yields $g_s/h_s = 3/4$. This ratio can be seen as an indicator for certain values of h_s, but we have to keep in mind, that the diquark spectrum is not observable in nature and thus the coupling constant h_s cannot be fitted to this spectrum. A possibility to solve this problem is fitting the baryon spectrum, where h_s is indirectly included in the scattering matrix as we will see in chapter 5. With equation (4.16), h_s can be expressed through the coupling constant in the particle-antiparticle channel by

$$h_s = \frac{N_c}{2(N_c - 1)} g_s. \tag{4.17}$$

Using the above relation, we can express the denominator of equation (4.13) in terms of the (scalar) meson coupling constant g_s. This yields, in case of on-shell diquarks ($q^2 = m_{sad}^2$), the mass for a certain diquark. Under a variation of the assumed number of colours N_c, we notice that for $N_c = 2$, the scalar antitriplet diquarks behave like the pions. Hence, the mass of the diquark and pion are degenerated when $h_s = g_s$ holds. Moreover, the scalar diquarks become massless in the chiral limit, such that they are Goldstone bosons whereas for three colours, this does not hold any more. For $N_c = 3$, the masses of the scalar diquarks are higher compared to the two colour
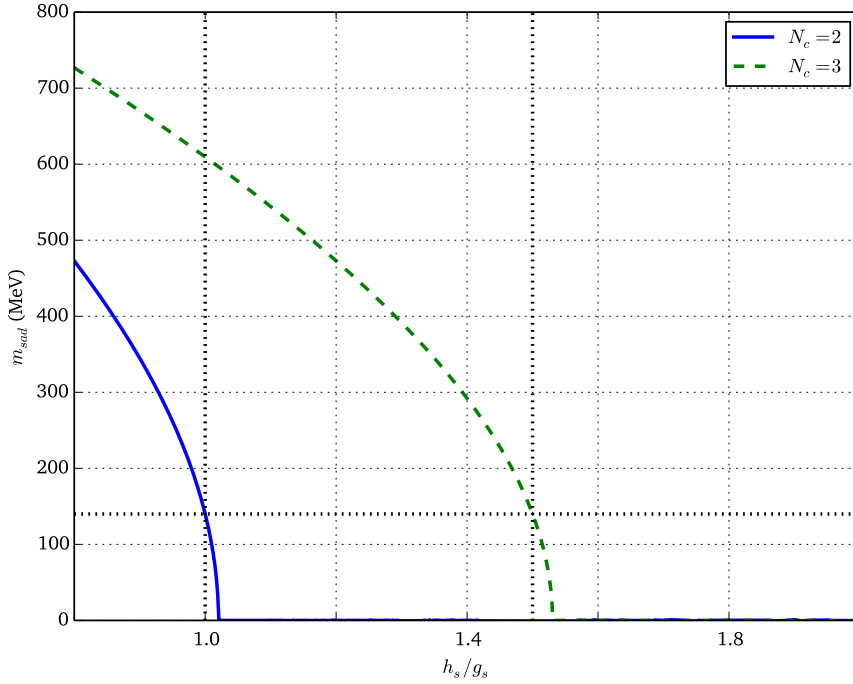

Figure 4.5.   Mass of the scalar antitriplet diquarks for different values of N_c. Parameter set [E] has been used.

case. The diquarks obtain the pion mass for $h_s = \frac{3}{2} g_s$ as shown in figure 4.5. The behaviour of the denominator in expression (4.13) for the different values of N_c is shown in figure 4.6. The roots of the denominator in equation (4.13) give rise to the masses of the diquarks. Furthermore, the emerging imaginary part of the integral I_2 for $q^2 > 4M^2$, cf. appendix D.1.1, leads to a critical value of the coupling constant, where only one root in the positive/negative hemisphere exists. The corresponding q_0 to this solution depends on the parameter set and is above the threshold for parameter set [A] and [B], while for [C]-[E] it lies directly on $q_0 = 2M$. Nevertheless, for all parameter sets the corresponding q_0 can be related to an unstable resonance within the particle-particle channel.

To obtain the value for the coupling constant, we can express the denominator of
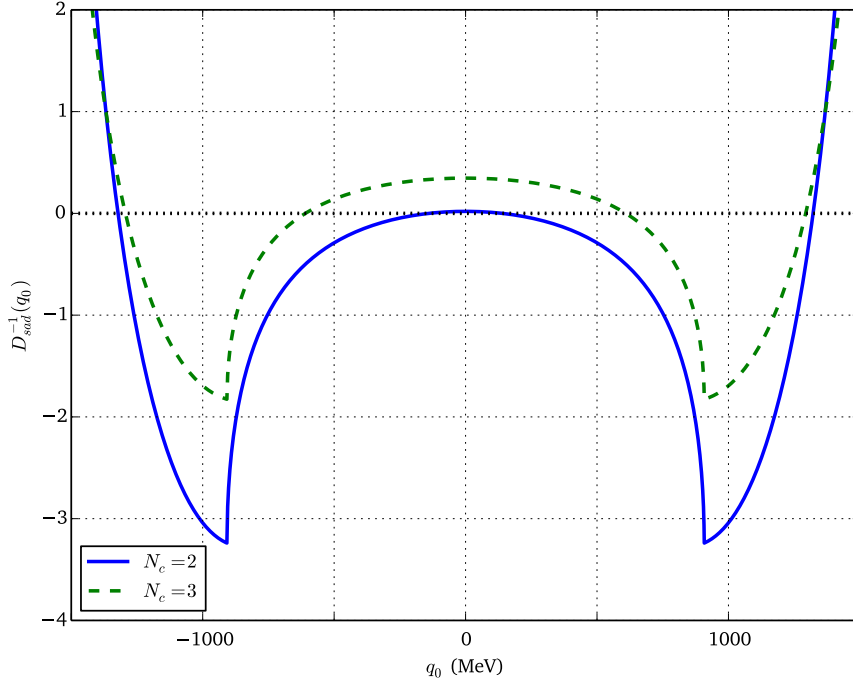
Figure 4.6. Denomiantor (real part) of the diquark propagator for different values of N_c for $h_s = g_s$ (parameter set [E]).

equation (4.13) in terms of g_s,

$$D_{sad}^{-1}(q) := 1 - 2r \cdot g_s(16iI_1 - 8q^2 iI_2(q)) \tag{4.18}$$

with $r := \frac{h_s}{g_s}$ and determine its minimum. The minimum can be found for parameter set [A] at $q_0^{\min} = 768.41$ MeV and hence $r_{crit} = 0.683$ for three colours.

Another point of interest is the coupling for the opening threshold, i.e. for a diquark mass equal to twice the quark's constituent mass $m_{sad} = 2M$. We find $r_{th} = 0.716$ for parameter set [A], cf. figure 4.7. In table 4.2 the critical and threshold ration r are shown for the different parameter sets of table 3.2. For the parameter sets [C], [D] and [E], r_{crit} is equal to r_{th} since the minimum of the inverse propagator is equal to the point of instability, i.e. $q_0 = 2M$. In case of $r > r_{crit}$, it is always possible to find multiple roots of the denominator of equation (4.13), due to the symmetry of the inverse propagator, cf. figure 4.4. As already mentioned, the root for $q_0 > 2M$ is related to a scalar diquark, whose mass is large enough to decay into its constituents and therefore can not be modelled as a particle with a simple pole approximation.

For the pseudoscalar diquarks (labeled with "pad"), we find that its mass is always larger than the scalar one, due to the difference of the polarisation loop

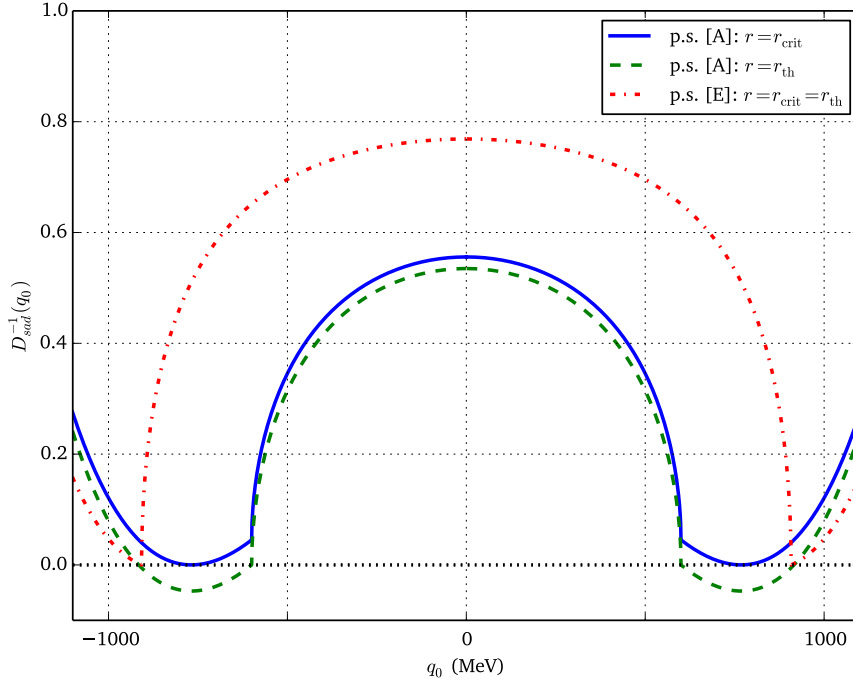$$\Pi^{pad}(q_0) = 16iI_1 - (q_0^2 - 4M^2)8iI_2(q_0^2) \tag{4.19}$$

Figure 4.7. Denomiantor (real part) of the diquark propagator (4.13) for the critical and threshold coupling constant with $N_c = 3$. For parameter set [E] $r_{crit} = r_{th}$ holds.

Table 4.2. Values of the critical and threshold coupling for different parameter sets.

	[A]	[B]	[C]	[D]	[E]
M [MeV]	300	350	400	450	453.811
q_0^{min} [MeV]	768.41	771.71	$2M$	$2M$	$2M$
r_{crit}	0.683	0.549	0.44	0.359	0.354
r_{th}	0.716	0.554	0.44	0.359	0.354

in the propagator. An analogous structure appears in the mesonic channel for the σ-meson. The corresponding mass of the pseudoscalar diquark is near the threshold $m_{pad}^2 = q_0^2 = 4M^2$ and for sufficiently small couplings even beyond it. For $h_s/g_s > 1.5$ the pseudoscalar diquark becomes bound, while for smaller values the opening imaginary part in the inverse propagator is responsible for the root and thus for the corresponding mass. As already mentioned this imaginary part is related to a decay
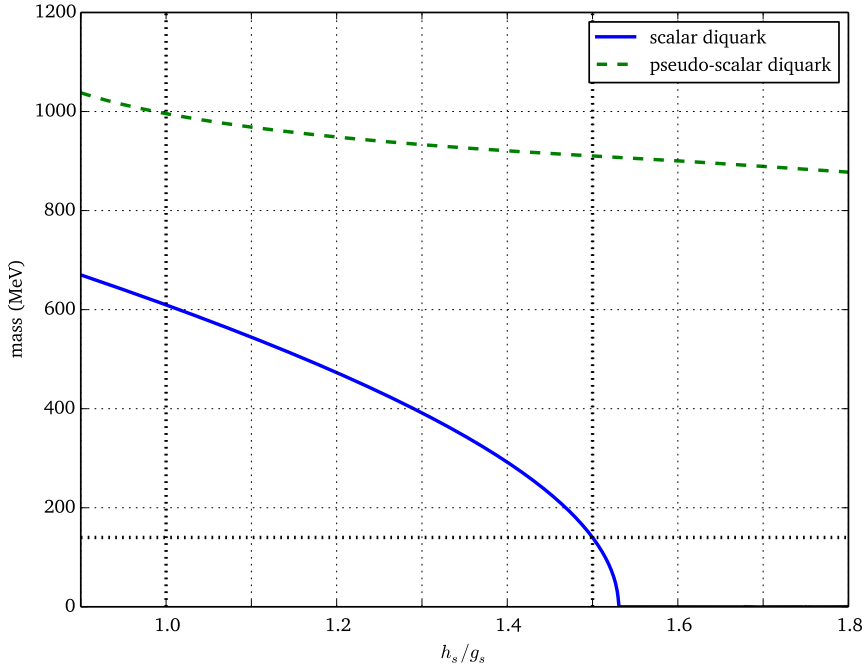

Figure 4.8. Scalar and pseudoscalar diquark masses for different coupling constants expressed in terms of g_s for parameter set [E].

of the diquark into its constituents, while diquark masses which satisfy $q^2 < 4M^2$ are bound states. However, figure 4.8 indicates that a very large coupling in the particle-particle channel has to be used in order to obtain a stable pseudoscalar diquarks. Even then, the obtained masses are close or even bigger than the nucleon mass itself. This will make it complicated to couple the pseudoscalar diquarks with a third quark into a bound state with the mass of a nucleon. In contrast to the scalar-diquark, which is much lighter than the pseudoscalar diquark, the latter is thus not suitable to build a nucleon. For completeness, the critical value r_{crit} for parameter set [E] for which no mass exists has been calculated and can be found around $r_{\mathrm{crit}} = 0.82$. Since this value is related to a pseudoscalar diquark in the unstable region and lies above the one we find for the scalar channel, the assumption that pseudoscalar diquarks are hardly bound in this region of h_s compared to the scalar diquarks seems to be valid. Hence, the pseudoscalar diquark will not be considered in further discussions.
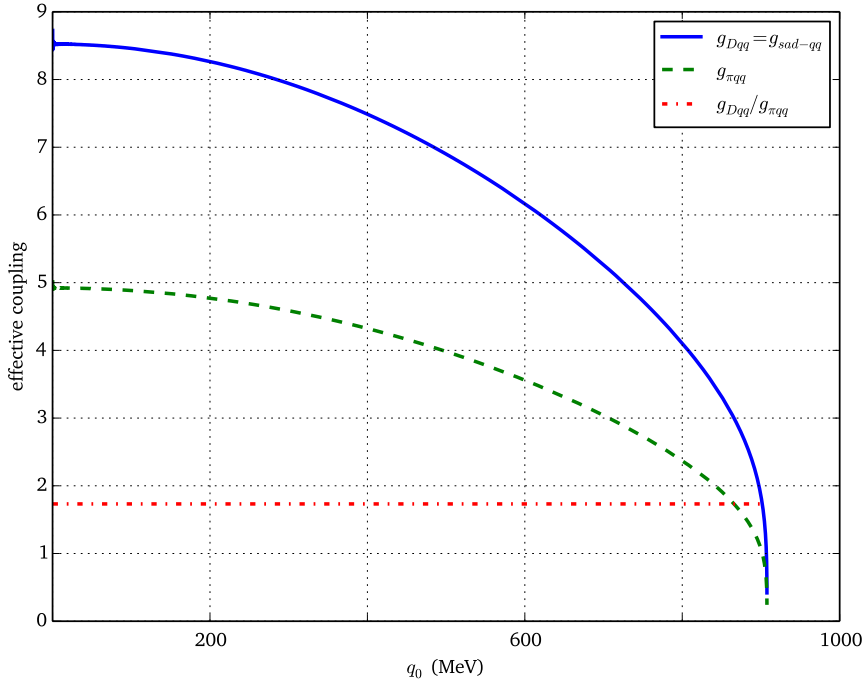
Figure 4.9. Pion-quark and scalar diquark-quark coupling constants as functions of q_0 ($N_c = 3$).

4.2. Diquark-quark coupling constant

Similar to the discussion of the mesons, a diquark-quark coupling constant can be defined, which will be suitable for the description of the baryons. Again, we start with the full scattering matrix

$$iT^D_{ij,kl} = \qquad\qquad = \bar{\Omega}_{ij}\frac{4ih_s}{1-2h_s\Pi^s(q)}\Omega_{kl}\,. \tag{4.20}$$

Analogously, to the mesons, the interaction between the two quarks can be interpreted as an exchange of a diquark. This leads to

$$iT^D = (-ig_{Dqq}(q)\Gamma^D C)\frac{i}{q^2 - m_D^2}(-ig_{Dqq}(q)C\Gamma^D)\,. \tag{4.21}$$

where the diquark-quark coupling is allowed to be momentum dependent as well. By assuming that this dependence is weak and comparing (4.20) with (4.21), we find for

the scalar diquarks

$$-\frac{g^2_{sad-qq}}{q^2 - m^2_{sad}} \approx \frac{4h_s}{1 - 2h_s \Pi^{sad}} = t_s ,$$ (4.22)

which, after applying the pole approximation yields

$$g^{-2}_{sad-qq} = \frac{1}{2} \left.\frac{\partial \Pi^{sad}(q^2)}{\partial q^2}\right|_{q^2 = m^2_{sad}} = \left.\frac{\frac{\partial \Pi^{sad}(q_0^2)}{\partial q_0}}{4q_0}\right|_{q_0 = m_{sad}} .$$ (4.23)

We have already seen, that in the two-colour case the scalar diquark polarisation loop is equal to the pion polarisation loop, cf. equation (4.15). Therefore, the coupling constants are equal too, while in the three-colour case the different pre-factors lead to a constant ratio $g_{sad-qq}/g_{\pi-qq} = \sqrt{N_c}$ of the couplings if treated as functions of q_0 and ignoring the on-shell condition. Compared to the meson-quark coupling constant, or more precisely the pion-quark coupling, the scalar diquarks seems to be coupled stronger to the constituent quarks despite the significantly higher mass of the diquarks.

To increase overview and due to the fact we neglect other diquark channels the effective scalar diquark coupling will be denoted by g_{Dqq}.

4.3. Medium diquarks

In this section we want to develop the medium expression for a diquark and study its behaviour for finite temperature and chemical potential. Again, the expression for the propagator will be similar to the one obtained in the vacuum case except for the polarisation loop (4.5), which has to be modified in accordance with the replacement given in (2.54). In contrast to mesons, which contain a quark and an antiquark, the constituents of diquark are two quarks. It follows that this kind of particles feel twice the chemical potential of a quark as we will find in the following discussion. Moreover, we do not have to distinguish between the quark chemical potentials, since we make use of the isopin limit.

The diquark polarisation loop (4.5) in the Matsubara formalism reads

$$\Pi^D(i\omega + 2\mu, \vec{q}) = -iT\sum_n \int \frac{d^3k}{(2\pi)^3} \text{Tr}\left[C\Gamma^D S(i\omega + i\nu_n + \mu, \vec{q} + \vec{k})\Gamma^D C S^T(-i\nu_n + \mu, -\vec{k})\right]$$ (4.24)

$$= iT\sum_n \int \frac{d^3k}{(2\pi)^3} \text{Tr}\left[\Gamma^D S(i\omega + i\nu_n + \mu, \vec{q} + \vec{k})\Gamma^D S(i\nu_n - \mu, \vec{k})\right] ,$$ (4.25)
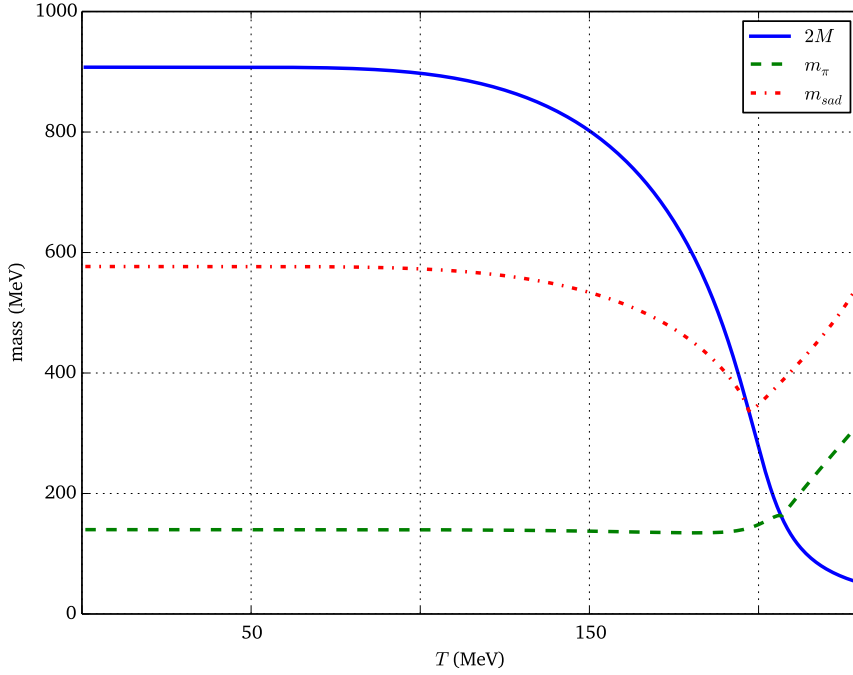
Figure 4.10. Diquark, pion and two times the constitutent mass for vanishing chemical potential.

where we have taken into account some of the relations given in appendix E.1. This looks similar to the mesonic channel. It turns out that the diquark polarisation loop also can be expressed in terms of elementary integrals. For the scalar color-antitriplet diquark we obtained

$$\Pi^{\text{sad}}(i\omega + 2\mu, \vec{q}) = 16iL_1 - \left((i\omega + 2\mu)^2 - \vec{q}^2\right)8i\tilde{L}(i\omega + 2\mu, \vec{q}), \qquad (4.26)$$

with

$$\tilde{L}(i\omega + 2\mu, \vec{q} = 0) := -T\sum_n \int \frac{\mathrm{d}^3 k}{(2\pi)^3} \frac{1}{[(i\omega + i\nu_n + \mu)^2 - E_k^2][(i\nu_n - \mu)^2 - E_k^2]}. \quad (4.27)$$

A detailed derivation of the polarisation loop and integral can be found in appendix E.1.1.

Compared to the medium discussion of the pion, the polarisation loop and thus the inverse propagator itself can be treated as function of $i\omega + 2\mu$, as expected. To be consistent to the earlier dicussions, we choose the analytical continuation $i\omega \mapsto q_0 + i\epsilon$. Again, the following discussion has been performed with parameter set [E] and a coupling $h_s = 1.169 g_s$ in the particle-particle channel.

At first, we keep the chemical potential at a constant value of zero and vary the temperature. In figure 4.10 the diquark mass compared to the pion mass and two
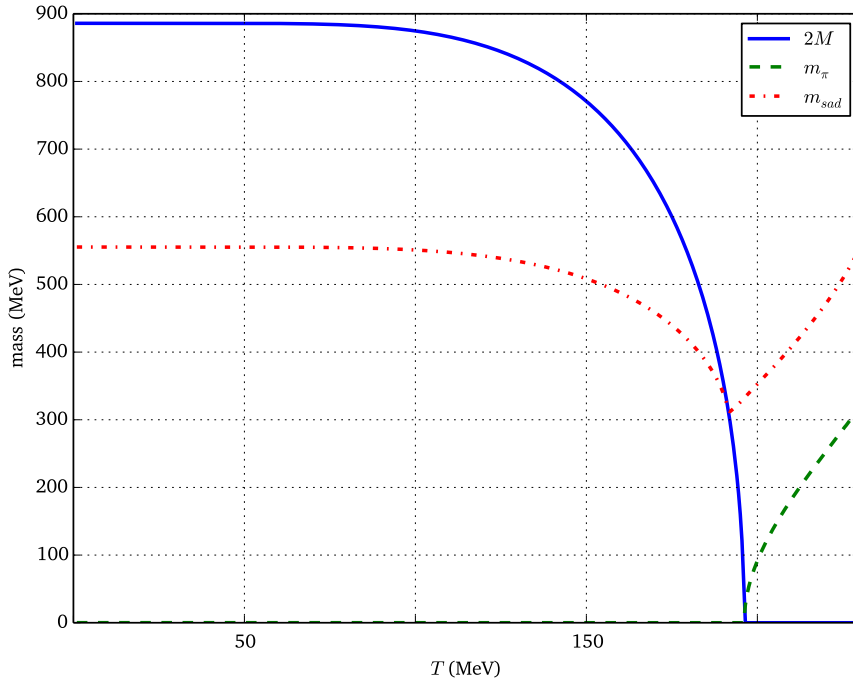
44

Figure 4.11.   Diquark, pion and two times the constitutent mass for vanishing chemical
potential in the chiral limit.

times the constituent mass is shown. We note that the behaviour of the scalar diquark
and pion are analogous. As seen in the derivation of the diquark scattering matrix the
behaviour of the scalar diquark strongly recalls the pseudoscalar pions. Especially, in
case of two colours they are expected to be equal in vacuum. However, this does not
hold for non-vanishing chemical potential any more, since the diquark polarisation
loop can not be expressed by the pion one. We already have found in the vacuum
investigation that the diquarks obtain an higher mass than the pions and thus are less
bound. For varying temperature, the melting temperature of the scalar diquark, at
which the imaginary part of the inverse diquark propagator opens, and thus allows the
diquark to decay into its constituents, lies at $T_m = 197$ MeV. For the pions meanwhile
we found the melting temperature at $T_m = 220$ MeV.

In the chiral limit, the diquarks have a non-vanishing mass while the pions are the
massless Goldstone bosons. For increasing temperature the mass continuously falls
down until the obtained mass reaches $2M$ and the decay into a quark pair becomes
possible. Of course this behaviour in the chiral limit, as well as for non-vanishing bare
quark mass, is related to the fact that the constituent mass decreases faster than the
bound state of two quarks.

A completely different behaviour shows for varying chemical potential at vanishing
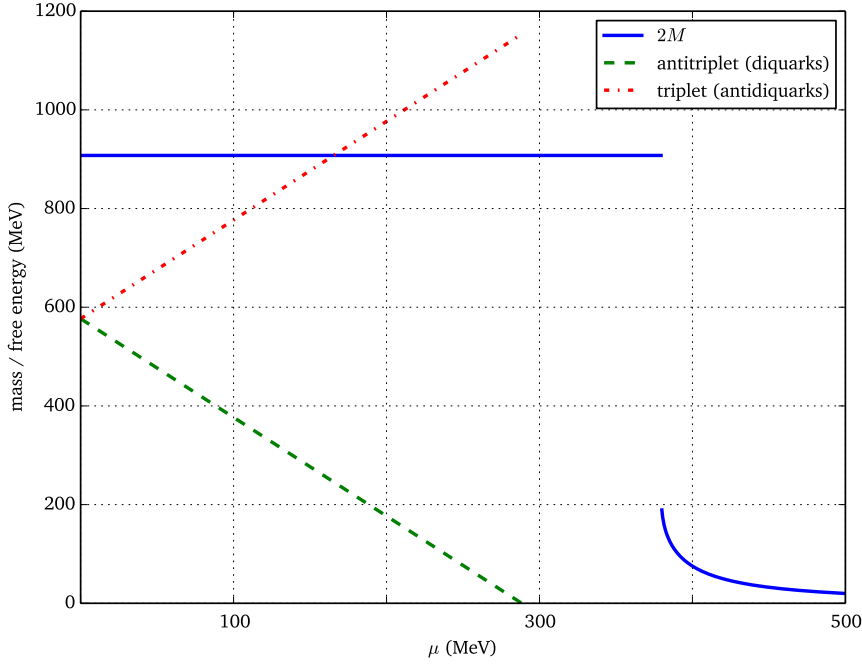
Figure 4.12. Free energy of diquark and antidiquark for finite μ ($T = 1$ MeV).

temperature. For non-vanishing chemical potential the poles of the diquark propagator are shifted. This can be directly seen if we take a look at the pole-approximation for $T = 0$ MeV. Therefore, the diquark propagator near the pole is expected to behave like a bosonic propagator

$$D_D(q_0, \vec{q}, \mu) = \frac{1}{(q_0 + 2\mu)^2 - E_D^2} \, . \tag{4.28}$$

The poles are given by

$$q_{\text{Pole}}^{\pm} = E_D^{\pm} - 2\mu \, , \tag{4.29}$$

with $E_D^{\pm} := \pm E_D = \pm\sqrt{\vec{q}^2 + m_D^2}$. Hence, the poles should not be identified with the physical mass of the particle. The poles $q_{\text{Pole}}^{\pm}$ meanwhile, are the excitation energy of the dense medium to obtain an antidiquark and diquark, respectively. In other words it is the free energy of the (anti)diquark. Since the free energy in the chiral limit behaves like the one obtained for $m = 9.046$ MeV, we concentrate on the latter case. While the pion mass stays constant before the chirally restored phase begins, the diquark energy becomes linearly smaller by increasing the chemical potential. At $\mu = m_{sad}/2$, where m_{sad} denotes the vacuum mass, the diquark obtains a free energy equal to zero still before the chirally restored phase begins. In comparison with the critical chemical potential for the quarks, cf. section 2.6, where we obtained
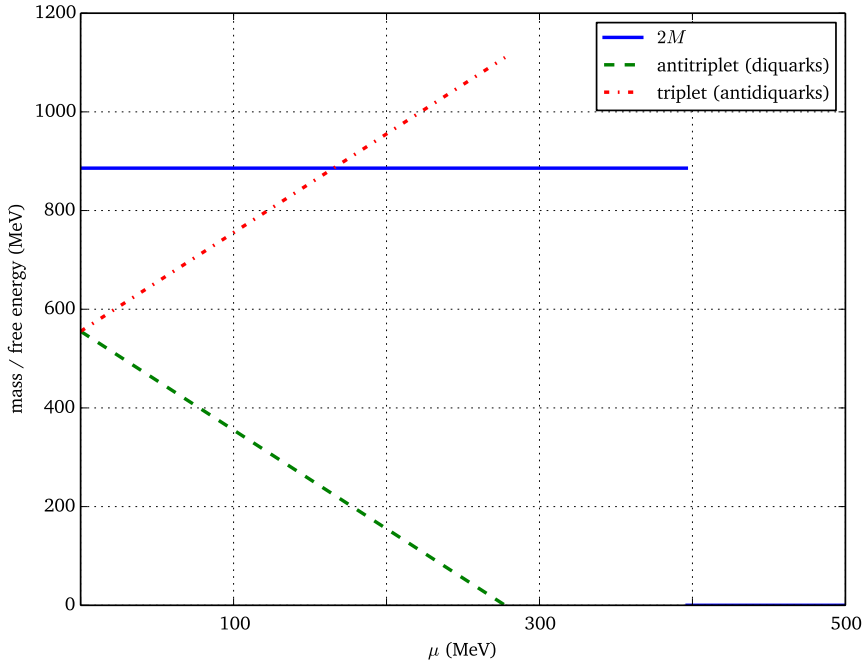
Figure 4.13. Free energy of diquark and antidiquark for finite μ in the chiral limit $(T = 1 \text{ MeV})$.

$\mu_c = 400$ MeV, diquarks have an additional phase transition which has not considered so far. In fact, it has been studied in reference [26] and other works that diquarks at $\mu = m_{sad}/2$ enter the two-flavour colour superconductivity (2SC) phase with non-vanishing diquark condensate, while in the colour symmetric phase, i.e. $\mu < m_{sad}/2$ the diquark condensate is zero. For a chemical potential beneath the threshold, the six diquark states in colour space split into an colour triplet and antitriplet state [26]. The corresponding free energies of the antitriplet diquark and triplet antidiquark are shown in figure 4.12 and 4.13 for $m = 0$ MeV. Moreover, it is known that for sufficiently large chemical potential and low temperature the condensation of two quarks is favoured over the chirally restored phase [27]. Notwithstanding the above, the physical mass of the diquark, and antidiquark as well, should not and indeed does not change until $\mu = m_{sad}/2$ due to the silver-blaze property.

As already mentioned at the beginning of this chapter the antitriplet in colour space is of particular interest in view of the baryon modelling in later chapters. Despite the fact the 2SC phase has interesting features to discuss, we focus on the colour symmetric phase. As a result of the upper discussion the diquark mass will be taken constant to its vacuum value until $\mu = m_{sad}/2$, due to the fact that the methods provided in this work are not able to investigate the 2SC phase. Therefore, diquarks will not be considered for $\mu > m_{sad}/2$. Of course, effects related to a temperature variation will

47

be taken into account.

In figure 4.14 the effective diquark-quark and pion-quark coupling in the medium are shown for a wide temperature range. The small peaks within the plots do not have any physical meaning and are related to numerical uncertainties only.
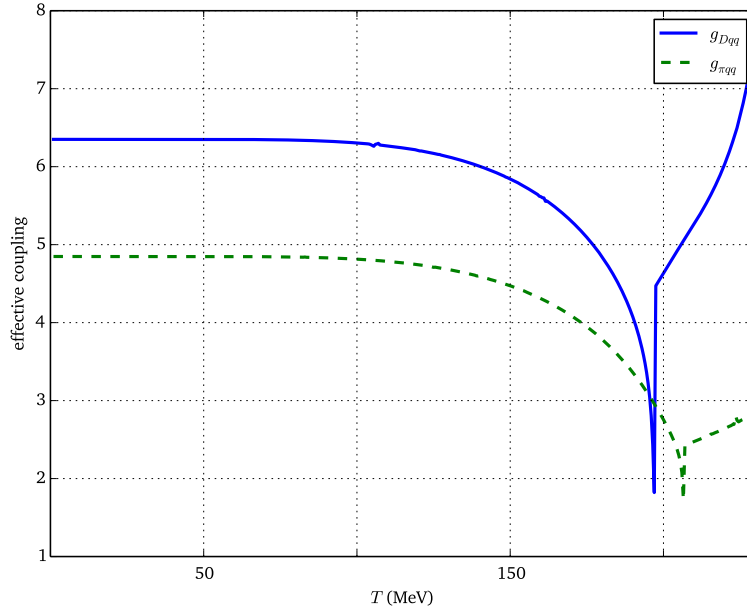For vanishing chemical potential both couplings are constant until a significant drop

Figure 4.14.   Effective coupling constant for the pion and diquark as functions of the temperature at $\mu = 0$.

occurs. Since the behaviour of the effective pion-quark and diquark-quark coupling are qualitatively equal in the corresponding region for both quantities, we will concentrate our discussion on the latter one.
In figure 4.15 the effective diquark-quark coupling has been calculated in the region of the kink. We find that the temperatures related to the kink labeled with "2", in figure 4.15, right after the drop coincides with the melting temperature of the pseudoscalar diquark. At this temperature, the diquark has zero binding energy since its mass is equal to twice the constitutes. Therefore, the effective coupling should smoothly fall down to almost zero, until the imaginary part of the corresponding polarisation loop opens. Increasing the temperature after this point leads to unstable particles such that the effective coupling also becomes complex.[2] The more or less smooth behaviour of the effective coupling is possibly related to the (crossover) into the chirally restored phase of the quarks for a non-vanishing bare mass. Taking a look at the chiral limit,

---

[2]Note that we always plot the real part of certain properties unless stated otherwise.
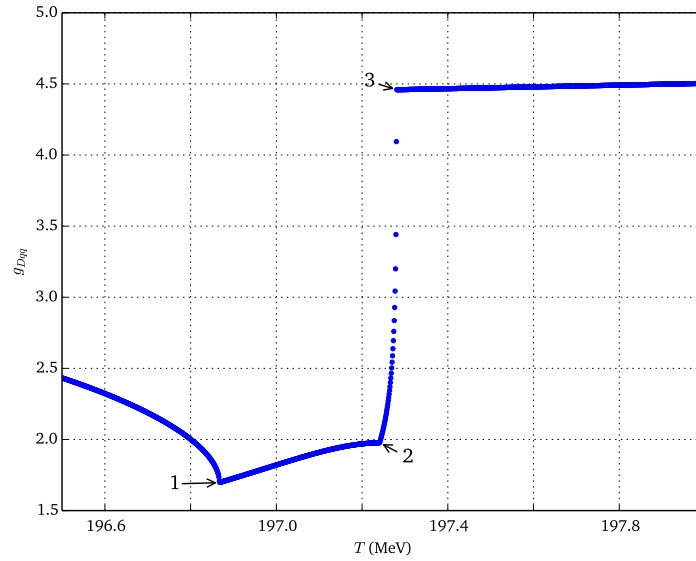
Figure 4.15. Effective coupling constant for the diquark as function of the temperature at $\mu = 0$ at the critical region.

where a second order phase transition appears, we find that the effective coupling is unsteady, which is shown in figure 4.16. Hence, we conclude that the behaviour of the effective coupling indeed could be related to the kind of phase transition for the quarks. Unfortunately, we do not find any good explanation for the kinks "1" and "3" in figure 4.15.

Again, a different picture arises for $T = 1$ MeV and varying chemical potential, cf. figure 4.17. In the derivation of the effective coupling we make use of the pole approximation. While for vanishing chemical potential the poles of the propagator are the mass of the diquark itself, the poles for non-vanishing chemical potential are related to the free energies shown in figure 4.12. Consequently, instead of inserting the diquark mass in (4.23), we have to evaluate (4.23) at $q_0 = E_D^+ - 2\mu$ for the antitriplet. The results for the diquark-quark coupling as a function of the chemical potential are shown in figure 4.17 for a constant diquark mass. If we consider the poles in equation (4.29) to be the mass of the diquark, we find that due to the decreasing free energy of the medium, which is related to an increasing binding energy, the diquark-quark coupling increases too until $\mu = m_{sad}/2$. After this critical chemical potential our methods are not reliable to further investigate the diquark-quark coupling.

The pion-quark coupling, however, stays constant until $\mu = 412$ MeV, because the pion mass itself does not change in this range. Then the coupling drops down and decreases for larger chemical potentials, which is related to the increasing mass of the pion. Overall, we note that the behaviour of the pion-quark coupling resemble the one obtained for the pion mass in dense matter as shown in figure 3.8.
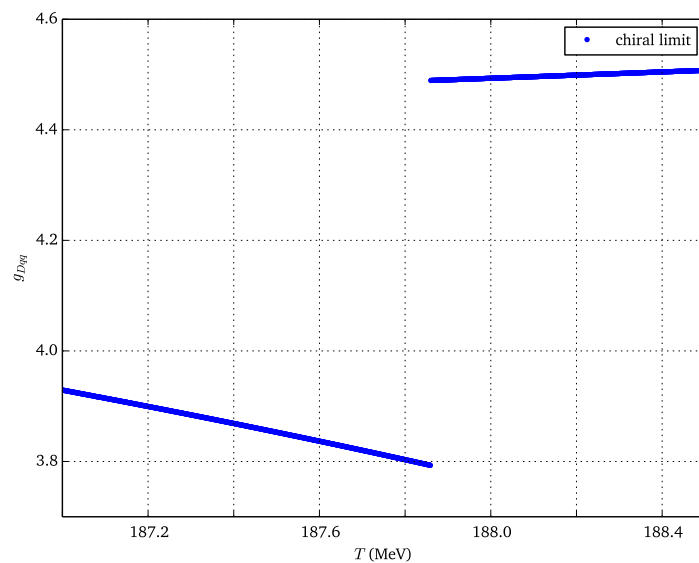
49

Figure 4.16.   Effective coupling constant for the diquark as a function of the temperature at $\mu = 0$ at the critical region for vanishing bare quark mass.
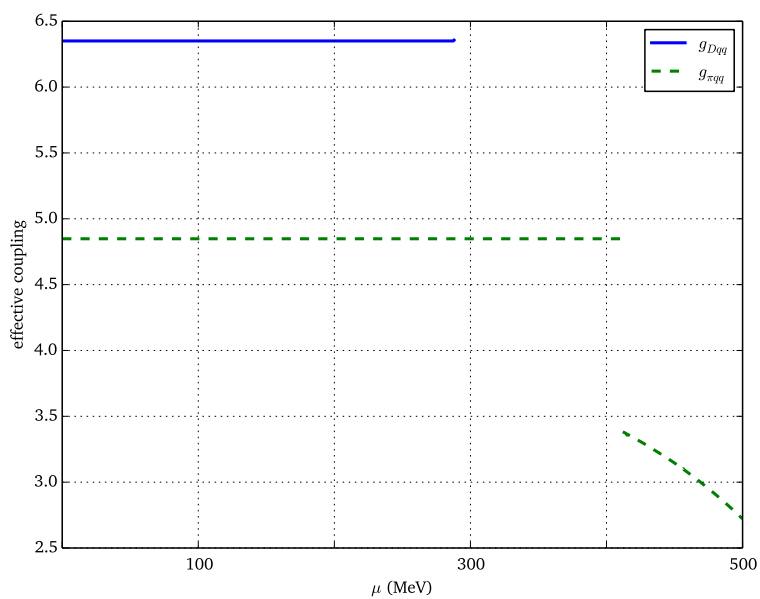

Figure 4.17.   Effective coupling constants of the pion and diquark channel for finite μ ($T = 1$ MeV).

50

Chapter 5

Baryon modelling for two flavours

In general, a baryon has to be described by a complex structure of three quarks, coupled through an exchange of gluons. We will reduce this problem in the framework of the NJL model to a more computationally friendly two-body interaction, where a diquark and a quark can form a baryon. Therefore, three-body irreducible diagrams, which contain a three fermion vertex, are ignored. For diquarks the flavour triplet and singlet states can take part in the baryon structure, but have to be combined carefully with certain spin channels to obtain an antisymmetric wave function, since baryons are a composition of three fermions. To simplify our discussion, we will restrict ourselves to the scalar diquarks, having the lowest mass in the particle-particle channel, as shown in the previous chapter, and thus might be bound stronger with a third quark. Note that the Dirac structure of a baryon is then determined by the third quark, due to lack of a Dirac structure in the scalar diquark channel. Furthermore, the pseudoscalar diquark will not be used to model baryons within the two flavour NJL framework, since it would require a binding energy in the order of the constituent quark mass itself (or even more) to obtain the nucleon mass of 940 MeV [28].

In contrast to the previous chapters, we will start from the Dyson equation and introduce Fadeev components for the baryon propagator as the solution of the three-body problem. While the non-relativistic Fadeev equation can be solved numerically in certain model potentials, the bound state problem of a three-quark system has to be truncated in quantum field theory approaches [29]. To reduce this problem, a commonly used assumption in QCD calculations is that the two-body correlation within the three quark system is separable. In our case, the two-body scattering matrix is already separable in the sense that it can be written as the product given in expression (4.7), due to the local four-point character of the considered Lagrangian (4.1). This leads to a BS-like equation for the effective baryon vertex function and can be used within the Dyson equation to obtain a computationally friendly matrix equation for the baryons. Compared to the modelling of the two-particle channels, the emerging

scattering kernel for the baryons does not have an elementary structure given in the Lagrangian and therefore has to be treated more carefully.

5.1. Dyson equation for the baryon propagator

We will begin, similar to the derivation of the dressed quark propagator in section 2.4, by introducing the full baryon propagator D_B, which can be described in leading-order as (non-interacting) propagation of three quarks denoted by $D_0 = S_i \otimes S_j \otimes S_k$. In the following discussions, we will omit the tensor structure to increase readability. In a simplified version, the corresponding Dyson equation reads

$$D_B = D_0 + D_0 K D_0 + D_0 K D_0 K D_0 + \dots \tag{5.1}$$
$$= D_0 + D_0 K D_B, \tag{5.2}$$

where K denotes the three-fermion scattering kernel, containing all two-particle irreducible graphs. Based on the approach that we neglect the three-particle irreducible graphs, the scattering kernel K is the sum over all possible two-quark interactions

$$K = k_1 + k_2 + k_3, \tag{5.3}$$

if we assume three distinguishable quarks. Then, k_i with $i \in 1,2,3$ denotes the interaction of the quarks labelled with j and k, while quark i is treated as a spectator. In particular, the k_i will be the scattering kernel of the quark-quark scattering process, introduced in the previous chapter up to an additional inverse quark propagator S_i^{-1} for the three particle space. The diquark propagator d_i fulfils its own Dyson equation,

$$d_i = D_0 + D_0 k_i d_i \tag{5.4}$$
$$= D_0 + D_0 \hat{T}_i D_0, \tag{5.5}$$

which is now defined in the three quark space. As already mentioned the diquark propagator within a three-particle Hilbert space contains an addition quark propagator S_i in the one particle subspace. One finds for the corresponding BS equation, after cutting of the external legs

$$\hat{T}_i = k_i + k_i D_0 \hat{T}_i, \tag{5.6}$$

where $\hat{T}_i = T_i \otimes S_i^{-1}$ denotes the two-body scattering matrix. This equation looks similar to the scattering matrix of the diquark channel in equation (4.6), but still

Figure 5.1. Diagrammatical representation of τ_i with reinserted leading order terms of τ_j and τ_k.

contains the contribution of the spectator quark. It is now convenient to introduce the so-called Faddeev components

$$D_i := D_0 k_i D_B \,. \tag{5.7}$$

By virtue of (5.2), (5.3) and (5.4) the Dyson equation can be expressed, cf. appendix F.1, as

$$D_B = d_i + d_i(k_j + k_k)D_B \,. \tag{5.8}$$

We found, that the three-particle Dyson equation in leading-order can be written as a two-particle propagator d_i, that contains an inverse free quark propagator in the one-particle sub-space. Using equation (5.5) and comparing the right-hand side with the right-hand side of (5.8), the Fadeev components D_i have to fulfil a set of coupled integral equations

$$D_i = D_0 \hat{T}_i D_0 + D_0 \hat{T}_i (D_j + D_k) \,. \tag{5.9}$$

Analogous to equation (5.3), the three-particle T-matrix $\tau := \tau_i + \tau_j + \tau_k$ can be defined, where only two-particle correlations are considered. After cutting off the external legs, i.e. multiply D_0^{-1} on both sides of equation (5.9), a certain T-matrix τ_i of the three particle scattering reads

$$\tau_i = \hat{T}_i + \hat{T}_i D_0 (\tau_j + \tau_k) \,. \tag{5.10}$$

Note that all quantities in the above equation are defined in a three-particle Hilbert-space. The diagrammatic representation of the expression (5.10) in figure 5.1 shows that the three-particle scattering matrix τ is a sum over connected two-body scatttering matrices $\hat{T}$, defined in a three-particle Hilbert-space. Since the three-particle matrix τ_i resembles the full scattering matrix for a 2+1 particle scattering process, the leading-order term in (5.10) can be interpreted as the non-interacting term of a two-body correlation with a third free quark within the S-matrix. Hence, the three-particle T-matrix τ can be identified with the full scattering matrix (S-matrix) within a 2+1 particle

space. Since we want to describe a baryon as a bound state of the diquark-quark scattering process, only the last term in (5.10) is of particular interest. In the following discussion we will successively develop a formalism to obtain a BS-like equation starting from the Dyson equation for the baryons where only two-particle correlations are assumed. For this purpose, it is convenient to rewrite equation (5.10) [30]

$$\tau_i = \hat{T}_i + \hat{T}_i D_0 (\tau_j + \tau_k) \tag{5.11}$$

$$= \hat{T}_i + \sum_m \tilde{Y}_{im} . \tag{5.12}$$

Here, we have introduced an operator $\tilde{Y}_{ij}$, that contains all possible interactions between the two-particle matrices $\hat{T}_i$ and $\hat{T}_j$

$$\sum_m \tilde{Y}_{im} := \hat{T}_i \sum_m Y_{im} \hat{T}_m . \tag{5.13}$$

This leads to

$$\tau_i = \hat{T}_i + \hat{T}_i \sum_m Y_{im} \hat{T}_m \tag{5.14}$$

$$= T_i S_i^{-1} + T_i S_i^{-1} \sum_m Y_{im} T_m S_m^{-1} \tag{5.15}$$

$$= T_i S_i^{-1} + T_i \sum_m S_i^{-1} Y_{im} S_m^{-1} T_m . \tag{5.16}$$

To obtain the definition equation for the quantity Y_{ij} one can insert (5.14) in (5.10) for j and k. Hence, we find

$$\hat{T}_i + \sum_m \hat{T}_i Y_{im} \hat{T}_m = \hat{T}_i + \hat{T}_i D_0 \left(\hat{T}_j + \sum_n \hat{T}_j Y_{jn} \hat{T}_n + \hat{T}_k + \sum_n \hat{T}_k Y_{kn} \hat{T}_n \right) \tag{5.17}$$

$$= \hat{T}_i + \hat{T}_i D_0 \left(\sum_m \hat{T}_m (1 - \delta_{im}) + \sum_{nn'} (1 - \delta_{in'}) \hat{T}_{n'} Y_{n'n} \hat{T}_n \right) \tag{5.18}$$

$$= \hat{T}_i + \hat{T}_i D_0 \left(\sum_m \hat{T}_m (1 - \delta_{im}) + \sum_{nn'} (1 - \delta_{in'}) \hat{T}_{n'} Y_{n'm} \hat{T}_m \right) , \tag{5.19}$$

where in the last step, the index n has been renamed to m. By comparing the l.h.s. of equation (5.17) with (5.19), Y_{im} satisfies the self-consistent equation

$$Y_{im} = D_0 (1 - \delta_{im}) + D_0 \sum_n (1 - \delta_{in}) \hat{T}_n Y_{nm} . \tag{5.20}$$

The Equation (5.16) for a certain scattering matrix τ_i is diagrammatically represented by

$$\tau_i = \boxed{\begin{array}{c} \text{T}_i \\ \end{array}}_{S_i^{-1}} + \sum_{m \neq i} \left(\boxed{\text{T}_i} \leftarrow \boxed{\text{T}_m} \right) + \ \text{\textbf{...}} , \tag{5.21}$$

where we have inserted the self-consistent equation (5.20) into (5.16). Hereby the interpretation arises that in leading-order, the quantity Y_{ij} describes the exchange of a quark between the two-particle scattering matrices T_i and T_m with $m \neq i$. Since equation (5.20) for the quantity Y_{im} is a self-consistent equation, all higher-order terms are of the same structure. To simplify the notation, we introduce $\chi_{ij} := S_i^{-1} Y_{ij} S_j^{-1}$. Thus, the equations (5.20) and (5.16) can be written in terms of χ as [30]

$$\chi_{ji} = (1 - \delta_{ijk}) S_k + \sum_{nn'} (1 - \delta_{jnn'}) S_n S_{n'} T_n \chi_{ni} \tag{5.22}$$

$$\tau_i = T_i S_i^{-1} + \sum_m T_i \chi_{im} T_m , \tag{5.23}$$

where we have used $D_0 = S_i S_j S_k$ and $\delta_{ijk} := 1$ for $i = j = k$ and zero otherwise. Equation (5.22) represents a set of coupled integral equations, which give the relation between the Faddeev components in terms of the particle-particle scattering matrix T_i. Since these matrices depend on the three-body scattering kernel k_i, cf. equation (5.6), one has to solve T_i to obtain a solution for the three-body problem. Furthermore, the Fadeev components depend on the two relative momenta between the three quarks, which significantly increases the difficulty of the problem. A commonly used simplification in QCD approaches is given by the approximation, that the particle-particle scattering matrix, that includes the three-body scattering kernel k_i, can be written as a sum over separable two-quark correlations [29]

$$iT_i = \sum_\alpha \bar{\Omega}^\alpha i t_i \Omega^\alpha . \tag{5.24}$$

Here, Ω^α denotes the vertex function of a certain two-quark correlation with flavour, colour and Dirac representation α and corresponding propagator t_i for pair (jk). The separability of the two-body contributions is based on the assumption, that the lowest lying poles in a particular three-body channel might be dominated by the two-body correlations in the kinetic regime relevant within the baryons at not too high energies [29]. However, in the NJL model with the random-phase approximation, we have already seen that the two-body correlations are separable in the sense as mentioned above. Moreover, in general approaches, the vertex function Ω is momentum dependent, while in the NJL model this does not hold as seen in the previous chapter. Then, the two-quark correlations in pole approximation are the same matrices as introduced in equation (4.7), except of a factor of two. This factor emerges from the fact that we treat indistinguishable particles, as seen in chapter 4. Nevertheless, we will call these separable correlations "diquarks". In our case, where only scalar diquarks in the two-flavour case are included the sum over the different diquark channels in equation (5.24), reduces to the contribution

$$iT_i = (\Gamma^{sad} C) i t_{sad}(q) (C \Gamma^{sad}) , \tag{5.25}$$

which is equal to the T-matrix (4.20) in the diquark discussion. As already mentioned, t_{sad} is the scalar diquark propagator given by equation (4.13). We will omit the index sad, but replace it with particle index i in the upcoming discussion.

Based on the previous discussion, the Dyson equation (5.2) thus can be brought into a form, where the leading order term is described by the free propagation of a diquark and a quark. Due to the construction of the diquarks without a third quark, this leading-order diagram meanwhile contains a quark-quark loop and hence an intermediate propagation of three quarks, which in general will not satisfy Pauli's principle.
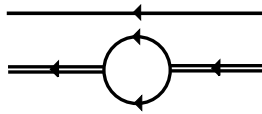

Figure 5.2. Leading-order contribution for the baryon propagator including an intermediate propagation of three quarks.

As we will see later, this problem will be solved by the exchange of a quark between the diquark and the quark, such that Pauli's principle will be restored in accordance with [31]. This quark exchange already emerges in equation (5.16) and is described by the quantity Y_{ij} in expression (5.20). We would like to emphasize at this point, that the existence of a two-quark bound state is not a necessary condition for a three-quark bound state [32]. However, it will be useful to have such a bound state in the two-quark correlations.

5.2. Momentum space representation

In this section we want to take a closer look at the momentum dependencies of the introduced quantities of the previous section. We follow more or less reference [30], but in more detail and with a slightly different notation.

In our discussion the three quarks are supposed to carry the momenta (k_1, k_2, k_3). Typically, one would assume to define a three-particle basis using these momenta. Due to the assumption of a bound state within a two-particle subsystem, it is more convenient to work in Jacobi variables, where the corresponding Jacobi momenta depend on the subsystem we want to describe. Let us disregard for a moment the

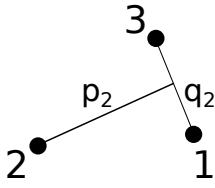colour and flavour degrees of freedom to focus on the complexity in momentum space only. For three distinguishable quarks, we have three different sets of subsystems as shown below.
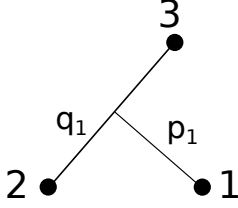
$$q_1 = \frac{1}{2}(k_2 - k_3) \tag{5.26}$$

$$p_1 = \frac{1}{2}(k_1 - (k_2 + k_3)) \tag{5.27}$$

$$q_2 = \frac{1}{2}(k_3 - k_1) \tag{5.28}$$

$$p_2 = \frac{1}{2}(k_2 - (k_3 + k_1)) \tag{5.29}$$
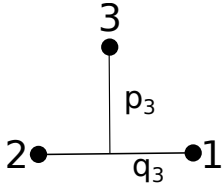
$$q_3 = \frac{1}{2}(k_1 - k_2) \tag{5.30}$$

$$p_3 = \frac{1}{2}(k_3 - (k_1 + k_2)) \tag{5.31}$$

In accordance with the notation used in the last section, we can define the Jacobi momenta as follows [30]:

$$q_i = \frac{1}{2}(k_j - k_k) \tag{5.32}$$

$$p_i = \frac{1}{2}(k_i - (k_j + k_k)) \tag{5.33}$$

Here, q_i denotes the relative momenta between the pair (jk), while p_i represents the relative momenta between the pair (jk) and particle i. The total momentum will be denoted by $P = k_i + k_j + k_k$ and is invariant under any permutation of the particle indices. Further, we find linear relations[1] between the three possible sets of the tuple (q_i, p_i)

$$q_j = -\frac{1}{2}q_i \mp \frac{3}{4}p_i \mp \frac{1}{8}P \tag{5.34}$$

$$p_j = \pm q_i - \frac{1}{2}p_i - \frac{1}{4}P. \tag{5.35}$$

---

[1]These relations are not unique in the pre-factors.

The upper sign holds for $(ij) = (12), (23)$ or (31), while the lower one will be used otherwise.

Since the momenta k_i, with $i \in (1, 2, 3)$, can be used to define a full basis in the three-particle Hilbert space by

$$\int \frac{d^4 k_1}{(2\pi)^4} \frac{d^4 k_2}{(2\pi)^4} \frac{d^4 k_3}{(2\pi)^4} |k_1 k_2 k_3\rangle \langle k_1 k_2 k_3| = \mathbb{1}, \tag{5.36}$$

a basis change to Jacobi momenta is given by

$$\begin{aligned}
\langle k_1 k_2 k_3 | p_i q_i P \rangle = & (2\pi)^4 \delta^{(4)} \left(2q_i - (k_j - k_k) \right) \times \\
& \times (2\pi)^4 \delta^{(4)} \left(2p_i - (k_i - (k_j + k_k)) \right) \times \\
& \times (2\pi)^4 \delta^{(4)} \left(P - (k_i + k_j + k_k) \right),
\end{aligned} \tag{5.37}$$

where (ijk) is a cyclic permutation of (123). We are now able to change the basis from a three particle-basis into a representation with the variables (q_i, p_i, P) defined in two-particle subsystems with spectator quark i. In the following discussion, the three-particle state in the (p, q, P) basis will be defined, but we have dropped the momentum P in the bra-ket notation, due to its invariant behaviour under particle permutations. It turns out that one and the same state of relative motion can be presented in three different ways

$$|q_1 p_1\rangle_1^{\alpha_1 \alpha_2 \alpha_3} = |q_2 p_2\rangle_2^{\alpha_2 \alpha_3 \alpha_1} = |q_3 p_3\rangle_3^{\alpha_3 \alpha_1 \alpha_2}. \tag{5.38}$$

To characterize the Dirac, flavour and colour structure for a certain particle i we introduced the index α_i. The lower index defines the subsystem and thus fixes the meaning of the momentum quantum numbers. For example, the index 1 denotes the state where particle 1 has the momentum k_1. Hence, q_1 is the relative momentum in the subsystem (23) while p_1 defines the relative momentum between particle 1 with respect to this subsystem. There exists more relations between the states in this notation. For a detailed explanation see appendix F.2.

In momentum space, based on the basis described by the two-body quantities q and p, the operator of a separable diquark scattering matrix from equation (5.25) has the expectation value

$$^{\alpha'_i \alpha'_j \alpha'_k}_{\quad i} \langle q'_i p'_i | T_i | q_i p_i \rangle_i^{\alpha_i \alpha_j \alpha_k} = (2\pi)^4 \delta^{(4)} (p'_i - p_i) \bar{\Omega}^{\alpha'_j \alpha'_k} t_i \left(\frac{1}{2} P - p_i \right) \Omega^{\alpha_j \alpha_k} \tag{5.39}$$

We can use this expectation value to obtain an operator representation for the two-body correlation besides the matrix representation. Therefore, we define the state [30]

$$|p_i\rangle_i^{\alpha_i} := \int \frac{d^4 q_i}{(2\pi)^4} \sum_{\alpha_j, \alpha_k} \Omega^{\alpha_j \alpha_k} |q_i p_i\rangle_i^{\alpha_i \alpha_j \alpha_k}, \tag{5.40}$$

which fulfils

$$
{}^{\alpha_i\alpha_j\alpha_k}_{\quad\; i}\langle q_i p_i | p_i'\rangle^{\alpha_i'}_i = (2\pi)^4 \delta^{(4)}(p_i' - p_i)\delta_{\alpha_i\alpha_i'}\Omega^{\alpha_j\alpha_k} . \tag{5.41}
$$

Hence, the operator for the two-particle T-matrix can be expressed by

$$
\hat{T}_i = \int \frac{\mathrm{d}^4 p_i}{(2\pi)^4} \sum_{\alpha_i} |p_i\rangle^{\alpha_i}_i \; {}^{\alpha_i}_i\langle p_i | t\left(\frac{1}{2}P - p_i\right) , \tag{5.42}
$$

but is not unique and one can imagine other representations. This representation, however, leads to a more or less straightforward derivation of the BS-like equation for the three-body problem. By using the operator (5.42) within equation (5.22) the matrix element

$$
X^{\beta\alpha}_{ji} := {}^{\beta}_j\langle p_j' | \chi_{ji} | p_i\rangle^{\alpha}_i \tag{5.43}
$$

$$
= \int \frac{\mathrm{d}^4 q_j'}{(2\pi)^4} \int \frac{\mathrm{d}^4 q_i}{(2\pi)^4} \bar{\Omega}^{\gamma\delta} \; {}^{\beta\gamma\delta}_{\quad\; j}\langle p_j' q_j' | \chi_{ji} | p_i q_i\rangle^{\alpha\zeta\eta}_i \Omega^{\zeta\eta} \tag{5.44}
$$

can be calculated, where a summation over the indices γ, δ, ζ and η has been suppressed for better readability. This matrix element represents the transition between a state with spectator particle i and pair (jk) to a state with spectator j and pair (ki) through a quark exchange described by the operator χ_{ji}. In other words, it can be interpreted as the scattering amplitude of a particle on a pair of particles. To obtain an expression for this scattering amplitude, we have to evaluate ${}^{\beta\gamma\delta}_{\quad\; j}\langle p_j' q_j' | \chi_{ji} | p_i q_i\rangle^{\alpha\zeta\eta}_i$, where we will use the representation of χ_{ji} of equation (5.22).

The leading-order term of equation (5.43) reads

$$
\mathcal{K}^{\beta\alpha}_{ji} := {}^{\beta}_j\langle p_j' | (1 - \delta_{ijk})S_k | p_i\rangle^{\alpha}_i \tag{5.45}
$$

$$
= (1 - \delta_{ijk}) \; {}^{\beta}_j\langle p_j' | S_k | p_i\rangle^{\alpha}_i \tag{5.46}
$$

$$
= (1 - \delta_{ijk}) \int \frac{\mathrm{d}^4 q_j'}{(2\pi)^4} \int \frac{\mathrm{d}^4 q_i}{(2\pi)^4} \bar{\Omega}^{\gamma\delta} \; {}^{\beta\gamma\delta}_{\quad\; j}\langle p_j' q_j' | S_k | p_i q_i\rangle^{\alpha\zeta\eta}_i \Omega^{\zeta\eta} . \tag{5.47}
$$

Since the states $|p_i\rangle^{\alpha}_i$ are a complete orthonormal basis in the three-particle momentum space, the emerging matrix element can be evaluated by virtue of relation (5.38). Using the completeness of the states $|p, q\rangle$, we find

$$
{}^{\beta\gamma\delta}_{\quad\; j}\langle p_j' q_j' | S_k | p_i q_i\rangle^{\alpha\zeta\eta}_i = {}^{\beta\gamma\delta}_{\quad\; j}\langle p_j' q_j' | S_k | p_j q_j\rangle^{\zeta\eta\alpha}_j \tag{5.48}
$$

$$
= (2\pi)^8 \delta^{(4)}(q_j' - q_j)\delta^{(4)}(p_j' - p_j)\delta_{\delta\alpha}\delta_{\beta\zeta} S^{\gamma\eta}_k\left(\frac{1}{4}P - q_i - \frac{1}{2}p_i\right) , \tag{5.49}
$$

where we assumed an even permutation (ijk) of (123) to permute the upper Greek indices. In case of an odd permutation the momentum dependence of the quark

propagator S_k will be the same as above, except for an index change from i to j. In order to express the momentum k_k dependency of the quark propagator in terms of (q, p), we have used the inverse relations of (5.32) and (5.33), respectively. Due to the delta distribution and Kronecker delta, the (omitted) sums as well as the integral in (5.47) simplify to

$$\mathcal{K}_{ji}^{\beta\alpha}(p_j', p_i) = (1 - \delta_{ijk}) \int \mathrm{d}^4 q_i \delta^{(4)}(p_j' - p_j) \bar{\Omega}^{\gamma\alpha} S_k^{\gamma\eta} \left(\frac{1}{4}P - q_i - \frac{1}{2}p_i\right) \Omega^{\beta\eta}. \tag{5.50}$$

Now, we can use expressions (5.34) and (5.35) to express the momentum dependence of S_k in terms of p_j' and p_i

$$\mathcal{K}_{ji}^{\beta\alpha}(p_j', p_i) = (1 - \delta_{ijk}) \int \mathrm{d}^4 q_i \delta^{(4)}(p_j' - p_j) \bar{\Omega}^{\gamma\alpha} S_k^{\gamma\eta} \left(\frac{1}{4}P - q_i - \frac{1}{2}p_i\right) \Omega^{\beta\eta} \tag{5.51}$$

$$= (1 - \delta_{ijk}) \bar{\Omega}^{\gamma\alpha} S_k^{\gamma\eta} \left(-p_i - p_j'\right) \Omega^{\beta\eta}. \tag{5.52}$$

At this point, we can already see, that this term can be interpreted as the interaction kernel of the diquark-quark scattering process. Compared to the scattering kernels introduced in previous sections, i.e. for mesons (3.9) and diquarks (4.3) respectively, the scattering kernel for the diquark-quark scattering has an explicit momentum dependence. Later, we will take a closer look at the diquark-quark scattering kernel to evaluate it in flavour- and colour-space.
The second contribution for the matrix element ${}^{\beta\gamma\delta}_{\quad j}\langle p_j' q_j' | \chi_{ji} | p_i q_i \rangle_i^{\alpha\zeta\eta}$, emerging from the second term of (5.22), reads

$$\begin{aligned}
&{}^{\beta}_{\ j}\langle p_j' | \sum_{nn'} (1 - \delta_{jnn'}) S_n S_{n'} T_n \chi_{ni} | p_i \rangle_i^{\alpha} \\
&= \sum_{nn'} (1 - \delta_{jnn'}) {}^{\beta}_{\ j}\langle p_j' | S_n S_{n'} T_n \chi_{ni} | p_i \rangle_i^{\alpha} \tag{5.53} \\
&= \sum_{nn'\beta'} (1 - \delta_{jnn'}) \int \frac{\mathrm{d}^4 \tilde{p}_n}{(2\pi)^4} {}^{\beta}_{\ j}\langle p_j' | S_n S_{n'} | \tilde{p}_n \rangle_n^{\beta'} {}^{\beta'}_{\ n}\langle \tilde{p}_n | t_n (\frac{1}{2}P - \tilde{p}_n) \chi_{ni} | p_i \rangle_i^{\alpha}, \tag{5.54}
\end{aligned}$$

where we have used (5.42). Again, we analyse the two emerging matrix elements separately: The first term gives [2]

$$\begin{aligned}
{}^{\beta}_{\ j}\langle p_j' | S_n S_{n'} | \tilde{p}_n \rangle_n^{\beta'} &= \int \frac{\mathrm{d}^4 q_j'}{(2\pi)^4} \int \frac{\mathrm{d}^4 \tilde{q}_n}{(2\pi)^4} \bar{\Omega}^{\gamma'\delta'} \, {}^{\beta\gamma'\delta'}_{\qquad j}\langle p_j' q_j' | S_n S_{n'} | \tilde{p}_n \tilde{q}_n \rangle_n^{\beta'\zeta'\eta'} \Omega^{\zeta'\eta'} \tag{5.55} \\
&= \int \frac{\mathrm{d}^4 q_j'}{(2\pi)^4} \int \frac{\mathrm{d}^4 \tilde{q}_n}{(2\pi)^4} \bar{\Omega}^{\gamma'\delta'} (2\pi)^8 \delta^{(4)}(p_j' - \tilde{p}_n) \delta^{(4)}(q_j' - \tilde{q}_j) \times \\
&\quad \times S_n^{\gamma'\beta'}(\frac{1}{4}P + \tilde{q}_j - \frac{1}{2}\tilde{p}_j) S_{n'}^{\delta'\zeta'}(\frac{1}{4}P - \tilde{q}_j - \frac{1}{2}\tilde{p}_j) \delta_{\beta\eta'} \Omega^{\zeta'\eta'}, \tag{5.56}
\end{aligned}$$

---

[2] Again, we suppressed the summation over the Greek indices.

where we have taken into account the relations (5.38). Hence, the delta distribution can be used to evaluate one of the integrals. After expressing the momentum dependence of the free quark propagators in terms of P and $(\tilde{p}_n, \tilde{q}_n)$ by using (5.35) with the lower sign[3] [30], we find

$$\begin{aligned}
&{}_j^\beta \langle p_j' | S_n S_{n'} | \tilde{p}_l \rangle_n^{\beta'} \\
&= \int \mathrm{d}^4 \tilde{q}_n \bar{\Omega}^{\gamma' \delta'} \delta^{(4)}(p_j' - \tilde{p}_j) S_n^{\gamma' \beta'}(\tfrac{1}{4}P + \tilde{q}_j - \tfrac{1}{2}\tilde{p}_j) S_{n'}^{\delta' \zeta'}(\tfrac{1}{4}P - \tilde{q}_j - \tfrac{1}{2}\tilde{p}_j) \Omega^{\zeta' \beta} \quad (5.57) \\
&= \int \mathrm{d}^4 \tilde{q}_n \bar{\Omega}^{\gamma' \delta'} \delta^{(4)}(q_j' - \tilde{q}_j) S_n^{\gamma' \beta'}(\tfrac{1}{2}P + \tilde{p}_n) S_{n'}^{\delta' \zeta'}(-\tilde{p}_j - \tilde{p}_n) \Omega^{\zeta' \beta} \quad (5.58) \\
&= \Omega^{\zeta' \beta} S_{n'}^{\delta' \zeta'}(-p_j' - \tilde{p}_n) \bar{\Omega}^{\gamma' \delta'} S_n^{\gamma' \beta'}(\tfrac{1}{2}P + \tilde{p}_n) \,. \quad (5.59)
\end{aligned}$$

The second matrix element of equation (5.54) leads to

$$ {}_n^{\beta'} \langle \tilde{p}_n | t_n(\tfrac{1}{2}P - \tilde{p}_l) \chi_{li} | p_i \rangle_i^\alpha = t_n(\tfrac{1}{2}P - \tilde{p}_n) X_{ni}^{\beta' \alpha}(\tilde{p}_n, p_i) \,. \quad (5.60) $$

since the diquark propagator t is just a scalar function. Moreover, the second order term in (5.44) can be expressed by the diquark-quark scattering kernel defined in equation (5.52)

$$\begin{aligned}
&{}_j^\beta \langle p_j' | \sum_{nn'} (1 - \delta_{jnn'}) S_n S_{n'} T_n \chi_{ni} | p_i \rangle_i^\alpha \\
&= \sum_{nn'} (1 - \delta_{jnn'}) \int \frac{\mathrm{d}^4 \tilde{p}_n}{(2\pi)^4} \Omega^{\zeta' \beta} S_{n'}^{\delta' \zeta'}(-p_j' - \tilde{p}_n) \bar{\Omega}^{\gamma' \delta'} S_n^{\gamma' \beta'}(\tfrac{1}{2}P + \tilde{p}_n) \times \\
&\quad \times t_n(\tfrac{1}{2}P - \tilde{p}_n) X_{ni}^{\beta' \alpha}(\tilde{p}_n, p_i) \quad (5.61) \\
&= \sum_{nn'} \int \frac{\mathrm{d}^4 \tilde{p}_n}{(2\pi)^4} \mathcal{K}_{jn'}^{\beta \gamma'}(p_j', \tilde{p}_n) S_n^{\gamma' \beta'}(\tfrac{1}{2}P + \tilde{p}_n) t_n(\tfrac{1}{2}P - \tilde{p}_n) X_{ni}^{\beta' \alpha}(\tilde{p}_n, p_i) \,. \quad (5.62)
\end{aligned}$$

Here, we have suppressed the summation over β'. Based on the assumption of an odd permutation (jnn') of (123), the latter term can be written as

$$\begin{aligned}
&{}_j^\beta \langle p_j' | \sum_{nn'} (1 - \delta_{jnn'}) S_n S_{n'} T_n \chi_{ni} | p_i \rangle_i^\alpha \\
&= \sum_n \int \frac{\mathrm{d}^4 \tilde{p}_n}{(2\pi)^4} \mathcal{K}_{jn}^{\beta \gamma'}(p_j', \tilde{p}_n) S_n^{\gamma' \eta'}(\tfrac{1}{2}P + \tilde{p}_n) t_n(\tfrac{1}{2}P - \tilde{p}_n) X_{ni}^{\beta' \alpha}(\tilde{p}_n, p_i) \,, \quad (5.63)
\end{aligned}$$

where we changed the index of the scattering kernel $\mathcal{K}$.

Combining the upper results, i.e. expressions (5.52) and (5.63), for the different terms

---

[3]This means, we assume an odd permutation of (jnn').

in (5.44), we find the self-consistent expression for $X_{ji}^{\beta\alpha}$ in momentum-space

$$
\begin{aligned}
X_{ji}^{\beta\alpha}(p_j', p_i) =& \mathcal{K}_{ji}^{\beta\alpha}(p_j', p_i) \\
&+ \sum_n \int \frac{\mathrm{d}^4 \tilde{p}_n}{(2\pi)^4} \mathcal{K}_{jn}^{\beta\gamma'}(p_j', \tilde{p}_n) S_n^{\gamma'\eta'}(\frac{1}{2}P + \tilde{p}_n) t_n(\frac{1}{2}P - \tilde{p}_n) X_{ni}^{\eta'\alpha}(\tilde{p}_n, p_i) .
\end{aligned}
$$
(5.64)

We want to emphasize at this point, that the above equation is already an effective two-body relation. It only depends on the relative momentum p between a single particle and a pair of particles. The next step is to transfer our results to identical quarks. Therefore, the corresponding transition amplitude X has to be antisymmetrised. As a consequence, the particle index n can be dropped for the quark and diquark propagators respectively, since we can not distinguish which particle has been exchanged. Thereupon, the only dependence of particle indices is given in the factor δ_{ijk}. In addition, we have to calculate the full three-particle T-matrix

$$
\tau = \sum_{i=[1,2,3]} \tau_i ,
$$
(5.65)

with τ_i from equation (5.23). We can use the definition (5.42) within expression (5.65) to obtain an operator representation of τ

$$
\begin{aligned}
\hat{\tau} =& \sum_i \int \frac{\mathrm{d}^4 p}{(2\pi)^4} \sum_\alpha |p\rangle_i^\alpha {}_i^\alpha\langle p| t_i \left(\frac{1}{2}P - p\right) S_i^{-1} \\
&+ \sum_{ij} \int \frac{\mathrm{d}^4 p}{(2\pi)^4} \int \frac{\mathrm{d}^4 p'}{(2\pi)^4} \sum_{\alpha\beta} |p\rangle_i^\alpha t_i \left(\frac{1}{2}P - p\right) X_{ij}^{\alpha\beta} t_j \left(\frac{1}{2}P - p'\right) {}_j^\beta\langle p'| .
\end{aligned}
$$
(5.66)

Now, we put this between antisymmetric states (characterized with index $\mathcal{A}$) in the three-particle Hilbert-space [30]

$$
|k_1 k_2 k_3\rangle_{\mathcal{A}}^{\alpha_1\alpha_2\alpha_3} = \sqrt{3!}\,\mathcal{A}|k_1 k_2 k_3\rangle
$$
(5.67)

$$
= \frac{1}{\sqrt{3!}} \sum_i \left(|q_i p_i\rangle_l^{\alpha_i\alpha_j\alpha_k} - |-q_i p_i\rangle_l^{\alpha_i\alpha_k\alpha_j} \right) ,
$$
(5.68)

with arbitrary index l. Here, the operator $\mathcal{A} := \frac{1}{3!}\sum_\pi \mathrm{sign}(\pi)\mathcal{P}_\pi$ is Hermitian, idempotent and ensures that the resulting state is antisymmetric under odd permutations of (123). For fixed index i, we suppose (ijk) to be an even permutation of (123). Hence,

we find for the matrix element

$$_{\mathcal{A}}^{\alpha_1'\alpha_2'\alpha_3'}\langle k_1'k_2'k_3'|\tau|k_1k_2k_3\rangle_{\mathcal{A}}^{\alpha_1\alpha_2\alpha_3}$$

$$= \sum_i \int \frac{\mathrm{d}^4p}{(2\pi)^4} \sum_\alpha {}_{\mathcal{A}}^{\alpha_1'\alpha_2'\alpha_3'}\langle k_1'k_2'k_3'|p\rangle_i^{\alpha}{}_i^{\alpha}\langle p|S_i^{-1}|k_1k_2k_3\rangle_{\mathcal{A}}^{\alpha_1\alpha_2\alpha_3} t_i\left(\frac{1}{2}P - p\right)$$

$$+ \sum_{i=j} \int \frac{\mathrm{d}^4p}{(2\pi)^4} \int \frac{\mathrm{d}^4p'}{(2\pi)^4} \sum_{\alpha\beta} {}_{\mathcal{A}}^{\alpha_1'\alpha_2'\alpha_3'}\langle k_1'k_2'k_3'|p\rangle_i^{\alpha} t_i\left(\frac{1}{2}P - p\right) X_{ij}^{\alpha\beta} t_j\left(\frac{1}{2}P - p'\right)_j^{\beta}\langle p'|k_1k_2k_3\rangle_{\mathcal{A}}^{\alpha_1\alpha_2\alpha_3}$$

$$+ \sum_{i\neq j} \int \frac{\mathrm{d}^4p}{(2\pi)^4} \int \frac{\mathrm{d}^4p'}{(2\pi)^4} \sum_{\alpha\beta} {}_{\mathcal{A}}^{\alpha_1'\alpha_2'\alpha_3'}\langle k_1'k_2'k_3'|p\rangle_i^{\alpha} t_i\left(\frac{1}{2}P - p\right) X_{ij}^{\alpha\beta} t_j\left(\frac{1}{2}P - p'\right)_j^{\beta}\langle p'|k_1k_2k_3\rangle_{\mathcal{A}}^{\alpha_1\alpha_2\alpha_3},$$

$$(5.69)$$

where we already separated the sums. The primed quantities in the upper relation denote properties of the outgoing state.

The leading-order term in the above equation is equal for all i except for the expectation value of the inverse quark-propagator, which depends on the index l within the antisymmetric state. Anyway, we can choose an arbitrary index and multiply the result with a factor of three but have to take care of the inverse quark propagator. An analogous argument holds for the second term. For the last contribution an extra factor of two arises from the fact that $X_{ij} = X_{ik}$ holds. Summarised, we find

$$_{\mathcal{A}}^{\alpha_1'\alpha_2'\alpha_3'}\langle k_1'k_2'k_3'|\tau|k_1k_2k_3\rangle_{\mathcal{A}}^{\alpha_1\alpha_2\alpha_3}$$

$$= 3 \int \frac{\mathrm{d}^4p}{(2\pi)^4} \sum_\alpha {}_{\mathcal{A}}^{\alpha_1'\alpha_2'\alpha_3'}\langle k_1'k_2'k_3'|p\rangle_1^{\alpha}{}_1^{\alpha}\langle p|S_l^{-1}|k_1k_2k_3\rangle_{\mathcal{A}}^{\alpha_1\alpha_2\alpha_3} t_1\left(\frac{1}{2}P - p\right)$$

$$+ 3 \int \frac{\mathrm{d}^4p}{(2\pi)^4} \int \frac{\mathrm{d}^4p'}{(2\pi)^4} \sum_{\alpha\beta} \left({}_{\mathcal{A}}^{\alpha_1'\alpha_2'\alpha_3'}\langle k_1'k_2'k_3'|p\rangle_1^{\alpha} t_1\left(\frac{1}{2}P - p\right) X_{11}^{\alpha\beta} t_1\left(\frac{1}{2}P - p'\right)_1^{\beta}\langle p'|k_1k_2k_3\rangle_{\mathcal{A}}^{\alpha_1\alpha_2\alpha_3} \right.$$

$$\left. + {}_{\mathcal{A}}^{\alpha_1'\alpha_2'\alpha_3'}\langle k_1'k_2'k_3'|p\rangle_1^{\alpha} t_1\left(\frac{1}{2}P - p\right) 2X_{12}^{\alpha\beta} t_2\left(\frac{1}{2}P - p'\right)_2^{\beta}\langle p'|k_1k_2k_3\rangle_{\mathcal{A}}^{\alpha_1\alpha_2\alpha_3} \right). \qquad (5.70)$$

Thus, we have to evaluate the matrix element $_1^{\alpha}\langle p|S_i^{-1}|k_1k_2k_3\rangle_{\mathcal{A}}^{\alpha_1\alpha_2\alpha_3}$ and elements of the form $_{\mathcal{A}}^{\alpha_1'\alpha_2'\alpha_3'}\langle k_1'k_2'k_3'|p\rangle_1^{\alpha}$. By using expression (5.68) for the antisymmetric state and (5.41) a straight forward calculation with $l = 1$ yields

$$_{\mathcal{A}}^{\alpha_1'\alpha_2'\alpha_3'}\langle k_1'k_2'k_3'|p\rangle_1^{\alpha} = \frac{1}{\sqrt{6}} \sum_i \left({}_1^{\alpha_i'\alpha_j'\alpha_k'}\langle q_i p_i|p\rangle_1^{\alpha} - {}_1^{\alpha_i'\alpha_j'\alpha_k'}\langle -q_i p_i|p\rangle_1^{\alpha} \right) \qquad (5.71)$$

$$= \frac{1}{\sqrt{6}} \sum_i (2\pi)^4 \delta^{(4)}(p - p_i)\delta_{\alpha_i'\alpha}\left(\Omega^{\alpha_j'\alpha_k'} - \Omega^{\alpha_k'\alpha_j'} \right) \qquad (5.72)$$

$$= \begin{cases} 0 & \text{for } \Omega^{\alpha_j'\alpha_k'} \text{ totally symmetric} \\ \frac{2}{\sqrt{6}} \sum_i (2\pi)^4 \delta^{(4)}(p - p_i)\delta_{\alpha_i'\alpha}\Omega^{\alpha_j'\alpha_k'} & \text{for } \Omega^{\alpha_j'\alpha_k'} \text{ totally antisymmetric} \end{cases}.$$

$$(5.73)$$

For the other matrix element a similar calculation yields

$$
{}_1^\alpha \langle p | S_l^{-1} | k_1 k_2 k_3 \rangle_{\mathcal{A}}^{\alpha_1 \alpha_2 \alpha_3}
$$

$$
= \begin{cases} 0 & \text{for } \bar{\Omega}^{\alpha_m \alpha_n} \text{ totally symmetric} \\ \frac{2}{\sqrt{6}} \sum_l (2\pi)^4 \delta^{(4)}(p - p_i) \bar{\Omega}^{\alpha_m \alpha_n} S_l^{-1}(\frac{1}{2} P + p_l) & \text{for } \bar{\Omega}^{\alpha_m \alpha_n} \text{ totally antisymmetric} \end{cases} ,
$$

$$ \tag{5.74} $$

where (lmn) is an even permutation of (123). For a totally symmetric diquark vertex function $\Omega^{\alpha\beta}$ the matrix element (5.70) vanishes. A analogous behaviour already occurs in the diquark discussion, cf. section 4.1, for the diquark scattering matrix. This is not surprising, since the three quarks which constitute the baryon are fermions and hence have to fulfil Pauli's principle. In section 5.6 we will see, how to project the vertex functions onto a physical nucleon state in colour and flavour space.

According to the fact that only antisymmetric diquark vertices give a contribution, it is convenient to introduce [30]

$$
X^{\beta\alpha}(p', p) := \frac{1}{6} \sum_{ij} X_{ji}^{\beta\alpha}(p', p) , \tag{5.75}
$$

which determines the full three-particle scattering matrix, when sandwiched between totally antisymmetric states. This quantity is often called baryon wave function. It is easy to see that the baryon wave function (5.75) fulfils

$$
X^{\beta\alpha}(p', p) = \mathcal{K}^{\beta\alpha}(p', p)
$$

$$
+ \int \frac{\mathrm{d}^4 p''}{(2\pi)^4} \mathcal{K}^{\beta\gamma}(p', p'') S^{\gamma\delta}(\frac{1}{2} P + p'') t(\frac{1}{2} P - p'') X^{\delta\alpha}(p'', p) . \tag{5.76}
$$

It follows that the matrix element (5.70), by virtue of equations (5.73) and (5.74), reads [30]

$$
{}_{\mathcal{A}}^{\alpha_1' \alpha_2' \alpha_3'} \langle k_1' k_2' k_3' | \tau | k_1 k_2 k_3 \rangle_{\mathcal{A}}^{\alpha_1 \alpha_2 \alpha_3}
$$

$$
= \sum_{(ijk),(lmn)} (2\pi)^4 \delta^{(4)}(p_l - p_i') \Omega^{\alpha_j' \alpha_k'} t(\frac{1}{2} P - p_l) \bar{\Omega}^{\alpha_m \alpha_n} S_{\alpha_i \alpha_l}^{-1}(\frac{1}{2} P + p_l)
$$

$$
+ \sum_{(ijk),(lmn)} \Omega^{\alpha_j' \alpha_k'} t(\frac{1}{2} P - p_i') X^{\alpha_i' \alpha_l}(p_i', p_l) t(\frac{1}{2} P - p_l) \bar{\Omega}^{\alpha_m \alpha_n} , \tag{5.77}
$$

with (ijk) and (lmn) are assumed to be even permutations of (123). The emerging factors of two in front of the diquark propagators in equation (5.70) have been absorbed to obtain the propagator for indistinguishable quarks, as treated in chapter 4. In this context, note that the diquark propagator in equation (5.70) still contains an index as expected for distinguishable quarks.

We have now reached a point where we have derived a BS-like equation for the determination of baryons within the NJL model, that only depends on an effective 2+1 interaction kernel. We can identify the self-consistent equation (5.76) with the BS equation for the diquark-quark scattering process and hence in certain ways with the baryon propagator itself. The corresponding diagrammatic representation is given in figure 5.3.

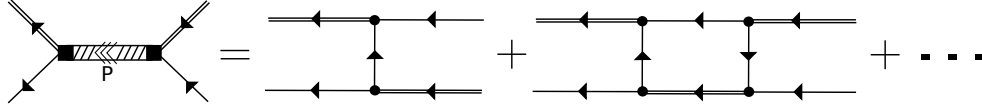Solving equation (5.76) for the baryon wave function $X^{\beta\alpha}$ and insert the result into

Figure 5.3. Diagrammatic representation of the Bethe-Salpeter equation for diquark-quark scattering.

(5.77) provides the solution of the three-body problem. Moreover, we note that the leading order term of equation (5.77) is related to a free propagation of a diquark and quark, while the following term describes the scattering of these two particles. We have already mentioned in the previous section that the T-matrix in the three-particle Hilbert space becomes the S-matrix in a 2+1 particle subspace.

For the upcoming discussion, it is practical to rewrite equation (5.76) into a matrix equation in the (two-dimensional) diquark-quark Hilbert-space. Therefore, we have to distinguish between the quarks and diquarks in colour and flavour space.

In order to go back to our notation in the meson and diquark chapter, with bared and non-bared Latin indices we take a closer look to the kernel $\mathcal{K}$

$$\mathcal{K}^{\beta\alpha}(p',p) = \quad \overset{\Omega^{\gamma\alpha}}{\underset{\bar{\Omega}^{\beta\eta}}{\mid S^{\gamma\eta}(\text{-p-p'})}} \quad = \bar{\Omega}^{\gamma\alpha} S^{\gamma\eta}\left(-p-p'\right)\Omega^{\beta\eta}. \tag{5.78}$$

If we consider the diquark vertices defined in chapter 4.1 (equation (4.7)) for the scalar diquarks, we find

$$\bar{\Omega}^{\gamma\alpha} = (\Gamma^D C)_{\gamma\alpha} = (i\gamma_5 C)_{\gamma\alpha} \otimes (\lambda_A)_{\gamma\alpha} \otimes (\tau_m)_{\gamma\alpha}. \tag{5.79}$$

Since we only assume the up and down quarks in our discussion, the (antisymmetric) second Pauli matrix describes the structure in flavour space. After introducing a new (upper) composite bared index $\bar{a} = (A, m = 2)$ that characterises the diquark channel and using the notation with non-bared Latin letters for the quarks as in the previous chapters we can rewrite (5.76) into

$$X^{\bar{a}\bar{b}}_{ij}(p',p) = \mathcal{K}^{\bar{a}\bar{b}}_{ij}(p',p)$$
$$+ \int \frac{\mathrm{d}^4 p''}{(2\pi)^4} \mathcal{K}^{\bar{a}\bar{b}'}_{ij'}(p',p'') S_{j'}(\tfrac{1}{2}P + p'') t^{\bar{b}'}(\tfrac{1}{2}P - p'') X^{\bar{b}'\bar{b}}_{j'i}(p'',p). \tag{5.80}$$

Note that these indices do not correspond to a certain particle any more. More precisely, they are related to the introduced Greek indices at the beginning of this section.
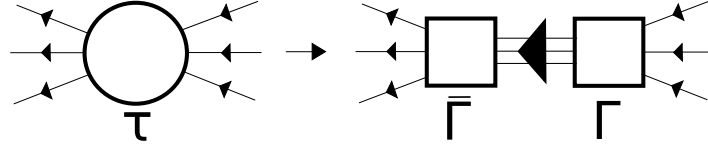
5.3. Vertex structure

Figure 5.4.   Seperation of the baryon T-matrix near the pole.

As already mentioned, equation (5.80) describes the scattering of a (bound) particle pair on a single particle. Since quarks are the degrees of freedom in the NJL model, the corresponding baryon vertex Γ with external propagators takes the form shown on the l.h.s. of figure 5.4.

Near its poles, the three-particle scattering matrix (5.65) can be written in pole-approximation as [30]

$$\tau = \frac{\bar{\Gamma}\Gamma}{P^2 - m_B^2 + i\epsilon}\,,\tag{5.81}$$

for $P^2 \longrightarrow m_B^2$. With the upper ansatz, the baryon wave function $X^{\alpha'_i \alpha_l}$ in equation (5.77) should separate as well, which leads to the vertex function Γ

$$\Gamma^{\alpha_1\alpha_2\alpha_3}(k_1, k_2, k_3) = \sum_{(lmn)} X^{\alpha_l}(p_l)t(\tfrac{1}{2}P - p_l)\bar{\Omega}^{\alpha_m\alpha_n}\,.\tag{5.82}$$

In accordance with the discussion in the previous section, the three-particle vertex Γ can be expressed by an effective 2+1 particle vertex, cf. figure 5.5. Note, that the
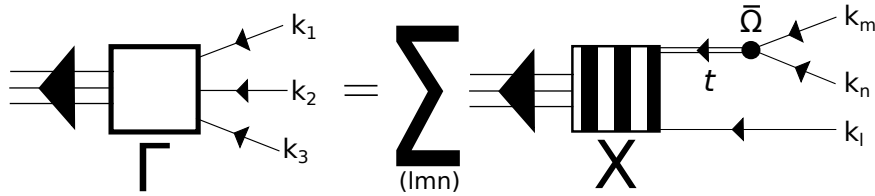

Figure 5.5.   Diagrammatical representation of the baryon vertex with external legs.

diquark vertex $\bar{\Omega}$ has been assumed to be antisymmetric in the upper Greek indices to obtain a non-vanishing scattering matrix. This leads to an antisymmetrized behaviour

of the baryon vertex Γ, too. The effective 2+1 particle vertex function $X^{\alpha_i}(p_i)$ fulfils, with the notation provided in the previous section, the homogeneous version of the BS equation [25]

$$\left(X_i^{\bar{a}}(p', P) - \int \frac{\mathrm{d}^4 p''}{(2\pi)^4} \mathcal{K}_{ij'}^{\bar{a}\bar{b}'}(p', p'') S_{j'}(\frac{1}{2}P + p'') t^{\bar{b}'}(\frac{1}{2}P - p'') X_{j'}^{\bar{b}'}(p'') \right) \Bigg|_{P^2 = m_B^2} = 0$$

(5.83)

and can be, more or less, directly read off the second term in equation (5.77). Hence, we can use this homogeneous BS equation to determine the bound state of three particles in the NJL model. An other possible way to obtain an analogous description of the baryons is to identify the baryon wave function $X_{ij}^{\bar{a}\bar{b}}(p', p)$ from the previous section with the full scattering matrix T of a diquark-quark scattering process, like in the meson and diquark channel, respectively. Thus, the denominator of the propagator at on-shell mass has to be evaluated. In case of the inhomogeneous BS equation, we have to solve the self-consistent expression (5.80) for $X_{ij}^{\bar{a}\bar{b}}(p', p)$. The difference between equation (5.83) and (5.80) lies in the kind of physical object. Equation (5.80) describes the complete scattering matrix with outgoing ($\bar{a}$ and i) and incoming ($\bar{b}$ and j) diquarks and quarks. By solving this expression for the baryon wave function we obtain a pole structure, which will be compared to the ansatz (5.81). In order to obtain the mass of the corresponding bound state, we have to evaluate the result at the on-shell condition $P^2 = m_B^2$.

Meanwhile, in equation (5.83) we start directly from the ansatz (5.81) and split the T-matrix (5.80) into two vertex functions $X_i^{\bar{a}}(p')$ based on the behaviour near the three-body bound state. These vertex functions only have one quark and diquark index since the "outgoing" quantity is a certain baryon propagator. Moreover, the vertex (5.83) only depends on the relative momentum p of the external quark and diquark.

For the sake of simplicity, we will use equation (5.83) to determine the mass of the baryon. We would like to emphasize at this point that in fact the quantities within equation (5.83) represents matrix elements due to the indices. However, these matrix elements will be treated as representative for the corresponding matrices in order to improve the understanding of the complete expression.

5.4. Baryon masses

To obtain the baryon mass we have to find the root of the matrix equation

$$\left(X_i^{\bar{a}}(p',P) - \int \frac{\mathrm{d}^4 p''}{(2\pi)^4} \mathcal{K}_{ij'}^{\bar{a}\bar{b}'}(p',p'') \mathcal{D}_{j'}^{\bar{b}'}(P,p'') X_{j'}^{\bar{b}'}(p'',P) \right) \Bigg|_{P^2=m_B^2} = 0. \tag{5.84}$$

Here, the elementary interaction $\mathcal{K}(p',p)$, introduced in equation (5.47), is given by

$$\mathcal{K}_{ji}^{\bar{a}\bar{b}}(p,p') := \quad \underset{(\Gamma^D C)_{jx}^{\bar{b}}}{\overset{(C\Gamma^D)_{xi}^{\bar{a}}}{\big|}} S_x(\text{-}\mathsf{p'}\text{-}\mathsf{p}) \quad = (\Gamma^D C)_{jx}^{\bar{b}} S_x(-p'-p)(C\Gamma^D)_{xi}^{\bar{a}}, \tag{5.85}$$

and represents the exchange of a quark with colour and flavour index x and four momentum $p' + p$. [4] The leading-order term of the Dyson equation, the (free) propagation of the corresponding quark and diquark, is denoted by

$$i\mathcal{D}_{j'}^{\bar{b}'}(P,p) := \quad \overset{it_{\bar{b}'}(P/2-p)}{\underset{iS_{j'}(P/2+p)}{\Longleftarrow}} \quad = -iS_{j'}(\tfrac{P}{2} - p)it^{\bar{b}'}(\tfrac{P}{2} + p). \tag{5.86}$$

As already mentioned, we will assume the diquarks to be in an antisymmetric state in colour and flavour space. This leads to the possible interpretation, that the diquark in a baryon plays the role of the antiquarks in the discussion of the mesonic spectrum.[5] Then, the kernel K of the interaction, can be interpreted as the combination of the free propagation of the baryon constituents with the elementary interaction $\mathcal{K}$

$$iK_{ij}^{\bar{a}\bar{b}}(p,p',P) := \mathcal{K}_{ji}^{\bar{a}\bar{b}}(p,p') \mathcal{D}_i^{\bar{b}}(P,p') \tag{5.87}$$

and is shown in figure 5.6.[6] To obtain a computable expression for the baryon masses, we can rewrite equation (5.84)

$$\int \frac{\mathrm{d}^4 p''}{(2\pi)^4} X_i^{\bar{a}}(p'',P)\delta^{(4)}(p''-p') - \int \frac{\mathrm{d}^4 p''}{(2\pi)^4} K_{ij'}^{\bar{a}\bar{b}'}(p',p'',P) X_{j'}^{\bar{b}'}(p'',P) \right) \Bigg|_{P^2=m_B^2} = 0 \tag{5.88}$$

$$\Rightarrow \int \frac{\mathrm{d}^4 p''}{(2\pi)^4} \left(\delta^{(4)}(p''-p')\delta^{\bar{b}'\bar{a}}\delta_{j'i} - K_{ij'}^{\bar{a}\bar{b}'}(p',p'',P) \right) X_{j'}^{\bar{b}'}(p'',P) \Bigg|_{P^2=m_B^2} = 0. \tag{5.89}$$

---

[4]We do not define a new momentum for the sum $p + p'$, since we want to maintain the p-dependence of this quantity for the further discussion.

[5]This is the reason we choose bared indices for the diquarks.

[6]The propagators on the l.h.s of the figure are added for illustrative purposes.
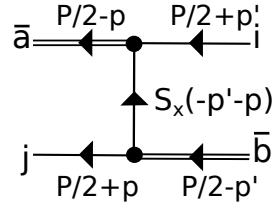
Figure 5.6.   Interaction kernel of the diquark-quark scattering.

Basically this equation describes an eigenvalue problem with eigenvalue zero for the on-shell condition. Therefore, we have to solve

$$\det\left(\mathbb{1}_{\text{Dirac}}\delta^{\bar{b}'\bar{a}}\delta_{j'i} - \int \frac{\mathrm{d}^4 p''}{(2\pi)^4}\, K_{ij'}^{\bar{a}\bar{b}'}(p',p'',P)\right)\Bigg|_{P^2=m_B^2} = 0\,. \tag{5.90}$$

Due to the p'' dependency of the interaction kernel $\mathcal{K}_{ij'}^{\bar{a}\bar{b}'}(p',p'')$ within the kernel $K(p',p'',P)$, the integration over p'' is a non-trivial task. In the upcoming chapter, we will see that applying an adequate approximation leads to a further simplification of equation (5.90). This allows us to perform the integration over the momentum p'' within the second term to obtain a quantity, which can be interpreted as a baryon polarisation loop, composed by a quark and a diquark. In addition, the remaining dependency of p' in the upper equation will disappear in this approximation. Before we evaluate the determinant in equation (5.90), the corresponding matrix within will be investigated.

5.5. Scattering kernel and static approximation

As already mentioned, the exchange of a quark is the elementary interaction for the diquark-quark scattering in order to ensure the Pauli exclusion principle. Then the interaction kernel can be expressed through (5.87) and is diagrammatically represented in figure 5.6. Basically, this kernel describes a quark exchange between two quark-quark scattering matrices. The emerging vertices in this Feynman diagram are the same vertices, cf. equation (4.12), as in the description of the diquark scattering matrix. A commonly used simplification of the scattering kernel, and thus for the Faddeev equation itself, is the static approximation [33]. Here the momentum dependence of the exchange quark is completely neglected by assuming that the mass of the quark is much larger than the typical momentum exchange. It follows that the (dressed) quark
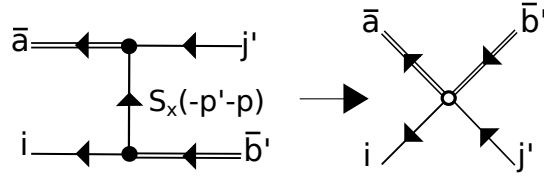
Figure 5.7. Visualisation of the static approximation for the baryonic scattering kernel.

propagator reduces to

$$iS_x(-p' - p) = i(-\not{p}' - \not{p} - M_x)^{-1} \to -i\frac{1}{M_x}\mathbb{1}\,,\tag{5.91}$$

which is illustrated for the kernel (5.87) in figure 5.7. The estimated uncertainty of this approximation, for the baryon masses in case of vanishing temperature and chemical potential, is about 5%, as discussed in [34]. The vertex structure of the baryons thus reduces in the case of the static approximation and only considering scalar diquarks to a momentum independent vertex function, that can be treated similar to the mesons and diquarks. Applying the static approximation to the integral kernel in equation (5.90), leads to

$$\det\left(\delta^{BB'} - \int \frac{\mathrm{d}^4 p''}{(2\pi)^4}\,\mathcal{K}^{\bar{a}\bar{b}'}_{ij'}\mathcal{D}^{\bar{b}'}_{j'}(P, p'')\right)\Bigg|_{P^2 = m_B^2} = 0 \tag{5.92}$$

where the elementary interaction is no longer momentum dependent. Here, the Kronecker-delta $\delta^{BB'} := \mathbb{1} \otimes \delta^{\mathrm{colour}}_{j'i}\delta^{\mathrm{colour}}_{\bar{b}'\bar{a}} \otimes \delta^{\mathrm{flavour}}_{j'i}\delta^{\mathrm{flavour}}_{\bar{b}'\bar{a}}$ denotes a certain baryon channel. The corresponding matrix of this eigenvalue problem can now be reduced to

$$\delta^{BB'} - \int \frac{\mathrm{d}^4 p''}{(2\pi)^4}\,\mathcal{K}^{\bar{a}\bar{b}'}_{ij'}\mathcal{D}^{\bar{b}'}_{j'}(P, p'') = \delta^{BB'} + i\frac{1}{M_x}\int \frac{\mathrm{d}^4 p''}{(2\pi)^4}\,\mathcal{D}^{\bar{b}'}_{j'}(P, p'')\,.\tag{5.93}$$

We can now insert expression (5.85) for the elementary interaction and (5.86) as the free quark and diquark propagator to obtain

$$\det\left(\delta^{BB'} + \frac{1}{M_x}\int \frac{\mathrm{d}^4 p''}{(2\pi)^4}\,(C\Gamma^D)^{\bar{a}}_{xj'}(\Gamma^D C)^{\bar{b}'}_{ix}S_{j'}(\frac{P}{2} - p'')it^{\bar{b}'}(\frac{P}{2} + p'')\right)\Bigg|_{P^2 = m_B^2} = 0\,.\tag{5.94}$$

The coupling constant of the baryonic channel can be read off directly. By comparing the upper equation with the propagators obtained in the meson or diquark channel, i.e. (3.22) and (4.13), leads to the assumption, that an appropriate Lagrangian for the baryons within the NJL model, as a diquark-quark bound state, should have a coupling-constant in the order of the inverse quark mass. Moreover, we note in this

explicit representation of the BS equation for the baryon that the complete baryonic channel only depends on the structure of the related diquark vertices.

The (general) vertex structure of the diquarks in this equation, meanwhile, is given by

$$(\Gamma^D C)_{ix}^{\bar{b}'} (C\Gamma^D)_{xj'}^{\bar{a}} = (\Delta^D C)_{ix} (C\Delta^D)_{xj'} \otimes \lambda_{ix}^{\bar{b}'} \lambda_{xj'}^{\bar{a}} \otimes \tau_{ix}^{\bar{b}'} \tau_{xj'}^{\bar{a}} \, , \qquad (5.95)$$

where Δ^D denotes a certain diquark (spin-)channel, cf. chapter 2.

5.6. Baryon projection

In order to obtain a description for the baryons emerging in nature, we have to project the matrix of the eigenvalue problem (5.94) onto physical states. For this purpose, projectors can be defined for certain spaces. As already stated, we want to describe baryons, which only include scalar diquarks, for which the structure in colour and flavour space is fully antisymmetric. In Dirac space we find

$$(\Delta^D C)(C\Delta^D) = -\Delta^D \Delta^D \, , \qquad (5.96)$$

where for the scalar diquarks $\Delta^D = i\gamma_5$ holds. The Dirac structure of a certain baryon therefore is given by the third quark. The contribution of pseudoscalar diquarks, i.e. $\Delta^D = \mathbb{1}$, in the modelling of the baryon will be neglected in accordance with the discussion provided in chapter 4.

The representation in colour space meanwhile can be expressed through an antisymmetric tensor as shown in appendix B.2. In the following, the bared indices run from 1 to 3 and denote the antisymmetric Gell-Mann matrices. This notation leads to

$$\lambda_{ix}^{\bar{a}} \lambda_{xj'}^{\bar{b}'} = i\epsilon_{ix}^{\bar{a}} i\epsilon_{xj'}^{\bar{b}'} \qquad (5.97)$$

$$= -\delta_i^{\bar{a}} \delta_{j'}^{\bar{b}'} + \delta^{\bar{a}\bar{b}'} \delta_{ij'} \, . \qquad (5.98)$$

A qualitative analysis of the kernel, shown in figure 5.6, in colour space already motivates that the first term in the above expression can be related to a singlet projector, while the last one represents the octet. Both vertices, corresponding to the incoming and outgoing diquark with (anti)colours $\bar{b}'$ and $\bar{a}$, respectively, are connected through a quark with colour index x. Hence, the first term yields both sides of figure 5.6 to be colourless.

For the second term in (5.98), the incoming and outgoing diquarks carry the same anticolour, which holds for the colour of the quarks in the scattering process as well. Overall, the state obtained by the second term is necessarily coloured, when the

incoming colours/anticolours, are not equal. As shown in appendix F.3, indeed the colour singlet and colour octet are eigenstates, of an operator related to equation (5.98). Moreover, the eigenvalue of the two multiplets have different signs. If we assume an attractive interaction in the colour-singlet state, the interaction therefore has to be repulsive in the octet channel due to the different signs. Furthermore, the singlet and octet do not mix and thus separate the expression (5.94) into these different states. Since the only observable states in nature are colour singlets, the octet channel is physically irrelevant and will be neglected. There are plenty of projectors onto singlet and octet states given in the literature, depending on the used conventions. To evaluate the baryons, as physical particles in a colour singlet state, the related projector used in this work reads

$$\mathcal{P}_{\bar{a}j}^{\text{colour},(1)} = \frac{1}{\sqrt{3}} \delta_j^{\bar{a}} \, . \tag{5.99}$$

For the colour singlet projector, we obtain for the first term in (5.94)

$$(\mathcal{P}_{\bar{a}j'}^{\text{colour},(1)})^\dagger \delta^{BB'} \mathcal{P}_{\bar{b}'i}^{\text{colour},(1)} = \frac{1}{3} \delta_{ij'}^{\text{colour}} \delta_{\bar{a}\bar{b}'}^{\text{colour}} \delta_{j'}^{\bar{a}} \delta_i^{\bar{b}'} \tag{5.100}$$

$$= \frac{1}{3} \text{tr} \left(\mathbb{1}_{\text{c}} \right) = 1 \, , \tag{5.101}$$

while for the integral term

$$(\mathcal{P}_{\bar{a}j'}^{\text{colour},(1)})^\dagger \lambda_{ix}^{\bar{a}} \lambda_{xj'}^{\bar{b}'} \mathcal{P}_{\bar{b}'i}^{\text{colour},(1)} = \frac{1}{3} i\epsilon_{ix}^{\bar{a}} i\epsilon_{xj'}^{\bar{b}'} \delta_{j'}^{\bar{a}} \delta_i^{\bar{b}'} = -\frac{1}{3} \epsilon_{ix}^{j'} \epsilon_{xj'}^{i} = -2 \tag{5.102}$$

holds.

https://de.wikipedia.org/wiki/Levi-Civita-Symbol The structure in flavour space is just given by the second Pauli matrix, since it is the only antisymmetric matrix for the $SU(2)$ representation. Due to the consideration of the isospin limit, for which the mass of up and down quarks are equal,https://de.wikipedia.org/wiki/Levi-Civita-Symbol the proton and neutron are degenerate in flavour space. Furthermore, since we cannot distinguish between the up and down quark in flavour space the indices of the mass M_x of the exchange quark as well as the free quark propagator $S_{j'}$ in equation (5.94) can be omitted. The structure in flavour space of the baryons therefore reduces to an identity with indices ij'. In detail, equation (5.93) thus represents a diagonal matrix in the two-flavour case due to the second Pauli matrix. Hence, the proton and neutron states do not mix, as expected. For three flavours and different masses for non-strange and strange quarks, off-diagonal elements will appear in matrix (5.94), which are related to the $\Sigma^0 - \Lambda$ mixing, such that a coupled set of equations has to be solved [25].

5.7. Dirac-like equation for the nucleon

Using the results from the previous section, the eigenvalue problem in equation (5.94) in Dirac-space takes the form

$$\det\left(\mathbb{1} - \frac{2}{M}\int\frac{\mathrm{d}^4 p''}{(2\pi)^4}\,S(\frac{P}{2}+p'')it_{sad}(\frac{P}{2}-p'')\right)\Bigg|_{q^2=m_B^2} = 0\,, \qquad (5.103)$$

where t_{sad} denotes the scalar antitriplet diquark propagator discussed in chapter 4.1. In the following steps, we want to rewrite equation (5.103), which already looks like a Dirac equation, to a more familiar form. Therefore, it is useful to define the nucleon polarisation loop

$$J^N(P) := \text{(diagram)} = \int\frac{\mathrm{d}^4 p''}{(2\pi)^4}\,S(\frac{P}{2}+p'')it_{sad}(\frac{P}{2}-p'')\,, \qquad (5.104)$$

which, compared to the mesonic and diquark polarisation loops, neither includes any vertex structure nor a trace. Furthermore, the polarisation loop (5.104) is not a closed fermion loop, since it is constructed of a fermion and a boson. As already mentioned in the previous discussions, the complete Dirac structure of the spin-half baryons is given, in the case of scalar diquarks, by the single quark. Now, we can insert the expressions (2.33) and (4.22) for the quark and diquark propagator in pole-approximation and change the variable $p'' \mapsto \frac{P}{2} - p''$, to obtain

$$J^N(P) = -ig_{Dqq}^2\int\frac{\mathrm{d}^4 p''}{(2\pi)^4}\,\frac{\slashed{P}-\slashed{p}''+M}{(P-p'')^2-M^2}\frac{1}{p''^2-m_{sad}^2}\,. \qquad (5.105)$$

This can be rewritten (see appendix F.4) as

$$J^N(P) = -ig_{Dqq}^2\left(\slashed{P}(I^0(P)-I^1(P))+MI^0(P)\right) \qquad (5.106)$$

with the introduced integral

$$I^n(P) := \int\frac{\mathrm{d}^4 p''}{(2\pi)^4}\left(\frac{Pp''}{P^2}\right)^n\frac{1}{(P-p'')^2-M^2}\frac{1}{p''^2-m_{sad}^2}\,, \qquad n=0,1\,. \qquad (5.107)$$

Note that for $n=0$ and $M=m_{sad}$ the integral in equation (5.107) is equal to the definition of I_2 in appendix D.1.1. Hence, the expression (5.103) reads

$$\det\left(\mathbb{1} - ig_{Dqq}^2\frac{2}{M}\left\{\slashed{P}(I^0(P)-I^1(P))+MI^0(P)\right\}\right)\Bigg|_{P^2=m_B^2} = 0\,. \qquad (5.108)$$

Basically, we find that the inhomogeneous BS equation (5.80) can be written as a Dirac-like equation for an appropriate (renormalised) nucleon wave function $X^{\text{nucl}}(P)$, which, in a compact version reads

$$\left(\slashed{P}A(P) - B(P)\right) X^{\text{nucl}}(P)\Big|_{P^2 = m_B^2} = 0\,. \tag{5.109}$$

Here, we have introduced the momentum-dependent pre-factors

$$A(P) := -ig_{Dqq}^2 \frac{2}{M}\left(I^0(P) - I^1(P)\right), \tag{5.110}$$

$$B(P) := ig_{Dqq}^2 M I^0(P) - \mathbb{1}\,. \tag{5.111}$$

Equation (5.109) also represents an eigenvalue problem and therefore can be solved by

$$\det\left(\slashed{P}A(P) - B(P)\right)\big|_{P^2 = m_B^2} \overset{!}{=} 0\,, \tag{5.112}$$

which leads, for a nucleon at rest, to

$$m_B^2 = \frac{B(P_0)}{A(P_0)}\Bigg|_{P_0^2 = m_B^2}\,. \tag{5.113}$$

Comparing equation (5.109) with the well known Dirac equation, the scalar part, or more precisely the fraction $B(P)/A(P)$, in equation (5.109) defines the mass of the nucleon in accordance with expression (5.113) and can be computed directly. The emerging divergent integrals I^0 and I^1 defined in (5.107) have to be regularised in a proper way, for example with Pauli-Villars regularisation. Furthermore, the pre-factors $A(P)$ and $B(P)$ are in general related to the spectral functions of the nucleon.

5.8. Nucleon propagator and mass

In this section we want to determine the vacuum nucleon propagator and investigate its behaviour under a variation of the free parameters of the NJL model. Hence, it will be possible to fit the still undetermined coupling constant h_s of the particle-particle channel onto the well known nucleon mass $m_N = 938$ MeV. Despite that we have already given an equation to obtain the nucleon mass in (5.109) through the coefficients $A(P)$ and $B(P)$, we will go a step back and consider the BS equation (5.103). By virtue

of the polarisation loop, defined in (5.104), the corresponding matrix reads

$$
\mathbb{1} + \frac{2}{M} J(P)
$$

$$
= \mathbb{1} - i \frac{2}{M} g_{Dqq}^2 \int \frac{\mathrm{d}^4 p''}{(2\pi)^4} \frac{\slashed{P} - \slashed{p}'' + M}{(P - p'')^2 - M^2} \frac{1}{p''^2 - m_{sad}^2} \tag{5.114}
$$

$$
= \mathbb{1} - i \frac{2}{M} g_{Dqq}^2 \int \frac{\mathrm{d}^4 p''}{(2\pi)^4} \frac{(P_0 - p_0'')\gamma_0 - (\vec{P} - \vec{p}'')\vec{\gamma} + M\mathbb{1}}{(P - p'')^2 - M^2} \frac{1}{p''^2 - m_{sad}^2} \tag{5.115}
$$

In Dirac-space, we can split the baryon polarisation loop into a scalar, related to the identity matrix, and a vector contribution, related to the γ_0-matrix. For a certain nucleon at rest, i.e. $\vec{P} = 0$, the scalar part is given by

$$
J_s(P_0) := -i g_{Dqq}^2 M I^0(P_0) \tag{5.116}
$$

while the vector one reads

$$
J_v(P_0) := -i g_{Dqq}^2 \int \frac{\mathrm{d}^4 p''}{(2\pi)^4} \frac{(P_0 - p_0'')}{(P - p'')^2 - M^2} \frac{1}{p''^2 - m_{sad}^2} . \tag{5.117}
$$

The remaining $\vec{p}''\vec{\gamma}$ contribution is antisymmetric and hence vanishes in case of an integration over the hole (three-dimensional) momentum space. A detailed treatment of both contributions can be found in appendix F.5. Due to the eigenvalue character of the original equation (5.84), we have to evaluate

$$
\det \left(\mathbb{1} + \frac{2}{M} J(P_0) \right) \bigg|_{P_0^2 = m_N^2} = \det \left(\mathbb{1} + \frac{2}{M}(J_s(P_0)\mathbb{1} + J_v(P_0)\gamma_0) \right) \bigg|_{P_0^2 = m_N^2} \overset{!}{=} 0. \tag{5.118}
$$

Since γ_0 is a diagonal 4×4 identity, except for a sign switch in the (last) 2×2 submatrix, the determinant can be evaluated directly. The matrix structure of the non-trivial part of the nucleon polarisation loop (5.104) reads

$$
\frac{2}{M} (J_s(P_0)\mathbb{1} + J_v(P_0)\gamma_0)
$$

$$
= \frac{2}{M} \begin{pmatrix} J_s(P_0) + J_v(P_0) & 0 & 0 & 0 \\ 0 & J_s(P_0) + J_v(P_0) & 0 & 0 \\ 0 & 0 & J_s(P_0) - J_v(P_0) & 0 \\ 0 & 0 & 0 & J_s(P_0) - J_v(P_0) \end{pmatrix} \tag{5.119}
$$

Hence, the determinant reads

$$
D_N^{-1}(P_0) := \det \left(\mathbb{1} + \frac{2}{M}(J_s(P_0)\mathbb{1} + J_v(P_0)\gamma_0) \right) \bigg|_{P_0^2 = m_N^2} \tag{5.120}
$$

$$
= [1 + \frac{2}{M} J_s(P_0) + \frac{2}{M} J_v(P_0)]^2 [1 + \frac{2}{M} J_s(P_0) - \frac{2}{M} J_v(P_0)]^2 \bigg|_{P_0^2 = m_N^2} \tag{5.121}
$$

$$
= \left([1 + \frac{2}{M} J_s(P_0)]^2 - \frac{4}{M^2} J_v^2(P_0) \right)^2 \bigg|_{P_0^2 = m_N^2} \overset{!}{=} 0. \tag{5.122}
$$

It turns out that one term of the determinant would be enough to determine the nucleon mass. Nevertheless, we choose the multiplication of the two different terms to obtain a symmetric behaviour of the nucleon-mass equation under a variation of P_0. For an arbitrary choice of input parameters [7], like the constituent quark-mass and coupling constant h_s of the diquark channel, the denominator of the baryon propagator represented by equation (5.122) is shown in figure 5.8.

In the discussion of the diquarks, we have already seen that for $h_s = \frac{3}{2}g_s$ the scalar diquarks and pseudoscalar mesons are degenerate. For increasing h_s the diquark becomes even lighter than the pion, cf. the discussion in chapter 4.1, before the mass vanishes. Hence, the upper limit for coupling h_s within the quark-quark channel will be set to $h_s = 1.5g_s$ in the following discussion. The lower limit for the diquark coupling is also given in chapter 4 and lies around $h_s = 0.7g_s$.

For $|P_0|$ between zero and approximately 1000 MeV, we recognise the stable region for baryons. The roots in this region are related to the mass of the nucleon. The first kink at a certain $P_0^2 = (M + m_{sad})^2$, indicates the beginning of a non-vanishing imaginary part and hence the possibility for the nucleon to decay. Therefore, roots after the first kink describe an unstable resonance of the nucleon that is allowed to decay into its constituents. In the following section we take a closer look at equation (5.122) to investigate the behaviour under various variations of the input parameters.

5.8.1. Constituent quark-mass / parameter set variation

Table 5.1.   Parameter set for fixed value of $h_S = 1.1g_S$

	[A]	[B]	[C]	[D]	[E]
M [MeV]	300	350	400	450	453
m [MeV]	7.57	8.46	8.89	9.04	9.05
$g_S\Lambda^2$	3.23	3.65	4.095	4.553	4.589
Λ [MeV]	696.676	647.491	624.828	615.359	615
m_{sad} [MeV]	472.186	490.169	514.274	542.188	544.437
g_{Dqq}	3.985	4.887	5.725	6.531	6.576

To get an idea of the behaviour of the inverse baryon propagator under a variation of the constituent quark-mass, or to be more precisely, the complete parameter set, we will use the parameter sets calculated in section 3.3. These sets are shown again in table 5.1. The coupling constant of the diquark-channel, i.e. h_s, in the upcoming

---

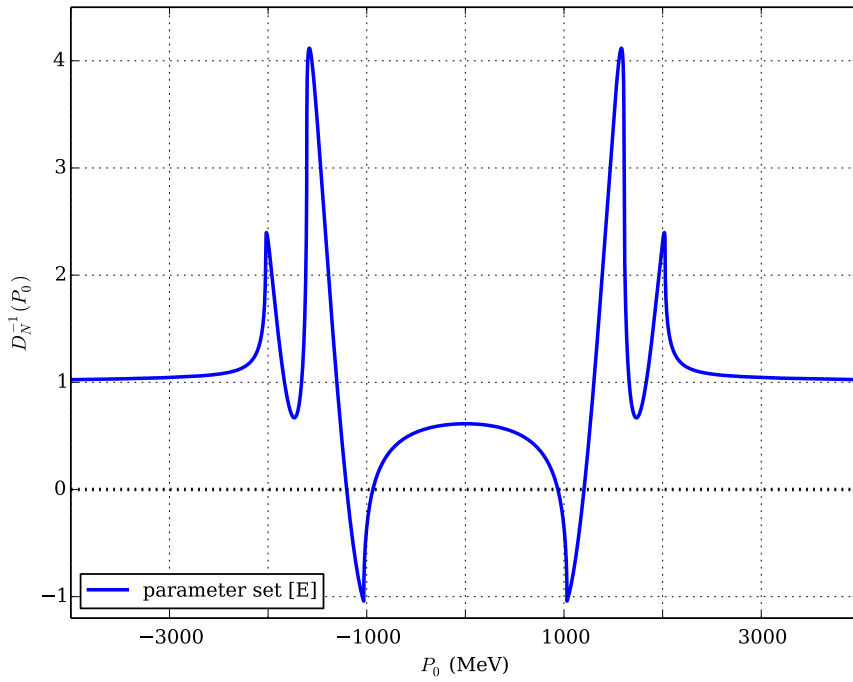[7]Here, parameter set [E] of table 5.1 has been used with $h_s = 1.1g_s$

Figure 5.8. Inverse nucleon propagator for parameter set [E] with $h_s = 1.1g_s$.
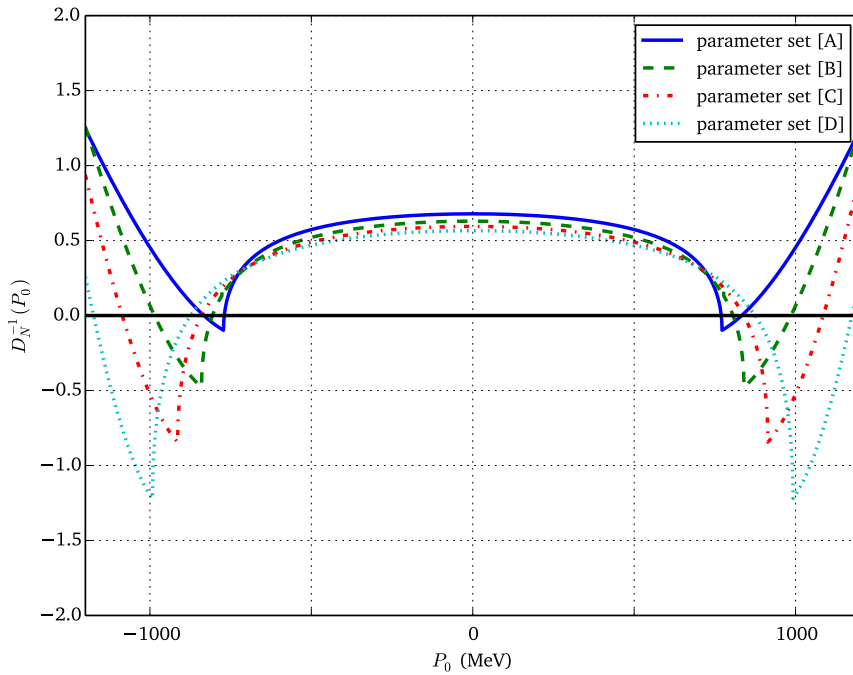

Figure 5.9. Behaviour of the inverse baryon propagator under a variation of M for fixed $h_s = 1.1g_s$. The related parameters for each M can be found in table 5.1.

77

discussion will be set to a fixed value of $h_s = 1.1g_s$. From this the scalar antitriplet diquark mass as well as the corresponding effective coupling g_{Dqq} have been calculated and added to the table.
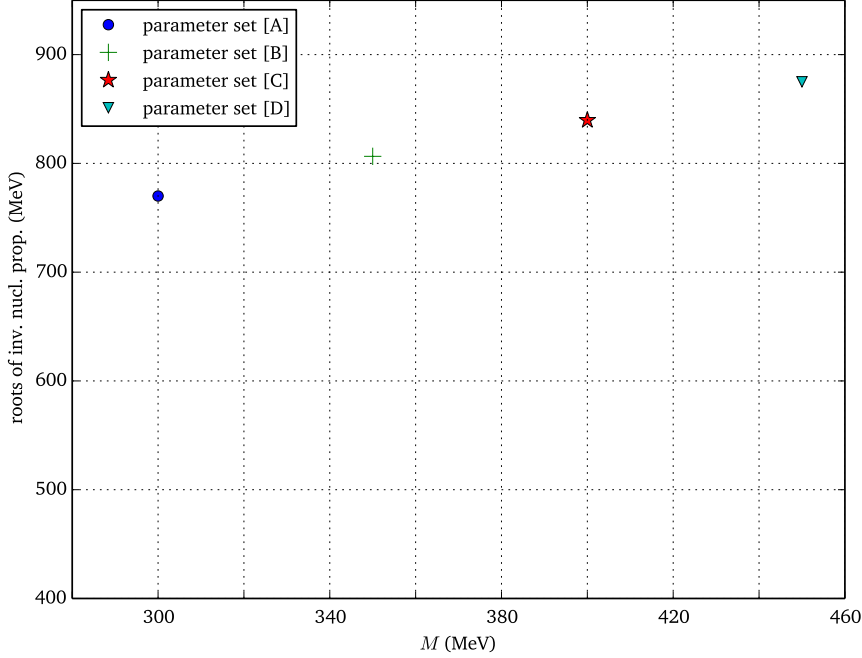

Figure 5.10. Roots for the inverse nucleon propagator for each parameter set of table 5.1.

Since we assume the nucleon to be stable, we will concentrate only on the region before the first kink. In case of constituent quark-masses lower than 350 MeV corresponding to parameter set [B], the roots, and thus the related nucleon mass, lies approximately 200 MeV over the diquark mass itself. However, increasing the constituent mass leads to a shift of the instability point to higher values of P_0. It seems that the form of the inverse propagator stays more or less constant for different parameter sets, except for a shift in the vertical axis and the position of the first kink due to the different constituent quark/diquark masses as well.

Physically, this behaviour could have been expected, since we vary the masses of the three constituents of a nucleon and consequently the diquark-quark coupling. The only possibility for an interaction between the quarks within a nucleon is given through the quark-quark coupling h_s. Note that the diquark masses are relatively close to each other in the parameter sets [A]-[D]. Due to the fact that we fix the quark-quark coupling to a certain value, the quarks can form a bound three-particle state, when their masses are high enough. From figure 5.9 it follows that a constituent mass of $M = 300$ MeV, related to parameter set [A] leads to root at $P_0 = 770$ MeV, while $M = 450$ MeV (parameter set [D]) gives $P_0 = 875$ MeV. Beside the quark masses, the

diquark-quark coupling changes as well. Since this coupling enters the two terms of the nucleon polarisation loop quadratic, it contributes to the roots significantly. It follows that the roots of the propagator and hence the related nucleon mass, hardly depends on the choice of parameter set, when we fix the quark-quark coupling h_s. In figure 5.10 the roots for each parameter set of table 5.1 can be found, which verifies our statement.

Unless stated otherwise, we choose the parameter set which represents the most stable nucleon, cf. figure 5.9. Parameter set [E], as well as [D], have the roots sufficiently far away from the point of instability with not to high coupling in the diquark channel. Nevertheless, as the next step in the analysis of the inverse baryon propagtor, we will increase the diquark coupling.

5.8.2. Variation of h_s

Table 5.2. Pseudo scalar diquark masses for parameter set [C] with different values of h_s.

h_s/g_s	0.7	0.9	1.1	1.3	1.5
m_{sad} [MeV]	725.504	629.096	514.274	372.305	140.002

We have seen, that a quark mass around 400 MeV leads to stable nucleons with not too strongly coupled diquarks. Now, we want to analyse the behaviour of the inverse baryon propagator in case of a variation of the diquark coupling h_s for parameter set [C].

For the various parameter sets, we noticed that the form of the inverse nucleon propagator stays relatively constant. In contrast, the inverse baryon propagator behaves slightly different when we tune h_s. Increasing h_s stretches the region of stability of the inverse nucleon propagator in the direction of P_0, while decreasing the diquark coupling squeezes it. In fact, varying h_s is related to the modification of the diquark mass. Based on our assumption of a nucleon built of a quark and a diquark, the mass of the latter should play an important role for the obtained nucleon propagator. Indeed, increasing h_s leads to lower masses for the diquarks and thus sharpens the region for stable nucleons. The point where the first kink emerges depends on the quark mass and diquark mass as well. Hence, for a coupling constant at the lower limit related to a diquark mass near the point of instability, i.e. $m_{sad}^2 = 4M^2$, the region of instability of the inverse nucleon propagator emerges around $P_0^2 \approx (3M)^2 = (1200)^2$ MeV^2. Despite that we do not find a root for such diquark masses, we find that in the inverse nucleon propagator, the interesting region of stability will be increased to its maximum. In general, it seems very complicated to
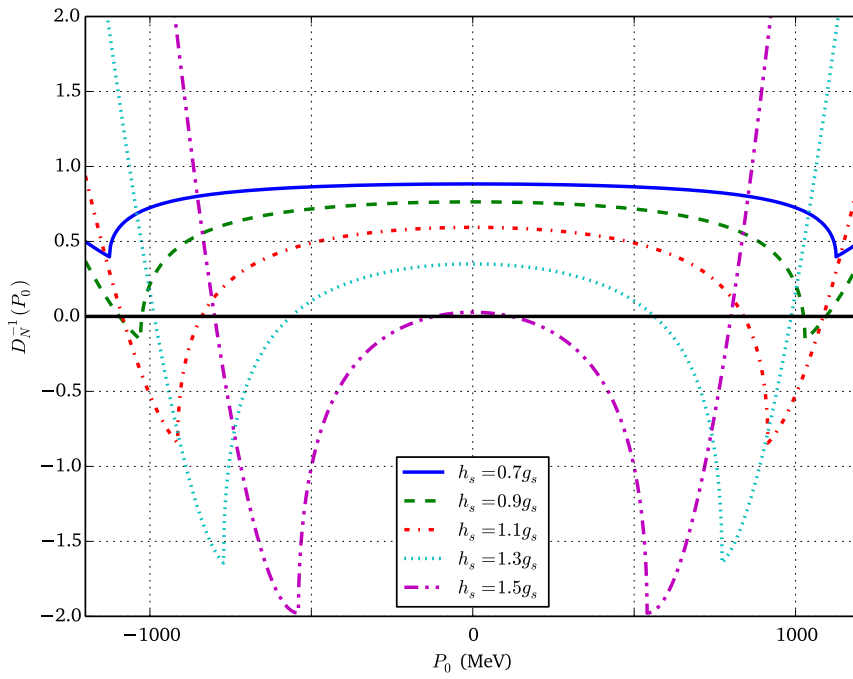
Figure 5.11. Behaviour of the inverse baryon propagator under a variation of h_s for fixed $M = 400$ MeV. The related diquark mass for each value of h_s can be found in table 5.2.

obtain a root within the region of stability of the inverse propagator at all with the restriction of not too strongly bound diquarks. In figure 5.12 the nucleon mass in terms of h_s/g_s has been calculated for the different parameter sets. One sees that the
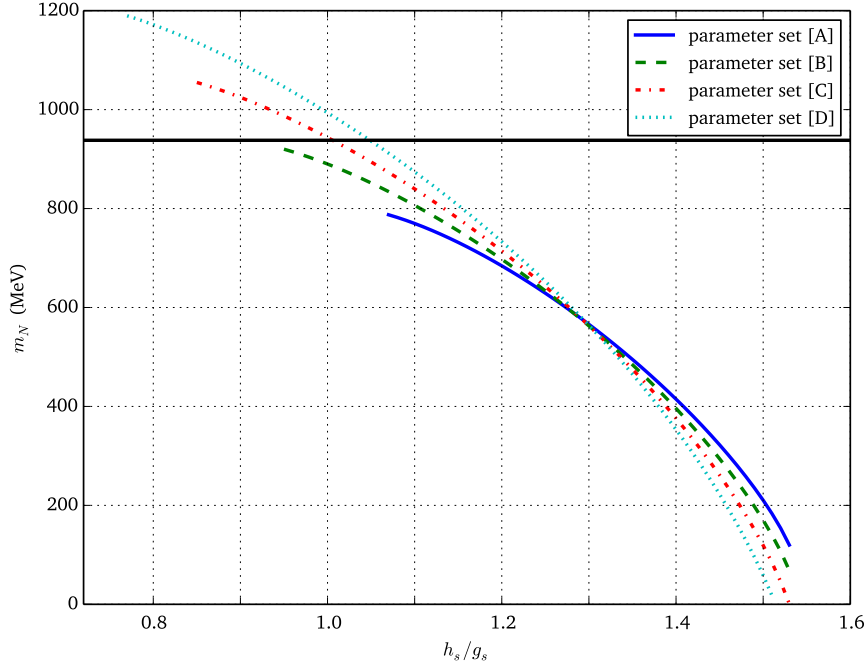

Figure 5.12. Nucleon masses as a function of h_s/g_s for all parameter sets. The solid black line show $m_N = 938$ MeV.

masses of the constituent quarks should lie around 450 MeV, whereas $M = 400$ MeV is also possible, in order to obtain a strongly bound nucleon. Then, a diquark mass of about 550 MeV can be obtained from a coupling h_s in the diquark channel between $(1 - 1.1)g_s$ depending on the other parameter as well. Parameter set [B], however, leads to a mass of 914 MeV for $h_s = 0.96g_s$, which is quite close to the mass of the nucleon. We will use this parameter set in further investigations as an example for nucleons near the point of instability. In table 5.3 we have summarised the best ratios h_s/g_s, if possible, for all parameter sets to fit the experimentally well known nucleon mass $m_N = 938$ MeV. In case of parameter set [A] no solution can be found in accordance with the upper discussion. Compared to the coupling obtained by the Fierz-transformation of the colour-current interaction, which yields $h_s = 3/4g_s$, the diquarks have to be significantly stronger bound to form a nucleon with a third quark. In the following discussion of the nucleons in the medium, parameter set [E] will be used with a coupling constant $h_s = 1.051g_s$ for the diquark channel.

Table 5.3. Parameter set for fixed value of the nucleon mass $m_N = 938$ MeV.

	[A]	[B]	[C]	[D]	[E]
M [MeV]	300	350	400	450	453
$g_s \Lambda^2$	3.23	3.65	4.095	4.553	4.589
h_s / g_s	-	-	1.006	1.049	1.05
m_{sad} [MeV]	-	-	570.742	576.121	576.78

5.9. Nucleon in the medium

It is now time to discuss the nucleon in dense hot matter in order to investigate the melting temperature and critical chemical potential of the nucleon. For this, the obtained vacuum description has to be transformed with the already introduced methods into the medium expressions. A slight difference compared to the mesons or diquark occurs due to the emerging effective coupling g_{Dqq} within the BS equation. Unlike the two particle channels, i.e. mesons and diquarks, the coupling in the three-body discussion itself depends on the temperature and quark chemical potential as well and is not given as an elementary coupling in the NJL Lagrangian. We want to refer at this point to the discussion encountered in section 4.3, where we have already investigated the in-medium behaviour of the effective diquark-quark coupling. Moreover, the inverse nucleon propagator has a more complicated structure due to mixture of a fermionic and bosonic contribution, but looks formally the same as in the vacuum. The polarisation loop for the nucleon in expression (5.105) within the Matsubara formalism thus reads

$$J^B(i\nu + \mu + \mu_D, \vec{P} = 0)$$

$$= T \sum_{\{i\omega\}} \int \frac{\mathrm{d}^3 p}{(2\pi)^2} \left((i\nu - i\omega + \mu)\gamma_0 + M\mathbb{1}\right) \frac{1}{(i\nu - i\omega + \mu)^2 - (E_P^Q)^2} \frac{1}{(i\omega + \mu_D)^2 - (E_P^D)^2},$$

$$(5.123)$$

with $(E_p^Q)^2 = p^2 + M^2$ and $(E_p^D)^2 = p^2 + m_{sad}^2$, the quark and diquark energy, respectively. Again, we found that in our baryon modelling, which is based on the assumption of a diquark-quark scattering process, the corresponding polarisation loop depends on the sum of a quark and diquark chemical potential. Hereby, the chemical potential μ_D is related to the diquark chemical potential and will be set to 2μ in accordance with section 4.3. Then, the baryon polarisation loop and the corresponding inverse baryon propagator depend on three times the quark chemical potential which would be expected for the three-body problem.

It follows directly from equation (5.123) that the polarisation loop yields the same two

contributions, i.e. a scalar and vector part, and thus will have the same structure as already found for the vacuum. A detailed investigation of the nucleon polarisation loop within the medium can be found in appendix F.5.1.

At first we want to take a closer look at the temperature behaviour for a fixed chemical potential $\mu = 0$. Our results are shown in figure 5.13 for parameter set [E]. For increasing temperature the nucleon mass decreases at first slowly and then faster until the limit of stability will be reached at $T_m = 193$ MeV and consequently is 4 MeV smaller than the one obtained for the diquarks. At this critical temperature, we would expect a melting of the nucleon into its constituents. Instead, we find that the nucleon indeed melts at first but becomes stable again for higher temperatures although the diquark is unstable. It turns out that within the gap in the region $193 < T < 198$ MeV, no roots of the inverse nucleon propagator, neither in the stable nor in the unstable region, can be found. Maybe the behaviour of the diquark-quark coupling, discussed in section 4.3, is responsible for this gap.

Increasing the temperature leads to new roots in the inverse propagator, which can be identified with a stable nucleon, but with unstable diquarks. Since we do not include the emerging imaginary part within the diquark propagator in this case, our results have to be treated with some care. However, in reference [35] it has been argued that due to this Borromean-state like behaviour the nucleon does not have a melting temperature at all. In order to verify this assumption within our investigation the binding energy of the nucleon has been calculated, cf. figure 5.14. While the diquark indeed becomes unstable for a certain value of T (the binding energy becomes zero), the nucleon obtains also a zero binding energy for nearly the same temperature, which is interesting.[8] Compared to reference [35] our binding energy for the nucleon shows a different behaviour, since it becomes zero before the Borromean-state emerges. Therefore, it is possible to identify a certain melting temperature T_m. A possible explanation of the different behaviour could be the simplification of the Dirac structure within the polarisation loop by performing a trace in reference [35]. Hence, the contribution of the integral proportional to γ_0 vanishes in this work. Due the observation in figure 5.14, we will use the temperature where the diquark-quark-nucleon binding energy (blue line) becomes zero, in the following discussion as the melting temperature of the nucleon. Nevertheless, we have to keep in mind that for higher temperatures, after the gap, a bound nucleon exists in our description.

Taking a look at the other parameter sets, with the upper definition of the melting temperature, leads to the results shown in figure 5.15, where we calculated the mass until the binding energy becomes zero. We note that the critical temperature depends significantly on the set of parameters, although the coupling h_s has been fitted to

---

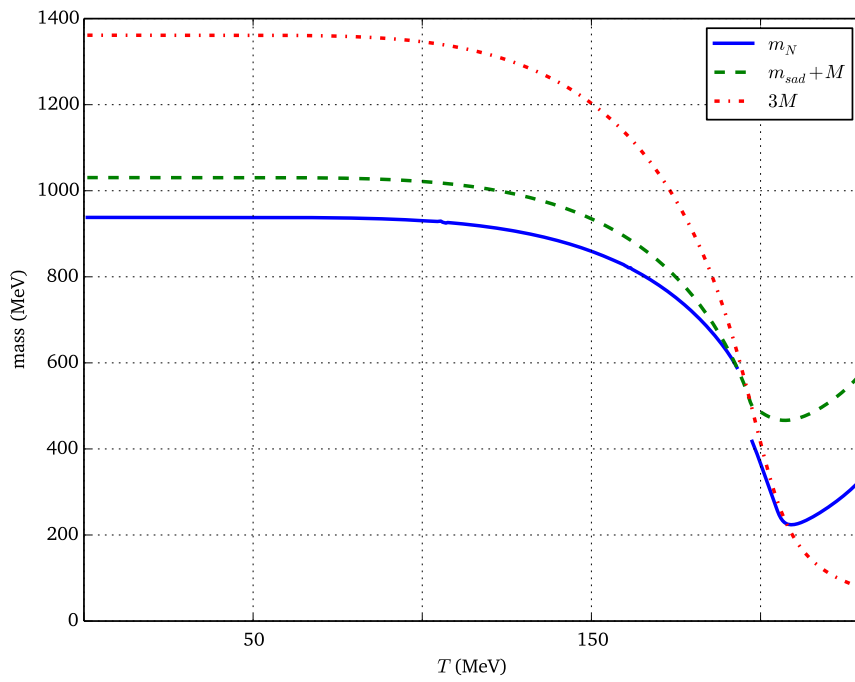[8]For $m_{sad} = 2M$, the blue line has to coincide with the red one.

Figure 5.13. Nucleon mass as a function of temperature for zero quark chemical potential.
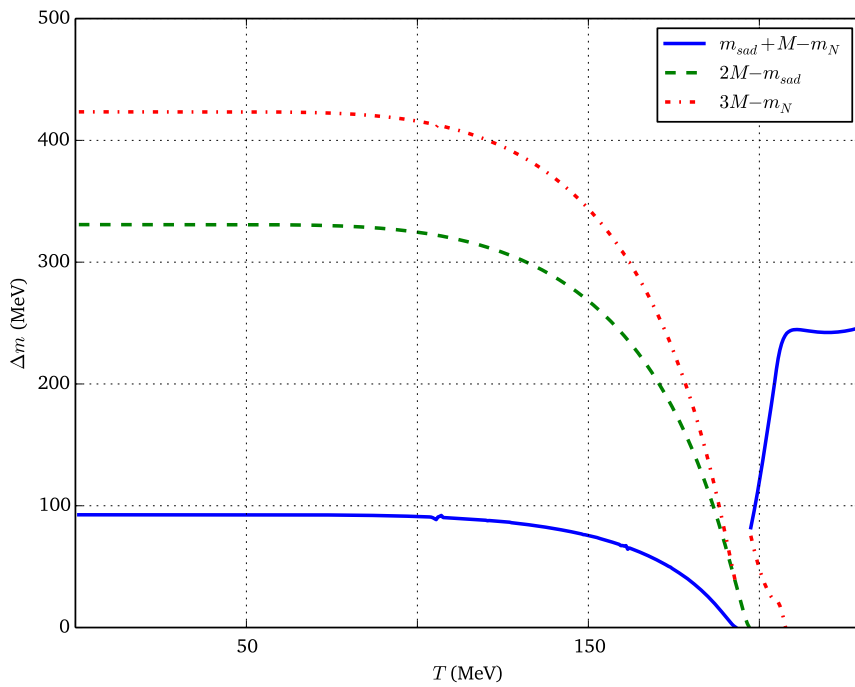

Figure 5.14. Binding energy of the nucleon and diquark as a function of T.

obtain the nucleon mass in the vacuum.[9] For parameter sets [B] and [C] we find $T_m = 107$ MeV and $T_m = 173$ MeV, respectively. This can be explained by the already discussed region in which the roots and thus the related nucleon mass of the inverse baryon propagator lies for the different parameter sets. While for set [B] the root is very close to the point of instability, the nucleon is much stronger bound in set [D] and especially [E]. Hence, we expect and find that the latter two have to have a higher melting temperature.

Comparing our results for the nucleon with the results provided in references [28] and [25] we found a good agreement. While in both investigations, a three-momentum cutoff rather than the PV regularisation in our discussion has been used, reference [28] also simplifies the Dirac structure in the baryon polarisation function by taking the trace in all spaces. Due to the different regularisation scheme, our result for the critical temperature is slightly smaller than in these references where melting temperatures larger than 200 MeV have been found. Moreover, in [25] a factor of two, based on the two different scattering kernels in the particle-particle channel, cf. equation (4.12), is missing in the modelling of the diquarks. Therefore, the baryons are less bound to the diquark and quark and melt earlier, which could explain why the melting temperatures of the baryons in reference [25] differs significantly from the diquark one.

For small (fixed) temperature $T = 1$ MeV and non-vanishing chemical potential the discussion is analogous to the one for the diquarks in the medium. Again, we note that our obtained nucleon propagator comes with an additional term of 3μ in the zero-component of the four-momentum P. A nucleon propagator for the pole-approximation reads

$$D_B(P_0, \vec{P}, \mu_B) = \frac{\slashed{P} + m_B}{(P_0 + \mu_B)^2 - E_B^2} \, , \qquad (5.124)$$

where m_B denotes the nucleon mass, $\mu_B = 3\mu$ the nucleon chemical potential and $E_B^2 = \vec{P}^2 - m_B^2$ the energy of the nucleon. The poles are given by

$$P_{\text{Pole}}^{\pm} = E_B^{\pm} - 3\mu \, , \qquad (5.125)$$

with $E_B^{\pm} := \pm E_B = \pm\sqrt{\vec{P}^2 + m_B^2}$. While the diquark is a boson and hence does not have a Dirac structure in the propagator, the third quark is a spin-half particle and thus does have a Dirac structure. In detail, the related nucleon Dirac structure is given by the scalar and vector contribution within the polarisation loop, namely J_s and J_v. Nevertheless, the poles of the nucleon propagator (5.124) are of particular interest and describe in the case of non-vanishing chemical potential the free energy of the nucleon, while the physical mass of the nucleon has to be constant, up to a certain

---

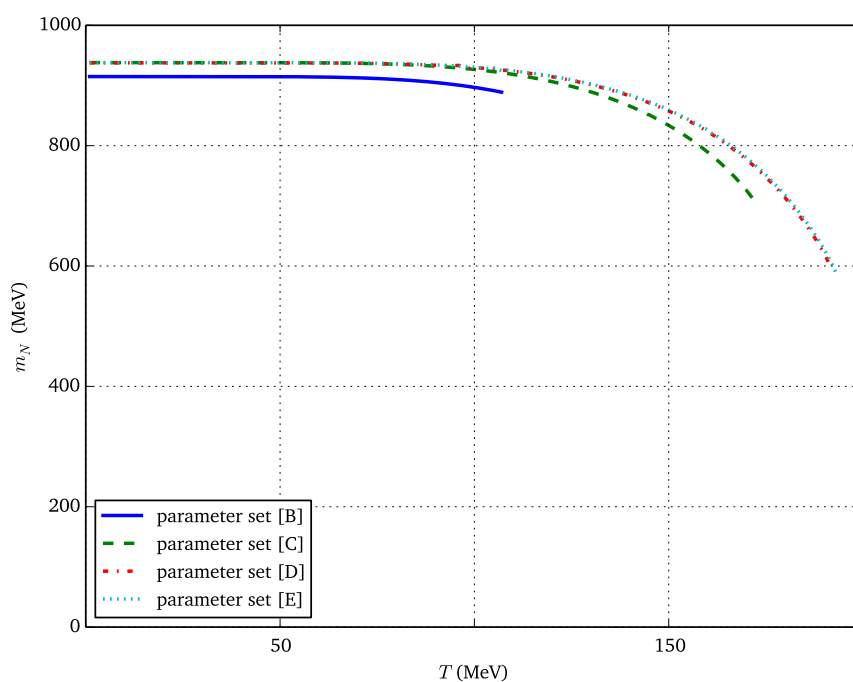[9]Except for parameter set [B], where we have used $m_N = 914$ MeV.

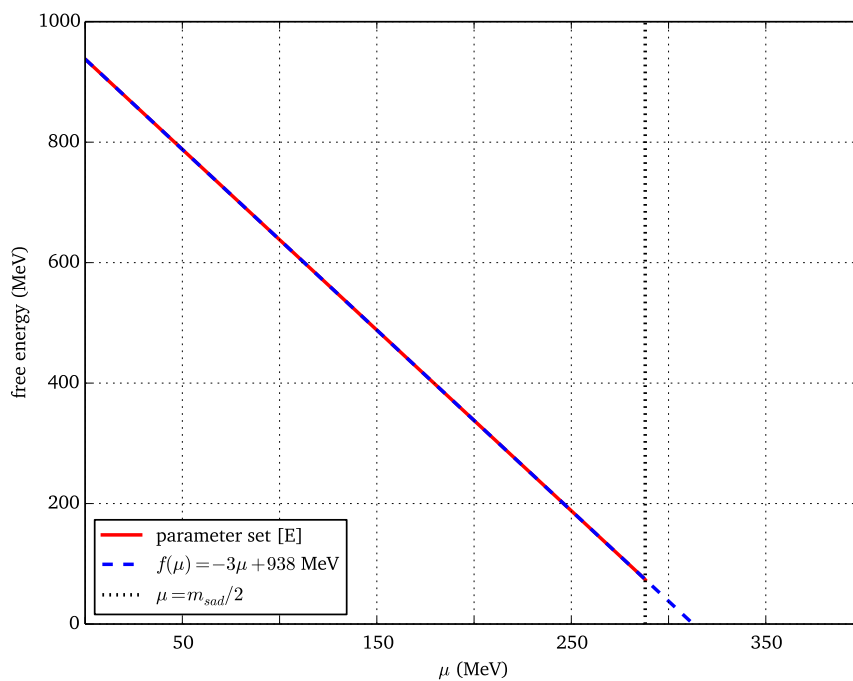**Figure 5.15.** Nucleon mass as a function of temperature for zero quark chemical potential.

Figure 5.16. Free energy of the nucleon as a function of the chemical potential for $T = 1$ MeV.
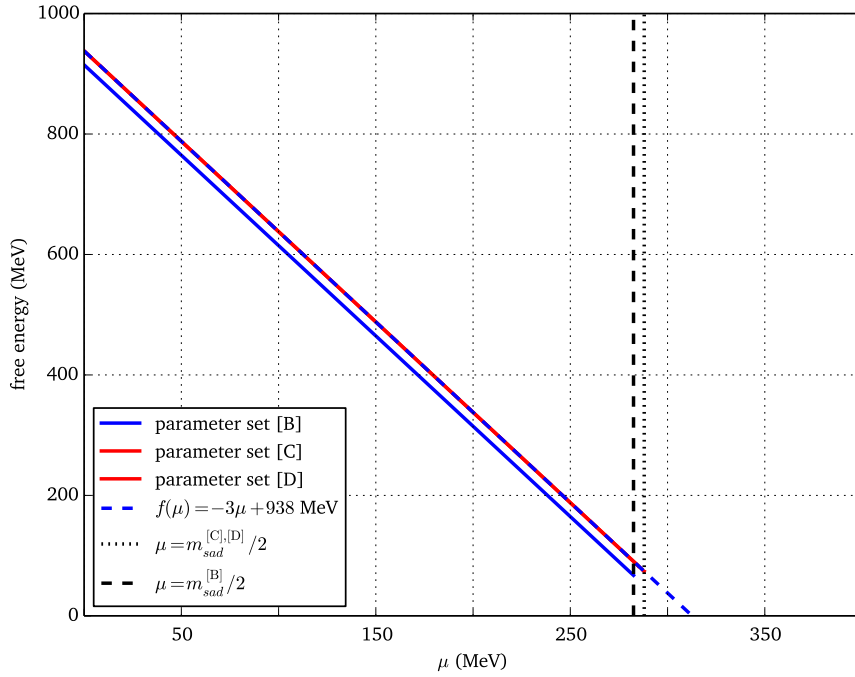
Figure 5.17. Free energy of the nucleon as a function of the chemical potential for $T = 1$ MeV for the different parameter sets of table 5.1.

threshold, based on the silver-blaze property. As shown in figure 5.16 the behaviour of the free energy for the nucleon bears a strong resemblance with the one obtained for the antitriplet diquark. Since the 2SC Phase has not been considered, our results are not reliable for chemical potentials greater than $\mu = m_{sad}/2$. However, we expect and find that the poles $P_{\text{Pole}}^{\pm}$ are given by (5.125) until $\mu = m_{sad}/2$, cf. figure 5.16 with $\vec{P} = 0$ and P_{Pole}^{+}.

For the other parameter sets and especially for parameter set [B], with a mass near to the point of instability, a similar behaviour is expected. Therefore, the fitting function coincide with equation (5.125) for all parameter sets, cf. figure 5.17. The line for parameter set [B] with a slightly lower mass of 914 MeV indicates that it crosses the μ-axis at 914/3 MeV, in accordance with the upper discussion.

As a conclusion, the behaviour of the nucleon in dense matter is independent of the choice of the parameters. The parameters, meanwhile, should reflect the vacuum observables of the treated physical particles, like the mass or decay constants. Furthermore, the position of the roots does not contribute for vanishing temperature in any way.

Chapter 6

Summary and outlook

In this thesis, we have modelled and studied mesons, diquarks and baryons in the framework of a two-flavour Nambu–Jona-Lasinio model in vacuum, as well as for finite temperature and quark chemical potential. Mesons have been described as a collective excitation of a quark-antiquark pair by using the Bethe-Salpeter equation in random-phase approximation. The physical masses of the pions and the pion decay constant have been used to generate a set of values for the bare quark masses, the coupling constant and other parameters. The in-medium behaviour of the quarks and mesons has been discussed with the Matsubara formalism. In addition, certain aspects like the phase transitions from the chirally broken into the restored phase have been found.

In order to describe diquarks as bound states of the quark-quark scattering process, the Fierz transformation has been introduced. This led to separate interaction Lagrangians in the particle-particle and the particle-antiparticle channel of the NJL model. Thus, we obtained a relation between the coupling constants g_s and h_s of the particle-antiparticle and particle-particle channel, respectively, based on the Fierz transformation of the colour-current interaction. However, the coupling h_s has been treated as a free parameter of the model and was later on fixed with the nucleon mass. In fact, diquarks are bound states of two quarks and thus are not observable in nature due to confinement. Nevertheless, to ensure Pauli's principle, we have discussed the possible channels that occur in Dirac, flavour and colour space. To simplify the discussion, we have restricted ourselves to the scalar channels in the antitriplet colour representation. For this, we have seen that the scalar diquarks obtain a smaller mass than the pseudoscalar ones. Just as for the mesonic channel, it was possible to introduce an effective diquark-quark coupling constant for the pole-approximation, which was needed for the baryon modelling. Besides the vacuum properties, we have also discussed the medium behaviour of the diquarks. In particular, we were interested in the melting temperature and the behaviour for finite chemical potential. We were

able to discuss the free energy of the diquarks for (nearly) vanishing temperature, while, due to the silver-blaze property, the masses have to be constant until a certain threshold emerges.

Since baryons are built out of three quarks, the modelling of such particles is more complicated compared to the two-particle spectrum. Therefore, we have started from the Dyson equation, and introduced the Faddeev components with separable two-particle correlations. For these correlations, we only considered scalar diquarks and two degenerate flavours, which led to a description of the nucleon. Then we have investigated our expression in momentum space, to obtain a Bethe-Salpeter-like equation. Furthermore, the vertex structure, as well as a Dirac-like equation of the nucleon have been derived and discussed. In order to simplify the complex structure of the diquark-quark scattering kernel within the Bethe-Salpeter equation, the static approximation has been introduced. This approximation is characterized by neglecting the four-momentum dependence of the exchanged quark and therefore can be interpreted as an infinitely heavy quark exchange. As a following step, the eigenvalue problem of the Bethe-Salpeter-like equation has been solved to obtain an expression for the nucleon mass. Therefore, it was possible to fix the coupling h_s of the particle-particle channel onto the well-known observable mass of the nucleon. Beside the discussion of the inverse nucleon propagator in vacuum, the Bethe-Salpeter equation of the nucleon has been transformed into the medium. Here, the temperature behaviour for vanishing chemical potential has been studied. Similar to the mesons and diquarks, the nucleon melts into its constituents at a certain temperature but seems to become stable again at higher temperatures. In this regime, where the diquarks are unstable, the nucleon seemed to be a Borromean-state. However, these results have to be treated with some care since the methods provided in this work are not reliable for unstable bound states. Furthermore, the results for the temperature behaviour of the nucleon, including the Borromean-state, has been compared to other already existent works. We found that our results resembled the results of these works, although some technical differences occur. Beside the temperature behaviour of the nucleon, the free energy of the nucleon in dense matter for vanishing temperature has been shortly discussed up to the chemical potential, for which the system enter the 2SC phase.

Since we have restricted ourselves to the two-flavour case in the chiral limit in order to simplify the discussion, it would be interesting to extend the investigation to three flavours. Then, it would be possible to describe the full baryon octet and decuplet as well, where for the latter it is required to include the axial diquarks into the baryon modelling. In order to describe the decay of diquarks and baryons, we could improve our methods by allowing an imaginary part within the propagators of the two-particle

and three-particle channel and thus get access to a finite decay width of the described particles. This would be, due to the already known imaginary parts of the expressions, more or less straightforward. In this context the question arises whether the baryon is stable when the diquark becomes unstable.

We have already seen in the in-medium discussion of the nucleon that the condition of a stable diquark within the nucleon is not necessary to obtain a stable three-particle state. Moreover, we have seen that the baryon seems to have a Borromean-state like behaviour for non-vanishing temperature and vanishing chemical potential. Therefore, a more detailed discussion of a possible melting temperature and the physics behind this Borromean-state would be of particular interest. For this purpose, the factors $A(P)$ and $B(P)$ as functions of the baryon momentum P within the derived Dirac-like equation can be used. These factors are known to be related to the spectral functions of a certain baryon, and thus can be used in upcoming discussions to investigate baryons in more detail. Especially, the spectral functions allow to get access to the different decay channels of the baryons and are therefore more suited for the in-medium discussion. Due to the fact that we have only studied the behaviour of particles either for vanishing chemical potential or (nearly) vanishing temperature, the discussion could be improved by studying the particles for the complete $T - \mu$ plane, where we expect that the silver-blaze property is no longer fulfilled. Hereby, we also have to take care of the 2SC phase. Of course, the spectral function formalism can be used in a three-flavour model as well.

Besides the upper mentioned extensions and improvements, the NJL model could be extended to the PNJL model, which includes Polyakov-loops, such that some aspects of confinement in medium will be part of the model. Even though some of these improvements have already been discussed in the literature, questions regarding the reliability of some approaches have been raised.

Appendix

Appendix A

Conventions

In this work we use the following structure of the Minkowski space

$$(x_\mu) = \begin{pmatrix} t \\ -x_1 \\ -x_2 \\ -x_3 \end{pmatrix} = \begin{pmatrix} t \\ -\vec{x} \end{pmatrix} \tag{A.1}$$

which implied the used metric

$$g_{\mu\nu} = g^{\mu\nu} = \text{diag}(1, -1, -1, -1). \tag{A.2}$$

Greek indices are elements of $[0, 1, 2, 3]$ and are summed over when they appear as upper and lower indices. Latin indices, meanwhile, can take values from one to eight unless stated otherwise. For the Dirac matrices, the following relation holds:

$$\{\gamma^\mu, \gamma^\nu\} = \gamma^\mu \gamma^\nu + \gamma^\nu \gamma^\mu = 2g^{\mu\nu} \cdot \mathbb{1}_{4\times4} \tag{A.3}$$

The Gell-Mann matrices, as a base for the $SU(3)$, are used in the minimal possible presentation

$$\lambda_0 = \sqrt{\frac{2}{3}} \begin{pmatrix} 1 & 0 & 0 \\ 0 & 1 & 0 \\ 0 & 0 & 1 \end{pmatrix} \qquad \lambda_1 = \begin{pmatrix} 0 & 1 & 0 \\ 1 & 0 & 0 \\ 0 & 0 & 0 \end{pmatrix}$$

$$\lambda_2 = \begin{pmatrix} 0 & -i & 0 \\ i & 0 & 0 \\ 0 & 0 & 0 \end{pmatrix} \qquad \lambda_3 = \begin{pmatrix} 1 & 0 & 0 \\ 0 & -1 & 0 \\ 0 & 0 & 0 \end{pmatrix}$$

$$\lambda_4 = \begin{pmatrix} 0 & 0 & 1 \\ 0 & 0 & 0 \\ 1 & 0 & 0 \end{pmatrix} \qquad\qquad \lambda_5 = \begin{pmatrix} 0 & 0 & -i \\ 0 & 0 & 0 \\ i & 0 & 0 \end{pmatrix}$$

$$\lambda_6 = \begin{pmatrix} 0 & 0 & 0 \\ 0 & 0 & 1 \\ 0 & 1 & 0 \end{pmatrix} \qquad\qquad \lambda_7 = \begin{pmatrix} 0 & 0 & 0 \\ 0 & 0 & -i \\ 0 & i & 0 \end{pmatrix}$$

$$\lambda_8 = \frac{1}{\sqrt{3}} \begin{pmatrix} 1 & 0 & 0 \\ 0 & 1 & 0 \\ 0 & 0 & -2 \end{pmatrix}$$

with the anti-commutator relation

$$\left[\lambda^i, \lambda^j \right] = \lambda^i \lambda^j - \lambda^j \lambda^i = 2i f_{ijk} \lambda^k . \tag{A.4}$$

Here f_{ijk} denote the complete antisymmetric structure constants of the Lie algebra. The non-vanishing ones read:

$$f_{123} = 1 \tag{A.5}$$

$$f_{213} = -1 \tag{A.6}$$

$$f_{147} = f_{165} = f_{246} = f_{257} = f_{345} = f_{376} = \frac{1}{2} \tag{A.7}$$

$$f_{458} = f_{678} = \frac{\sqrt{3}}{2} \tag{A.8}$$

The generators of an arbitrary $SU(N)$ matrix will be denoted by τ. In case of $N = 2$, the generators are given by the three Pauli matrices.

Moreover, all calculations will be performed in natural units, which means that

$$c_0 = \hbar = k_B = 1 \tag{A.9}$$

holds.

Appendix B

Fierz transformation

B.1. Dirac space

A general 4x4 matrix in Dirac space can be expressed by

$$M = A_S \mathbb{1} + A_P i \gamma_5 + A_V^\mu \gamma_\mu + A_A^\mu \gamma_\mu \gamma_5 + A_T^{\mu\nu} \sigma_{\mu\nu} \tag{B.1}$$

with scalar, pseudoscalar, vector, axial vector and tensor coefficients A_S, A_P, A_V^μ, A_A^μ and $A_T^{\mu\nu}$. In order to determine these coefficients we can project into each channel by taking the trace of M with certain factors

$$\text{tr}\,(M) = 4A_S \tag{B.2}$$

$$\text{tr}\,(i\gamma_5 M) = -4A_P \tag{B.3}$$

$$\text{tr}\,\left(\gamma^\lambda M\right) = 4A_V^\lambda \tag{B.4}$$

$$\text{tr}\,\left(\gamma^\lambda \gamma_5 M\right) = -4A_A^\lambda \tag{B.5}$$

$$\text{tr}\,\left(\sigma^{\alpha\beta} M\right) = 8A_T^{\alpha\beta}. \tag{B.6}$$

Hence, we are able to rewrite M

$$M = \frac{1}{4}\left(\text{tr}\,(M)\,\mathbb{1} - \text{tr}_{i\gamma_5 M}\,(i)\,\gamma_5 + \text{tr}\,(\gamma^\mu M)\,\gamma_\mu - \text{tr}\,(\gamma^{\mu\gamma_5} M)\,\gamma_\mu\gamma_5 + \frac{1}{2}\text{tr}\,(\sigma^{\mu\nu} M)\,\sigma_{\mu\nu}\right). \tag{B.7}$$

Thus, we find that the components of the Matrix M are given by

$$M_{ij} = \frac{1}{4}\Big[M_{mm}\delta_{ij} - (i\gamma_5)_{mn} M_{nm}(i\gamma_5)_{ij} + (\gamma^\mu)_{mn} M_{nm}(\gamma^\mu)_{ij}$$

$$- (\gamma^\mu\gamma_5)_{mn} M_{nm}(\gamma_\mu\gamma_5)_{ij} + \frac{1}{2}(\sigma^{\mu\nu})_{mn} M_{nm}(\sigma_{\mu\nu})_{ij} \Big]. \tag{B.8}$$

Therefore, it follows

$$M_{nm}\delta_{in}\delta_{jm} = \frac{1}{4}M_{nm}\Big[\delta_{mn}\delta_{ij} - (i\gamma_5)_{mn}(i\gamma_5)_{ij} + (\gamma^\mu)_{mn}(\gamma_\mu)_{ij}$$
$$- (i\gamma^\mu\gamma_5)_{mn}(i\gamma_\mu\gamma_5)_{ij} + \frac{1}{2}(\sigma^{\mu\nu})_{mn}(\sigma_{\mu\nu})_{ij}\Big], \qquad \text{(B.9)}$$

which leads for the Kronecker delta to

$$\delta_{in}\delta_{jm} = \frac{1}{4}\Big[\delta_{mn}\delta_{ij} - (i\gamma_5)_{mn}(i\gamma_5)_{ij} + (\gamma^\mu)_{mn}(\gamma_\mu)_{ij}$$
$$- (i\gamma^\mu\gamma_5)_{mn}(i\gamma_\mu\gamma_5)_{ij} + \frac{1}{2}(\sigma^{\mu\nu})_{mn}(\sigma_{\mu\nu})_{ij}\Big]. \qquad \text{(B.10)}$$

For each channel, we can now perform a Fierz transformation which is a long but straightforward calculation and therefore will not shown in detail. The summarised results for the particle-antiparticle channel reads

$$\begin{pmatrix} \mathbb{1}_{\bar{i}j}\mathbb{1}_{\bar{k}l} \\ (i\gamma_5)_{\bar{i}j}(i\gamma_5)_{\bar{k}l} \\ (\gamma^\mu)_{\bar{i}j}(\gamma^\mu)_{\bar{k}l} \\ (i\gamma_\mu\gamma_5)_{\bar{i}j}(i\gamma_\mu\gamma_5)_{\bar{k}l} \\ (\sigma_{\mu\nu})_{\bar{i}j}(\sigma_{\mu\nu})_{\bar{k}l} \end{pmatrix} = \begin{pmatrix} \frac{1}{4} & -\frac{1}{4} & \frac{1}{4} & -\frac{1}{4} & \frac{1}{8} \\ -\frac{1}{4} & \frac{1}{4} & \frac{1}{4} & -\frac{1}{4} & \frac{1}{8} \\ 1 & 1 & \frac{1}{2} & -\frac{1}{2} & 0 \\ -1 & -1 & \frac{1}{2} & -\frac{1}{2} & 0 \\ 3 & -3 & 0 & 0 & -\frac{1}{2} \end{pmatrix} \begin{pmatrix} \mathbb{1}_{\bar{i}l}\mathbb{1}_{\bar{k}j} \\ (i\gamma_5)_{\bar{i}l}(i\gamma_5)_{\bar{k}j} \\ (\gamma^\mu)_{\bar{i}l}(\gamma^\mu)_{\bar{k}j} \\ (i\gamma_\mu\gamma_5)_{\bar{i}l}(i\gamma_\mu\gamma_5)_{\bar{k}j} \\ (\sigma_{\mu\nu})_{\bar{i}l}(\sigma_{\mu\nu})_{\bar{k}j} \end{pmatrix}. \qquad \text{(B.11)}$$

In a more compact form the upper expression is given by

$$\Delta^N_{ij}\Delta^N_{st} = \sum_{N'} f_{NN'}\Delta^{N'}_{it}\Delta^{N'}_{sj}, \qquad \text{(B.12)}$$

where $f_{NN'}$ are the matrix-elements of the 4x4 matrix in equation (B.11).

Now we want to find a similar equation for the particle-particle channel. For this purpose, the charge conjugation operator $C := i\gamma_2\gamma_0$ will be introduced. As mentioned in the main-text, it satisfies the conditions given in equation (2.14) and (2.15). By applying this on the different spin channels yields

$$C^{-1}\mathbb{1}C = \mathbb{1}^T, \qquad \text{(B.13)}$$
$$C^{-1}i\gamma_5 C = i\gamma_5^T, \qquad \text{(B.14)}$$
$$C^{-1}\gamma_\mu C = -\gamma_\mu^T, \qquad \text{(B.15)}$$
$$C^{-1}\gamma_\mu\gamma_5 C = (\gamma_\mu\gamma_5)^T, \qquad \text{(B.16)}$$
$$C^{-1}\sigma_{\mu\nu}C = -\sigma_{\mu\nu}^T, \qquad \text{(B.17)}$$

which can also be brought into a more comfortable form

$$(\Delta^N)^T = -S^{(N)}C\Delta^N C. \qquad \text{(B.18)}$$

Here

$$S^{(N)} = \begin{cases} S^{(S)} = S^{(P)} = S^{(A)} = 1 \\ S^{(V)} = S^{(T)} = -1 \end{cases}, \tag{B.19}$$

holds By virtue of equation (B.18), the expression for the Fierz transformation in the particle-particle yields

$$\Delta_{\bar{i}j}^N \Delta_{\bar{k}l}^N = \Delta_{\bar{i}j}^N (\Delta_{l\bar{k}}^N)^T \tag{B.20}$$

$$= -S^{(N)} \Delta_{\bar{i}j}^N (C\Delta^N C)_{l\bar{k}} \tag{B.21}$$

$$= -S^{(N)} \Delta_{\bar{i}j}^N C_{l\bar{s}} \Delta_{\bar{s}t}^N C_{t\bar{k}} \tag{B.22}$$

$$= -S^{(N)} \sum_{N'} f_{NN'} \Delta_{\bar{i}t}^{N'} C_{l\bar{s}} C_{t\bar{k}} \Delta_{\bar{s}j}^{N'} \tag{B.23}$$

$$= -S^{(N)} \sum_{N'} f_{NN'} (\Delta^{N'} C)_{\bar{i}k} (C\Delta^{N'})_{lj} \tag{B.24}$$

where $f_{NN'}$ are again the components of the transformation matrix from (B.11). Hence we found:

$$\begin{pmatrix} \mathbb{1}_{\bar{i}j} \mathbb{1}_{\bar{k}l} \\ (i\gamma_5)_{\bar{i}j}(i\gamma_5)_{\bar{k}l} \\ (\gamma^\mu)_{\bar{i}j}(\gamma^\mu)_{\bar{k}l} \\ (i\gamma_\mu\gamma_5)_{\bar{i}j}(i\gamma_\mu\gamma_5)_{\bar{k}l} \\ (\sigma_{\mu\nu})_{\bar{i}j}(\sigma_{\mu\nu})_{\bar{k}l} \end{pmatrix} = \begin{pmatrix} \frac{1}{4} & -\frac{1}{4} & \frac{1}{4} & -\frac{1}{4} & \frac{1}{8} \\ -\frac{1}{4} & \frac{1}{4} & \frac{1}{4} & -\frac{1}{4} & \frac{1}{8} \\ 1 & 1 & \frac{1}{2} & -\frac{1}{2} & 0 \\ -1 & -1 & \frac{1}{2} & -\frac{1}{2} & 0 \\ 3 & -3 & 0 & 0 & -\frac{1}{2} \end{pmatrix} \begin{pmatrix} C_{\bar{i}k}C_{lj} \\ (i\gamma_5 C)_{\bar{i}k}(Ci\gamma_5)_{lj} \\ (\gamma^\mu C)_{\bar{i}k}(C\gamma^\mu)_{lj} \\ (i\gamma_\mu\gamma_5 C)_{\bar{i}k}(Ci\gamma_\mu\gamma_5)_{lj} \\ (\sigma_{\mu\nu}C)_{\bar{i}k}(C\sigma_{\mu\nu})_{lj} \end{pmatrix}. \tag{B.25}$$

B.2. Flavour and colour space

Since the flavour and colour symmetries are both members of the special unitary group $SU(N)$, we can discuss them simultaneously. So let τ_a, with $a = 1, \ldots, N^2 - 1$, be a traceless hermitian NxN matrices with normalisation condition

$$\text{tr}\left(\tau_a \tau_b\right) = 2\delta_{ab}. \tag{B.26}$$

It is commonly known that every complex NxN matrix can be written in a basis formed by $\mathbb{1}, i\mathbb{1}, \tau, i\tau$ as

$$A = (a + ib)\mathbb{1} + (c_j + id_j)\tau_j. \tag{B.27}$$

According to the commutator relation for a Lie-algebra, we find:

$$[\tau_a, \tau_b] = 2if_{abc}\tau_c \tag{B.28}$$

$$\{\tau_a, \tau_b\} = \frac{4}{N}\delta_{ab} + 2d_{abc}\tau_c \tag{B.29}$$

$$\mathrm{tr}\left([\tau_a, \tau_b]\tau_c\right) = 4if_{abc} \tag{B.30}$$

$$\mathrm{tr}\left(\{\tau_a, \tau_b\}\tau_c\right) = 4d_{abc} \tag{B.31}$$

with f_{abc} and d_{abc} are totally antisymmetric and totally symmetric quantities, respectively. We can now perform the same steps as in the last section for the Dirac space, in an other basis. At first, a general NxN matrix can be written as

$$M = A_0\mathbb{1} + A_a\tau_a \tag{B.32}$$

and projected into the different channels

$$M = \frac{1}{N}\mathrm{tr}\left(M\right)\mathbb{1} + \frac{1}{2}\mathrm{tr}\left(\tau_a M\right)\tau_a. \tag{B.33}$$

This leads to the Kronecker delta

$$\delta_{il}\delta_{kj} = \frac{1}{N}\delta_{ij}\delta_{kl} + \frac{1}{2}(\tau_a)_{ij}(\tau_a)_{kl}, \tag{B.34}$$

which is needed in the Fierz transformation for the particle–antiparticle channel. The result reads

$$\begin{pmatrix} \mathbb{1}_{\bar{i}j}\mathbb{1}_{\bar{k}l} \\ (\tau_a)_{\bar{i}j}(\tau_a)_{\bar{k}l} \end{pmatrix} = \begin{pmatrix} \frac{1}{N} & \frac{1}{2} \\ 2\left(\frac{N^2-1}{N^2}\right) & -\frac{1}{N} \end{pmatrix} \begin{pmatrix} \mathbb{1}_{\bar{i}l}\mathbb{1}_{\bar{k}j} \\ (\tau_a)_{\bar{i}l}(\tau_a)_{\bar{k}j} \end{pmatrix}. \tag{B.35}$$

For the particle-particle channel we can rewrite expression (B.34) to

$$\mathbb{1}_{\bar{i}j}\mathbb{1}_{\bar{k}l} = \mathbb{1}_{\bar{i}j}\mathbb{1}_{l\bar{k}} = \frac{1}{N}\delta_{\bar{i}\bar{k}}\delta_{lj} + \frac{1}{2}(\tau_a)_{\bar{i}\bar{k}}(\tau_a)_{lj} \tag{B.36}$$

and separate the symmetric (τ_S) and antisymmetric (τ_A) terms

$$\mathbb{1}_{\bar{i}l}\mathbb{1}_{l\bar{k}} = \frac{1}{N}\delta_{\bar{i}\bar{k}}\delta_{lj} + \frac{1}{2}(\tau_S)_{\bar{i}\bar{k}}(\tau_S)_{jl} - \frac{1}{2}(\tau_A)_{\bar{i}\bar{k}}(\tau_A)_{jl}. \tag{B.37}$$

In case of $N = 3$, $\tau_S \in \{\lambda_1, \lambda_3, \lambda_4, \lambda_6, \lambda_8\}$ and $\tau_A \in \{\lambda_2, \lambda_5, \lambda_7\}$ holds. The latter can also be expressed with the total antisymmetric tensor $\epsilon^i_{jk} := \epsilon_{ijk}$:

$$i\epsilon^1_{ab} := -\lambda_7 \tag{B.38}$$

$$i\epsilon^2_{ab} := \lambda_5 \tag{B.39}$$

$$i\epsilon^3_{ab} := -\lambda_2 \tag{B.40}$$

Thereupon, it follows that

$$(\tau_a)_{\bar{i}j}(\tau_a)_{\bar{k}l} = 2\left(\frac{N-1}{N^2}\right)\mathbb{1}_{\bar{i}k}\mathbb{1}_{jl} + \left(\frac{N-1}{N}\right)(\tau_S)_{\bar{i}k}(\tau_S)_{jl}$$

$$+ \left(\frac{N+1}{N}\right)(\tau_A)_{\bar{i}k}(\tau_A)_{jl}, \qquad (B.41)$$

holds, which in combination with $\tau_0 := \sqrt{\frac{2}{N}}\mathbb{1}$, leads to

$$\begin{pmatrix} \mathbb{1}_{\bar{i}j}\mathbb{1}_{\bar{k}l} \\ (\tau_a)_{\bar{i}j}(\tau_a)_{\bar{k}l} \end{pmatrix} = \begin{pmatrix} \frac{1}{N} & \frac{1}{2} \\ \left(\frac{N-1}{N}\right) & -\left(\frac{N+1}{N}\right) \end{pmatrix} \begin{pmatrix} (\tau_S)_{\bar{i}k}(\tau_S)_{jl} \\ (\tau_A)_{\bar{i}k}(\tau_A)_{jl} \end{pmatrix}. \qquad (B.42)$$

B.3. Example: Colour-current interaction

As an example we want perform a full Fierz transformation and separation of the particle-antiparticle and particle-particle channel, on the colour-current interaction Lagrangian given in equation (2.26). In the particle-antiparticle channel we have two types of diagrams: The first one is the direct particle-antiparticle vertex
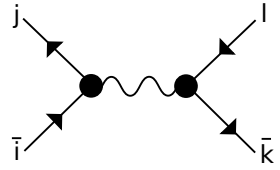
$$= -2ig(\gamma^\mu\lambda^a)_{j\bar{i}}(\gamma_\mu\lambda^a)_{\bar{k}l} \qquad (B.43)$$

The second one is the so-called exchange diagram and reads
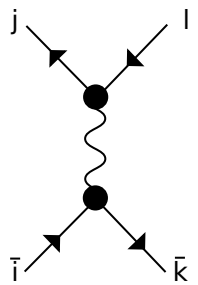
$$= 2ig(\gamma^\mu\lambda^a)_{jl}(\gamma_\mu\lambda^a)_{\bar{k}\bar{i}}, \qquad (B.44)$$

where the negative sign for the fermion exchange is already included. We can now perform a Fierz transformation in the exchange diagram to obtain the total vertex structure in the particle-antiparticle channel. In order to do this, we need the

transformation rules in the different spaces[1]

$$(\gamma^{\mu})_{jl}(\gamma_{\mu})_{\bar{k}\bar{i}} = \mathbb{1}_{j\bar{i}}\mathbb{1}_{kl} - (i\gamma_5)_{j\bar{i}}(i\gamma_5)_{kl} - \frac{1}{2}(\gamma^{\mu})_{j\bar{i}}(\gamma^{\mu})_{kl} - \frac{1}{2}(\gamma^{\mu}\gamma_4)_{j\bar{i}}(\gamma_{\mu}\gamma_5)_{kl} \quad (B.45)$$

$$(\mathbb{1}_f)_{jl}(\mathbb{1}_f)_{\bar{k}\bar{i}} = \frac{1}{2}(\mathbb{1}_f)_{j\bar{i}}(\mathbb{1}_f)_{kl} + \frac{1}{2}(\tau_m)_{j\bar{i}}(\tau_m)_{kl} \quad (B.46)$$

$$(\lambda^a)_{jl}(\lambda^a)_{\bar{k}\bar{i}} = 2\frac{N_c^2 - 1}{N_c^2}(\mathbb{1}_c)_{j\bar{i}}(\mathbb{1}_c)_{kl} - \frac{1}{N_c}(\lambda^a)_{j\bar{i}}(\lambda^a)_{kl} \quad (B.47)$$
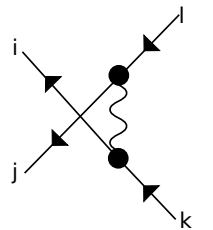
which leads to the (full) particle-antiparticle channel:

$$2ig\left\{\frac{N_c^2 - 1}{N_c^2}\left[\mathbb{1}_{j\bar{i}}\mathbb{1}_{\bar{k}l} + (i\gamma_5)_{j\bar{i}}(i\gamma_5)_{\bar{k}l} - \frac{1}{2}(\gamma^{\mu})_{j\bar{i}}(\gamma_{\mu})_{\bar{k}l} - \frac{1}{2}(\gamma^{\mu}\gamma_5)_{j\bar{i}}(\gamma_{\mu}\gamma_5)_{\bar{k}l}\right.\right.$$

$$+ (\tau_m)_{j\bar{i}}(\tau_m)_{\bar{k}l} + (i\gamma_5\tau_m)_{j\bar{i}}(i\gamma_5\tau_m)_{\bar{k}l} - \frac{1}{2}(\gamma^{\mu}\tau_m)_{j\bar{i}}(\gamma_{\mu}\tau_m)_{\bar{k}l} -$$

$$\frac{1}{2}(\gamma^{\mu}\gamma_5\tau_m)_{j\bar{i}}(\gamma_{\mu}\gamma_5\tau_m)_{\bar{k}l}\Big]$$

$$- \frac{1}{2N_c}\left[(\lambda^a)_{j\bar{i}}(\lambda^a)_{\bar{k}l} + (i\gamma_5\lambda^a)_{j\bar{i}}(\gamma_5\lambda^a)_{\bar{k}l} + (2N_c - \frac{1}{2})(\gamma^{\mu}\lambda^a)_{j\bar{i}}(\gamma_{\mu}\lambda^a)_{\bar{k}l}\right.$$

$$- \frac{1}{2}(\gamma^{\mu}\gamma_5\lambda^a)_{j\bar{i}}(\gamma_{\mu}\gamma_5\lambda^a)_{\bar{k}l} + (\tau_m\lambda^a)_{j\bar{i}}(\tau_m\lambda^a)_{\bar{k}l}$$

$$+ (i\gamma_5\tau_m\lambda^a)_{j\bar{i}}(i\gamma_5\tau_m\lambda^a)_{\bar{k}l} - \frac{1}{2}(\gamma^{\mu}\tau_m\lambda^a)_{j\bar{i}}(\gamma_{\mu}\tau_m\lambda^a)_{\bar{k}l}$$

$$\left.\left. - \frac{1}{2}(\gamma^{\mu}\gamma_5\tau_m\lambda^a)_{j\bar{i}}(\gamma_{\mu}\gamma_5\tau_m\lambda^a)_{\bar{k}l}\right]\right\} \quad (B.48)$$

For the particle-particle channel we can also find two diagrams
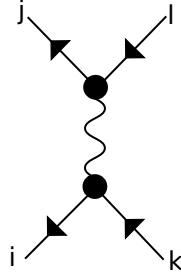
$$= 2ig(\gamma^{\mu}\lambda^a)_{jl}(\gamma_{\mu}\lambda^a)_{ik}, \quad (B.49)$$

$$= -2ig(\gamma^{\mu}\lambda^a)_{jl}(\gamma_{\mu}\lambda^a)_{ik}. \quad (B.50)$$

---

[1]We set $N_f = 2$, but do not fix the number of colours, because later we want to make different assumptions.

Here, the diagram shown in B.50 will be implemented later when we model the diquarks. As we want to perform a Fierz transformation into the particle-particle channel the upper transformation rules have been modified with the charge conjugation operator mentioned in the previous section

$$
(\gamma^\mu)_{jl}(\gamma_\mu)_{ik} = C_{ji}C_{kl} + (i\gamma_5 C)_{ji}(Ci\gamma_5)_{kl} - \frac{1}{2}(\gamma^\mu C)_{ji}(C\gamma_\mu)_{kl} - \frac{1}{2}(\gamma^\mu\gamma_5 C)_{ji}(C\gamma_\mu\gamma_5)_{kl}
$$

(B.51)

$$
(\mathbb{1}_f)_{jl}(\mathbb{1}_f)_{ik} = \frac{1}{2}(\tau_S)_{ji}(\tau_S)_{kl} + \frac{1}{2}(\tau_A)_{ji}(\tau_A)_{kl}
$$

(B.52)

$$
(\lambda^a)_{jl}(\lambda^a)_{ik} = \frac{N_c-1}{N_c}(\lambda_S)_{ji}(\lambda_S)_{kl} - \frac{N_c+1}{N_c}(\lambda_A)_{ji}(\lambda_A)_{kl}\,.
$$

(B.53)

Here, the index S denote the symmetric and A the antisymmetric matrices of a certain space, i.e. the Gell-Mann matrices in colour and Pauli matrices in flavour space. Hence, we find for the particle-particle channel the vertex structure

$$
2ig\Bigg\{ \frac{N_c+1}{2N_c}\Big[(C\tau_A\lambda_{A'})_{ji}(C\tau_A\lambda_{A'})_{kl} + (i\gamma_5 C\tau_A\lambda_{A'})_{ji}(Ci\gamma_5\tau_A\lambda_{A'})_{kl}
$$

$$
- \frac{1}{2}(\gamma^\mu\gamma_5 C\tau_A\lambda_{A'})_{ji}(C\gamma_5\gamma_\mu\tau_A\lambda_{A'})_{kl} - \frac{1}{2}(\gamma^\mu C\tau_S\lambda_{A'})_{ji}(C\gamma_\mu\tau_S\lambda_{A'})_{kl}\Big]
$$

$$
- \frac{N_c-1}{2N_c}\Big[(C\tau_A\lambda_{S'})_{ji}(C\tau_A\lambda_{S'})_{kl} + (i\gamma_5 C\tau_A\lambda_{S'})_{ji}(Ci\gamma_5\tau_A\lambda_{S'})_{kl}
$$

$$
- \frac{1}{2}(\gamma^\mu C\tau_A\lambda_{S'})_{ji}(C\gamma_\mu\tau_A\lambda_{S'})_{kl} - \frac{1}{2}(\gamma^\mu\gamma_5 C\tau_A\lambda_{S'})_{ji}(C\gamma_\mu\gamma_5\tau_A\lambda_{S'})_{kl}\Big]
$$

$$
+ \text{total symmetric terms} \Bigg\}\,.
$$

(B.54)

Appendix C

Medium Version of I_1

In order to obtain an expression for the in-medium contribution gap equation, we have to modify the integral I_1. Due to the simplicity of I_1, we will introduce the techniques that can be used for other integrals as well. The integral I_1 in the setting of finite temperature field theory with respect to the Matsubara formalism reads

$$L_1(M, T, \mu) := iI_1(M, T, \mu) = -T \sum_{\{i\nu\}} \int \frac{\mathrm{d}^3 k}{(2\pi)^3} \frac{1}{(i\nu + \mu)^2 + E_k^2} \, . \tag{C.1}$$

A commonly used trick to evaluate the sum over Matsubara frequencies is to rewrite it as a contour integral. Indeed, using the residuum theorem backwards and taking into account

$$\operatorname*{Res}_{\substack{z=i\nu \\ z=i\omega}} \left(\frac{1}{\exp(\beta z) \pm 1} \right) = \mp T \, , \tag{C.2}$$

where the upper sign holds for fermionic Matsubara frequencies and the lower for bosonic ones. The corresponding function are the Fermi-Dirac distribution function

$$n_F(z) := \frac{1}{\exp(\beta z) + 1} \tag{C.3}$$

and the Bose-Einstein distribution function

$$n_B(z) := \frac{1}{\exp(\beta z) - 1} \, , \tag{C.4}$$

respectively. Hence, we can rewrite equation (C.1)

$$iI_1(M, T, \mu) = \int \frac{\mathrm{d}^3 k}{(2\pi)^3} \oint_{\mathcal{C}} \frac{\mathrm{d}z}{(2\pi)i} n_F(z) \frac{1}{(z + \mu)^2 - E_k^2} \, . \tag{C.5}$$

The contour $\mathcal{C}$ is shown on the left hand side of figure C.1. Note, that the integrand has two additional poles on the real axis at $z_\pm = \pm E_k - \mu$. Since the integrand of
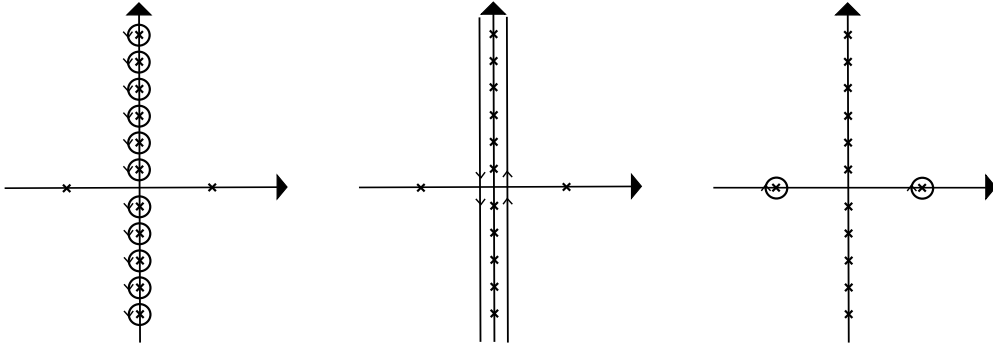
101

Figure C.1. Contour modification for Integral L_1. The left one in the original integration path, while the second one can be obtained by merging the circles around n_F or n_B, respectively. Evaluating L_1 with the last contour leads to equation (C.6).

equation (C.1) behaves like $1/z^2$, it is possible to redraw the contour in a way that we can use the residuum theorem again, but this time around the poles $z_\pm$, cf. figure C.1. We can always redraw the contour in this way of all integrals emerging in this work. After performing a partial-fraction decomposition of the integrand and evaluating the resulting expression at the two poles $z_\pm$, we arrive at

$$L_1(M,T,\mu) = \int \frac{\mathrm{d}^3k}{(2\pi)^3} \frac{1}{2E_k} (1 - n_F(E_k - \mu) - n_F(E_k + \mu)). \qquad (C.6)$$

The leading term is equal to the integrand we already found in the vacuum case. Since this integral is divergent, it will be regularised with the Pauli-Villar regularisation. To increase overview we will separate the vacuum and medium contribution

$$L_1(M,T,\mu) = L_1^{\mathrm{vac}}(M,\Lambda) + L_1^{\mathrm{med}}(M,T,\mu). \qquad (C.7)$$

Compared to the vaccum part, the medium contribution

$$L_1^{\mathrm{med}}(M,T,\mu) = - \int \frac{\mathrm{d}^3k}{(2\pi)^3} \frac{1}{2E_k} (n_F(E_k - \mu) + n_F(E_k + \mu)) \qquad (C.8)$$

is not divergent and therefore will not be regularised. More over, the medium part vanishes for $T \to 0$ due to the exponential character of $n_{F,B}$.

C.1. Properties of distribution functions

At this point some properties of the bosonic and fermionic distribution functions will be pointed out. At first, under an inversion of the argument we find

$$n_F(-z) = 1 - n_F(z) \tag{C.9}$$

$$n_B(-z) = -1 - n_B(z). \tag{C.10}$$

At some point in the discussion of mesons, diquarks and baryons we have to evaluate the distributions as functions of bosonic or fermionic Matsubara frequencies. It is easy to see how the Fermi distribution behaves under such shifts

$$n_F(z + i\omega) = n_F(z), \tag{C.11}$$

$$n_F(z + i\nu) = -n_B(z). \tag{C.12}$$

Here, we have taking into account that $e^{2n\pi i} = 1$ and $e^{(2n+1)\pi i} = -1$. For the Bose distribution a similar calculation leads to

$$n_B(z + i\omega) = n_B(z), \tag{C.13}$$

$$n_B(z + i\nu) = -n_F(z). \tag{C.14}$$

Moreover, an integration of the plain distributions yields

$$\int \mathrm{d}x\, n_F(x) = -T \ln\left(1 + e^{-\frac{x}{T}}\right), \tag{C.15}$$

$$\int \mathrm{d}x\, n_F(x) = T \ln\left(1 - e^{-\frac{x}{T}}\right). \tag{C.16}$$

Appendix D

Mesons
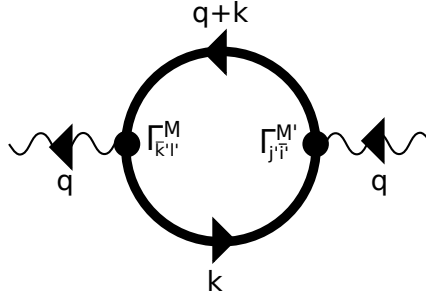
D.1. Pion polarisation loop

Figure D.1. Mesonic polarisation loop.

As mentioned in the main text, we have to evaluate the diagram shown in figure D.1 which leads to

$$-i\Pi^{M,M',f,f'} = \int \frac{\mathrm{d}^4k}{(2\pi)^4} \Gamma^{M,f}_{\bar{k}'l'} iS_{l'i'}(q+k)\Gamma^{M',f'}_{i'\bar{j}'} iS_{\bar{j}'\bar{k}'}(k) \tag{D.1}$$

$$= i \int \frac{\mathrm{d}^4k}{(2\pi)^4} \mathrm{Tr}\left(\Gamma^{M,f} iS_q(q+k)\Gamma^{M',f'} iS_{\bar{q}}(k)\right) \tag{D.2}$$

$$= \delta^{MM'}\mathrm{tr}_c\left(\mathbb{1}\right)\tau^f_{\bar{k}'i'}\tau^{f'}_{i'\bar{k}'} i \int \frac{\mathrm{d}^4k}{(2\pi)^4} \mathrm{tr}_D\left(i\gamma_5 iS_q(q+k)i\gamma_5 iS_{\bar{q}}(k)\right). \tag{D.3}$$

In the isospin limit the three pions, i.e. $|\pi^\pm\rangle$ and $|\pi^0\rangle$, are completely degenerated and thus, we can restrict ourself to the $|\pi^0\rangle$, which is physical represented when $\tau^{f'} = \tau^{f'} = \tau^3$ holds. For the charged pions one have to insert the Projectors given in table 3.1 with respect to

$$\tau^f_{\bar{k}'i'}\tau^f_{i'\bar{k}'} = \mathrm{tr}\left(\tau^f\tau^{f'}\right) = 2\delta^{ff'}, \tag{D.4}$$

which implies that the quark flavour of the mesons do not change in the propagation. After inserting the relation (D.4) into expression (D.3), we find

$$-i\Pi^{\pi^0} = -2\delta^{ff'}N_c i \int \frac{\mathrm{d}^4k}{(2\pi)^4} \, \mathrm{tr}_D \left(i\gamma_5 i S_q(q+k) i\gamma_5 i S_{\bar{q}}(k) \right) \tag{D.5}$$

$$= -2\delta^{ff'}N_c \int \frac{\mathrm{d}^4k}{(2\pi)^4} \, \mathrm{tr}_D \left(S_q(-q-k) S_{\bar{q}}(k) \right) , \tag{D.6}$$

where $\gamma_5 S(q)\gamma_5 = S(-q)$ has been used. The Dirac trace can now be evaluated which leads to

$$-i\Pi^{\pi^0}(q) = -2N_c \int \frac{\mathrm{d}^4k}{(2\pi)^4} \frac{qk + k^2 + M^2}{[(q+k)^2 - M^2] \cdot [k^2 - M^2]} \tag{D.7}$$

$$= -8N_c \left[-\int \frac{\mathrm{d}^4k}{(2\pi)^4} \frac{1}{2} \left(\frac{1}{(q+k)^2 - M^2} + \frac{1}{k^2 - M^2} \right) \right.$$

$$\left. + \frac{p^2}{2} \int \frac{\mathrm{d}^4k}{(2\pi)^4} \frac{1}{[(q+k)^2 - M^2] \cdot [k^2 - M^2]} \right] . \tag{D.8}$$

After a certain variable shift $k \mapsto k - q$, the first two integrals are equal, thus the integral I_1 appears. Hence, we find

$$-i\Pi^{\pi^0}(q) = 8N_c \int \frac{\mathrm{d}^4k}{(2\pi)^4} \frac{1}{k^2 - M^2} - 8N_c \frac{p^2}{2} \underbrace{\int \frac{\mathrm{d}^4k}{(2\pi)^4} \frac{1}{[(q+k)^2 - M^2] \cdot [k^2 - M^2]}}_{=:I_2(q)}$$
$$\tag{D.9}$$

$$= 8N_c I_1 - 4N_c q^2 I_2(q) , \tag{D.10}$$

where we have defined the integral I_2, which will be discussed in detail in the following section.

D.1.1. Integral iI_2

The integral iI_2 is defined by

$$iI_2(q) := i \int \frac{\mathrm{d}^4k}{(2\pi)^4} \frac{1}{[(q+k)^2 - M^2 + i\epsilon] \cdot [k^2 - M^2 + i\epsilon]} \tag{D.11}$$

and can be bought into a more general form

$$iI_2'(q^2) := i \int \frac{\mathrm{d}^4k}{(2\pi)^4} \frac{1}{[(q-k)^2 - M_1^2 + i\epsilon] \cdot [k^2 - M_2^2 + i\epsilon]} , \tag{D.12}$$

when we distinguish between the masses in the denominators. This new integral I_2' will be useful, when we discuss the baryons, thus we will concentrate on I_2' in the following short discussion. The results can be used for I_2 when $M_1 = M_2$ holds. An important difference between the integral I_2 and I_2' can be found by analysing its behaviour in the complex area.

Analogous to I_1, the q_0 integration of I_2' can be separated and performed with the residue theorem after rewriting the integrand and switching into the rest frame, i.e. $\vec{q} = 0$,

$$i I_2'(q_0, \vec{q} = 0) = i \int \frac{\mathrm{d}^4 k}{(2\pi)^4} \frac{1}{4 E_k E_k'} \left(\frac{1}{(q_0 - k_0) - E_k + i\epsilon} - \frac{1}{(q_0 - k_0) + E_k - i\epsilon} \right) \times \tag{D.13}$$

$$\times \left(\frac{1}{k_0 - E_p' + i\epsilon} - \frac{1}{k_0 + E_p' - i\epsilon} \right) .$$

Here, the energies with various masses are given by $E_k^2 = k^2 + M_1^2$ and $(E_k')^2 = k^2 + M_2^2$. Unlike the integral I_1 the Integral I_2' have four poles corresponding to the mass-shell of the two included particles, but only two of them will contribute to the integral. Using the residue theorem for the k_0 integration thus yields

$$i I_2'(q_0, \vec{q} = 0) = \int \frac{\mathrm{d}^3 k}{(2\pi)^3} \frac{1}{4 E_k E_k'} \left(\frac{1}{q_0 + E_k + E_k' - i\epsilon} - \frac{1}{q_0 - E_k - E_k' + i\epsilon} \right) . \tag{D.14}$$

Since this expression only depends on $\vec{k}^2 = k^2$, we can transform it easily into spherical coordinates

$$i I_2'(q_0, \vec{q} = 0) = \frac{1}{2\pi} \int_0^\infty \mathrm{d}k \, k^2 \frac{1}{4 E_k E_k'} \left(\frac{1}{q_0 + E_k + E_k' - i\epsilon} - \frac{1}{q_0 - E_k - E_k' + i\epsilon} \right) \tag{D.15}$$

$$= -\frac{1}{2\pi} \int_0^\infty \mathrm{d}k \, k^2 \frac{1}{2 E_k E_k'} \left(\frac{E_k + E_k'}{q_0^2 - (E_k + E_k')^2 + i\epsilon} \right) , \tag{D.16}$$

where we have already performed the angle integration.

The imaginary part of expression (D.16) can be determined with the identity

$$\lim_{\epsilon \to 0} \mathrm{Im} \left(\frac{1}{x + i\epsilon} \right) = -\pi \delta(x) . \tag{D.17}$$

Hence, we find

$$\mathrm{Im} \, i I_2'(q_0) = -\frac{1}{16\pi} \frac{\sqrt{[(M_1 + M_2)^2 - q_0^2][(M_2 - M_1)^2 - q_0^2]}}{\sqrt{q_0^2}} \Theta(q_0^2 - (M_1 + M_2)^2) . \tag{D.18}$$

The real part can be obtained by taking into account the Kramers-Kronig relation [36, 37]

$$\text{Re}(f(x)) = \frac{1}{\pi}\text{P.V.} \int \text{d}x' \, \frac{\text{Im}(f(x'))}{x' - x} \,, \tag{D.19}$$

which connects the imaginary part of a certain function f to its real part by a principal value integration. This integration will be performed numerically to be consistent with the treatment of later integral expressions. Unlike the later discussed integrals an additional factor of $\text{sign}(q)$ for I_2 and I_2' has to be multiplied to (D.18) in order to reproduce the analytical expression provided in reference [17] and other works. The sign function ensures that the real part has the right symmetry. For $q^2 > (M_1 + M_2)^2$
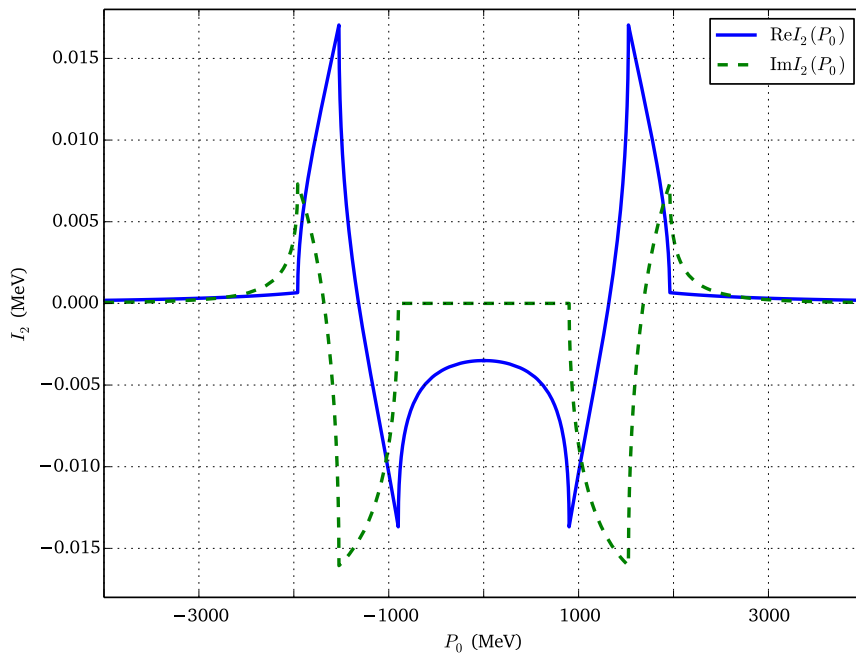

Figure D.2. Real and imaginary part of the integral I_2, where $M_1 = M_2$ holds.

the integral I_2' or I_2, respectively, obtains a non vanishing imaginary part, which leads to masses related to unstable particles and a non-real effective coupling as well. In the case of I_2 the imaginary part rises for $M_1 = M_2$ yields $q^2 > 4(M_1)^2$. A more detailed discussion of the physical consequences are given in the main text.

D.2. Medium version of pion polarisation loop

Since the propagator of a quark and an antiquark are identical in their functional form, the polarisation loop has the same structure as in the vacuum case. Beside the

integral iI_1, which has already been discussed in appendix C, we have to transform the integral iI_2 into its medium version. In accordance with the Matsubara formalism, the medium version of iI_2 reads

$$L_2(q_0, \vec{q}; T, \mu) := iI_2(q; T, \mu) \tag{D.20}$$

$$= -T \sum_{\{i\nu\}} \int \frac{\mathrm{d}^3 k}{(2\pi)^3} \frac{1}{\left((i\omega + i\nu + \mu)^2 - E_{q+k}^2\right) \cdot \left((i\nu + \mu)^2 - E_k^2\right)}, \tag{D.21}$$

with $E_{q+k}^2 := (\vec{q} + \vec{k})^2 + M^2$. Here, $i\omega$ is related to a bosonic frequence, while $i\nu$ is related to a fermionic one. Next, we will evaluate the upper integral expression.

D.2.1. The integral L_2

To simplify the discussion we assume $\vec{q} = 0$. Hence, equation (D.21) reduces to

$$L_2(i\omega, \vec{q} = 0; T, \mu) = -T \sum_{i\nu} \int \frac{\mathrm{d}^3 k}{(2\pi)^3} \frac{1}{\left((i\omega + i\nu + \mu)^2 - E_k^2\right) \cdot \left((i\nu + \mu)^2 - E_k^2\right)}. \tag{D.22}$$

A backward evaluation of the residue theorem with the Fermi distribution yields

$$L_2(i\omega, \vec{q} = 0; T, \mu) = \int \frac{\mathrm{d}^3 k}{(2\pi)^3} \oint_{\mathcal{C}} \frac{\mathrm{d}z}{2\pi i} n_F(z) \frac{1}{\left((i\nu + z + \mu)^2 - E_k^2\right) \cdot \left((z + \mu)^2 - E_k^2\right)}. \tag{D.23}$$

Compared to the integral L_1, L_2 has two additional poles in the complex plane due to $i\nu$ in the denominator of equation (D.22). The four poles are given by

$$z_{1\pm} = -i\omega - \mu \pm E_k, \tag{D.24}$$

$$z_{2\pm} = -\mu \pm E_k. \tag{D.25}$$

Again, it is possible to redraw the contour $\mathcal{C}$, which is shown in figure D.3. Evaluating the integral with the new contour on the right hand side of fig. D.3 around the 4 poles yields

$$L_2(i\omega, \vec{q} = 0; T, \mu) = -\int \frac{\mathrm{d}^3 k}{(2\pi)^3} \frac{1}{2E_k \cdot (i\omega)} \left(-\frac{n_F(-E_k - \mu)}{2E_k - i\omega} - \frac{n_F(E_k - \mu)}{2E_k + i\omega} \right. \tag{D.26}$$

$$\left. + \frac{n_F(-E_k - \mu - i\omega)}{2E_k + i\omega} + \frac{n_F(E_k - \mu - i\omega)}{2E_k - i\omega} \right).$$

Under virtue of equations (C.11)-(C.16) the upper expression can be simplified to

$$L_2(i\omega, \vec{q} = 0; T, \mu) = \int \frac{\mathrm{d}^3 k}{(2\pi)^3} \frac{1}{E_k} \frac{1}{(i\omega)^2 - 4E_k^2} \left(1 - n_f(E_k - \mu) - n_f(E_k + \mu) \right).$$
(D.27)

Therefore, the vacuum contribution can be identified directly

$$L_2^{\mathrm{vac}}(i\omega, \vec{q} = 0; T, \mu) = \int \frac{\mathrm{d}^3 k}{(2\pi)^3} \frac{1}{E_k} \frac{1}{(i\omega)^2 - 4E_k^2},$$
(D.28)

while the medium contribution reads

$$L_2^{\mathrm{med}}(i\omega, \vec{q} = 0; T, \mu) = - \int \frac{\mathrm{d}^3 k}{(2\pi)^3} \frac{1}{E_k} \frac{1}{(i\omega)^2 - 4E_k^2} \left(n_f(E_k - \mu) + n_f(E_k + \mu) \right).$$
(D.29)

In order to obtain the retarded version of the integral, we have to performe the analytical continuation $i\omega \mapsto q_0 + i\epsilon$. Hence, the vacuum and medium part yields

$$L_2^{\mathrm{vac}}(q_0, \vec{q} = 0; T, \mu) = \int \frac{\mathrm{d}^3 k}{(2\pi)^3} \frac{1}{E_k} \frac{1}{q_0^2 - 4E_k^2 + \mathrm{sign}(q_0)i\epsilon},$$
(D.30)

$$L_2^{\mathrm{med}}(q_0, \vec{q} = 0; T, \mu) = - \int \frac{\mathrm{d}^3 k}{(2\pi)^3} \frac{1}{E_k} \frac{1}{q_0^2 - 4E_k^2 + \mathrm{sign}(q_0)i\epsilon} \left(n_f(E_k - \mu) + n_f(E_k + \mu) \right),$$
(D.31)

where terms of ϵ^2 have been neglected. Since we treat the retarded version of the integral the vacuum part differs from I_2 by the sign in front of $i\epsilon$. In the following discussion we want to determine the imaginary part of equations (D.30) and (D.31). The real part, which is necessary to determine the roots of the inverse propagator, can be calculated by the Kramers-Kronig relation (D.19).
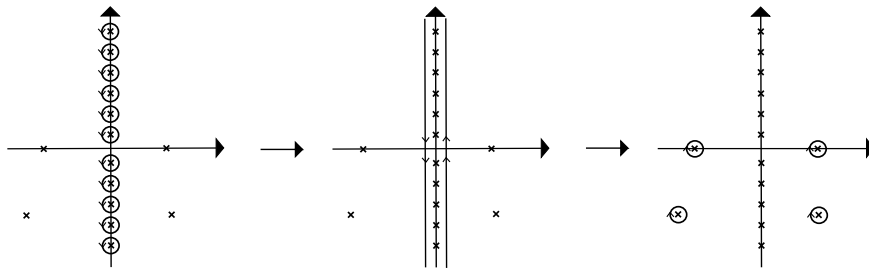

Figure D.3. Contour modification of integral L_2

Imaginary part of L_2^{vac}

As already mentioned, the imaginary part of equation (D.30) can be calculated by virtue of relation (D.17). Up to an addition factor of $\text{sign}(q_0)$ the imaginary part is equal to the one we find for iI_2', when $M_1 = M_2$ holds, cf. expression (D.18). For completeness, the imaginary part of L_2^{vac} reads

$$\text{Im}(L_2^{\text{vac}}(q_0, \vec{q} = 0; T, \mu)) = -\text{sign}(q_0)\frac{1}{16\pi}\frac{\sqrt{q_0^2 - 4M^2}}{q_0^2}\Theta(q_0^2 - 4M^2) \qquad \text{(D.32)}$$

Using the Kramers-Kronig relation (D.19) gives rise to the real part of L_2^{vac}.

Imaginary part of L_2^{med}

The medium contribution L_2^{med} in a compact form reads

$$L_2^{\text{med}}(q_0, \vec{q} = 0; T, \mu) = -\int \frac{\mathrm{d}^3 k}{(2\pi)^3}\frac{1}{E_k}\frac{1}{q_0^2 - 4E_k^2 + \text{sign}(q_0)i\epsilon}n_f(E_k \pm \mu). \qquad \text{(D.33)}$$

We can perform a simply variable transformation from the momentum integration into an energy integration to obtain

$$L_2^{\text{med}}(q_0, \vec{q} = 0; T, \mu) = -\int_{-\infty}^{\infty} \mathrm{d}E_k\,\Theta(E_k - M)\sqrt{E_k^2 - M^2}\,n_f(E_k \pm \mu)\frac{1}{q_0^2 - 4E_k^2 + \text{sign}(q_0)i\epsilon}. \tag{D.34}$$

Performing a second variable transformation with $x(E_k) := q_0^2 - 4E_k^2$ and taking into account the relation D.17 we have to evaluate the integral at $x = 0$. Finally, the imaginary part of L_2^{med} reads

$$\text{Im}(L_2^{\text{med}}(q_0, \vec{q} = 0; T, \mu)) = \text{sign}(q_0)\frac{1}{16\pi}\frac{\sqrt{q_0^2 - 4M^2}}{q_0^2}n_f\left(\frac{|q_0|}{2} \pm \mu\right)\Theta(q_0^2 - 4M^2), \tag{D.35}$$

where we have to sum over the possible signs. Again, the real part can be obtained by virtue of (D.19).

Appendix E

Diquaks

E.1. Diquark polarisation loop

The diquark polarisation loop, which we want to investigate, is diagrammatic represented in figure E.1. A carefull evaluation of the this diagram yields

$$\Pi^D_{f,f'}(q) = i \int \frac{\mathrm{d}^4 k}{(2\pi)^4} \, (C\Gamma^D)_{k'l'} iS_{l'i'}(k+q)(\Gamma^D C)_{i'j'} iS_{k'j'}(-k) \tag{E.1}$$

$$= i \int \frac{\mathrm{d}^4 k}{(2\pi)^4} \, (C\Gamma^D)_{k'l'} iS_{l'i'}(k+q)(\Gamma^D C)_{i'j'} iS^T_{j'k'}(-k) \tag{E.2}$$

$$= -i \int \frac{\mathrm{d}^4 k}{(2\pi)^4} \, \mathrm{Tr}\left(C\Gamma^D S(k+q)\Gamma^D C S^T(-k)\right) \tag{E.3}$$

$$= -i \int \frac{\mathrm{d}^4 k}{(2\pi)^4} \, \mathrm{Tr}\left(\Gamma^D S(k+q)\Gamma^D C S^T(-k)C\right) , \tag{E.4}$$

where, we have used the property of the trace to be invariant under a cyclic permutation. The transposed quark propagator in equation (E.4) can now be simplified
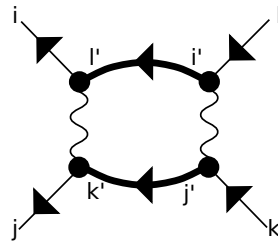

Figure E.1. Diquark polarisation loop.

through the relation

$$CS_q^T(-k)C = -S(k)\,,\tag{E.5}$$

which yields

$$\Pi^D(q) = -i \int \frac{\mathrm{d}^4 k}{(2\pi)^4} \operatorname{Tr}\left(\Gamma^D S(k+q)\Gamma^D S(k)\right)\,.\tag{E.6}$$

The diquark polarisation loop for the scalar antitriplet diquarks, with $\Gamma^D = i\gamma_5 \otimes \lambda_A \otimes \tau_A$, thus reads

$$\Pi^{sad}(q) = -i \int \frac{\mathrm{d}^4 k}{(2\pi)^4} \operatorname{Tr}\left(\Gamma^{sad} S_q(k+q)\Gamma^{sad} S_q(k)\right)\tag{E.7}$$

$$= \operatorname{tr}_c\left(\lambda_A \lambda_A\right)\operatorname{tr}_f\left(\tau_A \tau_A\right) \int \frac{\mathrm{d}^4 k}{(2\pi)^4} \operatorname{tr}_D\left(i\gamma_5 S_q(k+q)i\gamma_5 S_q(k)\right)\,,\tag{E.8}$$

with λ_A and τ_A are the antisymmetric Gell-Mann and Pauli matrices, respectively. Taking into account

$$\operatorname{tr}_c\left(\lambda_A \lambda_A\right) = \operatorname{tr}_f\left(\tau_A \tau_A\right) = 2\,,\tag{E.9}$$

in order to performing the traces in the three different spaces and finally, leads to

$$\Pi^{sad}(q) = 16iI_1 - 8q^2 iI_2(q)\,.\tag{E.10}$$

The calculations for the pseudoscalar diquark is completely analogous up to the different structure in Dirac space, i.e. $\Delta^{sad} = \mathbb{1}$. For the polarisation loop of the pseudoscalar diquarks we find

$$\Pi^{pad}(q) = 16iI_1 - (q^2 - 4M^2)8iI_2(q^2)\,.\tag{E.11}$$

E.1.1. Medium version of the diquark polarisation loop

We start from equation (4.25),

$$\Pi^D(i\omega + 2\mu, \vec{q}) = iT \sum_n \int \frac{\mathrm{d}^3 k}{(2\pi)^3} \operatorname{Tr}\left[\Gamma^D S(i\omega + i\nu_n + \mu, \vec{q} + \vec{k})\Gamma^D S(i\nu_n - \mu, \vec{k})\right]\,.\tag{E.12}$$

For the scalar diquarks, the traces in flavour- and colour-space give a factor of 2. Then, the trace in Dirac-space can be evaluated directly,

$$\Pi^{sad}(i\omega + 2\mu, \vec{q}) = -16T \sum_n \int \frac{\mathrm{d}^3 k}{(2\pi)^3} \frac{(i\omega + i\nu_n + \mu)(i\nu_n - \mu) - (\vec{q} + \vec{k})\vec{k} - M^2}{[(i\omega + i\nu_n + \mu)^2 - E_{q,k}^2][(i\nu_n - \mu)^2 - E_k^2]}\,.\tag{E.13}$$

The numerator can be expressed as

$$(i\omega + iv_n + mu)(iv_n - \mu) - (\vec{q} + \vec{k})\vec{k} - M^2 \tag{E.14}$$

$$= (iv_n)^2 - \mu^2 + (i\omega)(iv_n) - \mu(i\omega) - k^2 - \vec{q}\vec{k} - M^2 \tag{E.15}$$

$$= \frac{1}{2}\left((i\omega + iv_n + \mu)^2 - E_{q,k}^2 + (iv_n - \mu)^2 - E_k^2 - (i\omega)^2 - 4\mu - 4(i\omega)\mu + q^2\right) \tag{E.16}$$

$$= \frac{1}{2}\left((i\omega + iv_n + \mu)^2 - E_{q,k}^2 + (iv_n - \mu)^2 - E_k^2 - ((i\omega) + 2\mu)^2 - q^2\right). \tag{E.17}$$

Using this in the polarisation loop yields

$$\Pi^{\text{sad}}(i\omega + 2\mu, \vec{q}) = -8T\sum_n \int \frac{\mathrm{d}^3k}{(2\pi)^3}\left(\frac{1}{(i\omega + iv_n + \mu)^2 - E_{q,k}^2} + \frac{1}{(iv_n - \mu)^2 - E_k^2}\right) \tag{E.18}$$

$$+ 8T\left((i\omega) + 2\mu^2 - q^2\right)\sum_n \int \frac{\mathrm{d}^3k}{(2\pi)^3}\frac{1}{[(i\omega + iv_n + \mu)^2 - E_{q,k}^2][(iv_n - \mu)^2 - E_k^2]}.$$

If we assume a vanishing external momentum, i.e. $\vec{q} = 0$, the energies E_k and $E_{q,k}$ are equal. Moreover, we can replace $iv_n + i\omega \longrightarrow iv_n$ and $iv_n \longrightarrow -iv_n$. Then, the first integral is equal to L_1, cf. (C.6). The latter integral will be defined as

$$L_3(i\omega + 2\mu, \vec{q} = 0) := -T\sum_n \int \frac{\mathrm{d}^3k}{(2\pi)^3}\frac{1}{[(i\omega + iv_n + \mu)^2 - E_k^2][(iv_n - \mu)^2 - E_k^2]} \tag{E.19}$$

We will take a closer look at this integral in the following section.

E.1.2. The integral L_3

The integral L_3 will be evaluated similar to L_2 in the discussion of the mesons. After using the residue theorem backwards by virtue of the Fermi distribution n_F we can deform the contour to the poles on the complex plane as shown in previous chapters. Then, the residue theorem again, yields

$$L_3(i\omega + 2\mu, \vec{q} = 0) = -\int \frac{\mathrm{d}^3k}{(2\pi)^3}\frac{1}{4E_k^2}\left[n_F(-E_k + \mu)\left(\frac{1}{i\omega + 2\mu} - \frac{1}{i\omega + 2\mu - 2E_k}\right)\right. \tag{E.20}$$

$$+ n_F(E_k + \mu)\left(\frac{1}{i\omega + 2\mu} - \frac{1}{i\omega + 2\mu + 2E_k}\right)$$

$$- n_F(-E_k - \mu - i\omega)\left(\frac{1}{i\omega + 2\mu} - \frac{1}{i\omega + 2\mu + 2E_k}\right)$$

$$\left.- n_F(E_k - \mu - i\omega)\left(\frac{1}{i\omega + 2\mu} - \frac{1}{i\omega + 2\mu - 2E_k}\right)\right].$$

Taking into account the properties of the Fermi distribution given in section C.1, this can be expressed as

$$L_3(i\omega + 2\mu, \vec{q} = 0) = -\int \frac{\mathrm{d}^3 k}{(2\pi)^3} \frac{1}{2E_k^2} \Big[-\frac{2E_k}{(i\omega + 2\mu)^2 - 4E_k^2}$$

$$+ 2n_F(E_k - \mu) \left(\frac{E_k}{(i\omega + 2\mu)^2 - 2E_k(i\omega + 2\mu)} \right)$$

$$+ 2n_F(E_k + \mu) \left(\frac{E_k}{(i\omega + 2\mu)^2 + 2E_k(i\omega + 2\mu)} \right) \Big]. \tag{E.21}$$

As expected the integrand depends on $i\omega + 2\mu$, such as the complete diquark polarisation loop does. Now, an analytical continuation of the form $i\omega \mapsto q_0$ leads to

$$L_3(q_0, 0) = \int \frac{\mathrm{d}^3 k}{(2\pi)^3} \frac{1}{E_k} \Big[\frac{1}{(q_0 + 2\mu)^2 - 4E_k^2}$$

$$- n_F(E_k - \mu) \frac{1}{(q_0 + 2\mu)^2 - 2q_0 E_k} - n_F(E_k + \mu) \frac{1}{(q_0 + 2\mu)^2 + 2q_0 E_k} \Big]. \tag{E.22}$$

The first term describes the vacuum contribution for $\mu = 0$ MeV, similar to L_2^{vac}. Hence, we can can decompose the integral into a vacuum and medium contribution

$$\tilde{L}(q_0, 0) = \tilde{L}^{\mathrm{vac}}(q_0, 0) + \tilde{L}^{\mathrm{med}}(q_0, 0), \tag{E.23}$$

with

$$L_3^{\mathrm{vac}}(q_0, 0) := \int \frac{\mathrm{d}^3 k}{(2\pi)^3} \frac{1}{E_k} \frac{1}{(q_0 + 2\mu)^2 - 4E_k^2}, \tag{E.24}$$

$$L_3^{\mathrm{med}}(q_0, 0) := -\int \frac{\mathrm{d}^3 k}{(2\pi)^3} \frac{1}{E_k} \left(n_F(E_k - \mu) \frac{1}{(q_0 + 2\mu)^2 - 2q_0 E_k} \right.$$

$$\left. + n_F(E_k + \mu) \frac{1}{(q_0 + 2\mu)^2 + 2q_0 E_k} \right). \tag{E.25}$$

Since the evaluation of the vacuum contribution is straightforward and similar to the one discussed in appendix D.2.1, we will evaluate the imaginary part of the medium contribution in the following section. The real part can be obtained by performing a principal value integration in accordance with the Kramers-Kronig relation in (D.19).

Imaginary part

Again, we can use identity (D.17) to determine the imaginary part of L_3. The integrand of (E.25) can be rewritten

$$L_3^{\text{med}}(q_0, 0) = -\sum_{\pm} \int \frac{\mathrm{d}^3 k}{(2\pi)^3} \frac{1}{E_k} \frac{n_F(E_k \pm \mu)}{(q_0 + 2\mu)^2 \pm 2E_k(q_0 + 2\mu)} . \tag{E.26}$$

Here, the sum with index $\pm$ denotes a summation over the different signs. The integrand only depends on k^2 rather than the vector $\vec{k}$. Hence, we can perform the angle integration without any problems. After transforming the momentum integration into an energy integration, we have

$$L_3^{\text{med}}(q_0, 0) = -\frac{1}{2\pi^2} \sum_{\pm} \int_{-\infty}^{\infty} \mathrm{d}E_k \, \Theta(E_k - M) \sqrt{E_k^2 - M^2} n_F(E_k \pm \mu) \frac{1}{(q_0 + 2\mu)^2 \pm 2E_k(q_0 + 2\mu)} . \tag{E.27}$$

Since we are interested in the retarded version of the integral we replace $q_0 \to q_0 + i\epsilon$ as in the mesonic channel. Compared to L_2 the sign of ϵ depends on the integration variable. Hence, we have to be careful by substitutions within the integral. Nevertheless, the following steps are similar to the one performed for L_2. The final result, for the imaginary part of the medium contribution reads

$$\mathrm{Im}L_3^{\text{med}}(q_0, 0) = \sum_{\pm} \frac{1}{8\pi(q_0 + 2\mu)} \Theta(\mp \frac{q_0 + 2\mu}{2} - M) \sqrt{(q_0 + 2\mu)^2 - 4M^2} n_F(\mp \frac{q_0}{2}) . \tag{E.28}$$

Appendix F

Baryons

F.1. Derivation of equation (5.8)

We start with equation (5.2) and (5.3)

$$D_B = D_0 + D_0(k_i + k_j + k_k)D_B \tag{F.1}$$

$$= D_0 + (D_0 k_i + D_0 k_j + D_0 k_k)D_B \tag{F.2}$$

with (ijk) be an permutation of (123). Under virtue of equation (5.4) for the two-quark correlation function d_i it follows

$$D_B = D_0 + \left((1 - D_0 d_i^{-1}) + D_0 k_j + D_0 k_k\right)D_B \tag{F.3}$$

$$= D_0 + \left(1 - D_0 d_i^{-1} + D_0(k_j + k_k)\right)D_B \tag{F.4}$$

$$\Leftrightarrow 0 = D_0 - D_0 d_i^{-1}D_B + D_0(k_j + k_k)D_B \tag{F.5}$$

$$\Leftrightarrow 0 = 1 - d_i^{-1}D_B + (k_j + k_k)D_B \tag{F.6}$$

$$\Leftrightarrow D_B = d_i + d_i(k_j + k_k)D_B \,. \tag{F.7}$$

F.2. States of relative motion

In section 5.2 we have introduced the basis states $|q_m p_m\rangle_l^{\alpha_i \alpha_j \alpha_k}$. Here, particle l carries the Dirac, flavour and colour structure α_i and momentum k_i. Therefore, equation (5.38) is the trivial case in which particle 1 has momentum k_1 and structure α_1, as well as for the other two particles with corresponding indices. Hence, equation (5.38) arises by
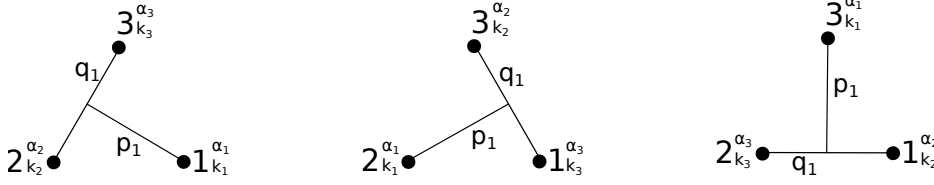
Figure F.1. The three different possibilities to define momentum and the Dirac, flavour and colour structure of a certain particle.

rotating the inner cross in figure F.1 and changing the index of p and q in accordance with their definition given in the beginning of section 5.2.

The other possible relations can be found by changing the momenta and structure indices of a certain particle. For example particle 2 carries momentum k_1 and structure α_1. Again, a rotation of the inner cross yields

$$|q_1 p_1\rangle_2^{\alpha_1 \alpha_2 \alpha_3} = |q_2 p_2\rangle_3^{\alpha_2 \alpha_3 \alpha_1} = |q_3 p_3\rangle_1^{\alpha_3 \alpha_1 \alpha_2} . \tag{F.8}$$

A similar relation can be obtained by defining particle 3 with momentum k_1 and structure α_1

$$|q_1 p_1\rangle_3^{\alpha_1 \alpha_2 \alpha_3} = |q_2 p_2\rangle_1^{\alpha_2 \alpha_3 \alpha_1} = |q_3 p_3\rangle_2^{\alpha_3 \alpha_1 \alpha_2} . \tag{F.9}$$

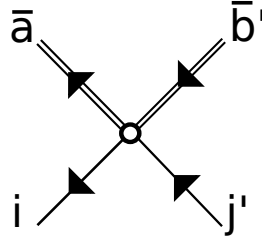## F.3. Colour structure for baryons

Figure F.2. Interaction kernel of the diquark-quark scattering.

We start with the interaction kernel of the baryons in static approximation shown in figure F.2 which yields the corresponding operator in colour space

$$i\hat{\mathcal{C}} = i\frac{1}{M_x} \lambda_{ix}^{\bar{b}'} \lambda_{xj'}^{\bar{a}} \tag{F.10}$$

$$= -i\frac{1}{M_x} \left(\delta_i^{\bar{a}} \delta_{j'}^{\bar{b}'} - \delta^{\bar{a}\bar{b}'} \delta_{ij'} \right) . \tag{F.11}$$

In order to investigate the colour structure, we denote a diquark-quark state by

$$|\bar{b}', j'\rangle ,\tag{F.12}$$

with $b', j' = R, G, B$. Hereby the bared letter is related to the antitriplet diquark. If we consider this as the incoming state of the diquark-quark vertex, the related outgoing state expressed by the indices of the upper figure is given by

$$i\hat{\mathcal{C}}|\bar{b}', j'\rangle = -i\frac{1}{M_x} \left(\delta_i^{\bar{a}} \delta_{j'}^{\bar{b}'} - \delta^{\bar{a}\bar{b}'} \delta_{ij'} \right) |\bar{a}, i\rangle .\tag{F.13}$$

It is well known that for three colours coupled with three anticolours leads to a singlet and octet states. The singlet state reads

$$|\psi_0\rangle = \frac{1}{\sqrt{3}} \left(|\bar{R}, R\rangle + |\bar{G}, G\rangle + |\bar{B}, B\rangle \right) ,\tag{F.14}$$

and the octet states are

$$|\psi_1\rangle = |\bar{R}, B\rangle ,\tag{F.15}$$

$$|\psi_2\rangle = |\bar{R}, G\rangle ,\tag{F.16}$$

$$|\psi_3\rangle = |\bar{B}, G\rangle ,\tag{F.17}$$

$$|\psi_4\rangle = |\bar{B}, R\rangle ,\tag{F.18}$$

$$|\psi_5\rangle = |\bar{G}, R\rangle ,\tag{F.19}$$

$$|\psi_6\rangle = |\bar{G}, B\rangle ,\tag{F.20}$$

$$|\psi_7\rangle = \frac{1}{\sqrt{2}} \left(|\bar{R}, R\rangle - |\bar{G}, G\rangle \right) ,\tag{F.21}$$

$$|\psi_8\rangle = \frac{1}{\sqrt{3}} \left(|\bar{R}, R\rangle + |\bar{G}, G\rangle - 2|\bar{B}, B\rangle \right) .\tag{F.22}$$

Indeed, a simple calculation shows that the singlet and octet states are eigenstates the operator $\hat{\mathcal{C}}$ with different eigenvalues

$$i\hat{\mathcal{C}}|\psi_0\rangle = 2i|\psi_0\rangle\tag{F.23}$$

and

$$i\hat{\mathcal{C}}|\psi_i\rangle = -i|\psi_i\rangle \qquad\qquad i = 1, 2, \ldots, 8 .\tag{F.24}$$

The sign change in the octet here is important. Since we find bound states in the colour singlet state, it follows from the different sign in equation (F.23) and (F.24) that the octet has to be repulsive in colour space.

F.4. Baryon Dirac-like equation

We start with the definition of the baryon polarisation loop

$$iJ^N(P) := i \int \frac{\mathrm{d}^4 p''}{(2\pi)^4} \, S_u(\frac{P}{2} + p'') t_s(\frac{P}{2} - p'') \,. \tag{F.25}$$

By multiplying p'' with $P_\mu P^\mu / P^2 = 1$ and switching into the baryon rest frame ($\vec{P} = 0$), the above equation can be written, in accordance with [33, 34] as

$$iJ^N(P) = -g^2_{Dqq} i \int \frac{\mathrm{d}^4 p''}{(2\pi)^4} \frac{\not{P}(1 - \frac{\not{P} p''}{P^2}) + M_u}{(P - p'')^2 - M_u^2} \frac{1}{p''^2 - m^2_{sad}} \,. \tag{F.26}$$

The antisymmetric term proportional to $P_0 \vec{p}'' \gamma_0 \vec{\gamma}$ vanishes due to the integration. Therefore, the polarisation loop splits into a term proportional to $\not{P}$ and one scalar term. With

$$I^n(P) := \int \frac{\mathrm{d}^4 p''}{(2\pi)^4} \left(\frac{P p''}{P^2} \right)^n \frac{1}{(P - p'')^2 - M_u^2} \frac{1}{p''^2 - m^2_{sad}} \tag{F.27}$$

the polarisation loop finally reads

$$iJ^N(P) = -ig^2_{Dqq} \left(\not{P}(I^0(P) - I^1(P)) + M_u I^0(P) \right) \,. \tag{F.28}$$

F.5. Baryon polarisation loop

The baryon polarisaion loop in the baryon rest frame reads

$$J(P_0, \vec{P} = 0) = J_s(P_0, \vec{P} = 0)\mathbb{1} + J_v(P_0, \vec{P} = 0)\gamma_0 \tag{F.29}$$

$$= -ig^2_{Dqq} \int \frac{\mathrm{d}^4 p}{(2\pi)^4} \frac{(P_0 - p_0)\gamma_0 + M\mathbb{1}}{(P - p)^2 - M^2 + i\epsilon'} \frac{1}{p^2 - m^2_{sad} + i\epsilon'} \,. \tag{F.30}$$

This can be rewritten to

$$J(P_0, \vec{P} = 0) = -g^2_{Dqq} \int \frac{\mathrm{d}^4 p}{(2\pi)^4} \frac{(P_0 - p_0)\gamma_0 + M\mathbb{1}}{(P - p)^2 - M^2} \frac{1}{p^2 - m^2_{sad}} \tag{F.31}$$

$$= -ig^2_{Dqq} \int \frac{\mathrm{d}^4 p}{(2\pi)^4} ((P_0 - p_0)\gamma_0 + M\mathbb{1}) \times \tag{F.32}$$

$$\times \frac{1}{(P_0 - p_0) - E_p^Q} \frac{1}{(P_0 - p_0) + E_p^Q} \frac{1}{p_0 - E_p^D} \frac{1}{p_0 + E_p^D} \,,$$

where we have introduced the energy of the diquark $(E_p^D)^2 = p^2 + m_{sad}^2$ and quark $(E_p^Q)^2 = P_0^2 + M^2$, respectively. After a partial fraction decomposition of the denominator we find

$$J(P_0, \vec{P} = 0) = -ig_{Dqq}^2 \int \frac{\mathrm{d}^4 p}{(2\pi)^4} \left((P_0 - p_0)\gamma_0 + M\mathbb{1} \right) \times \tag{F.33}$$

$$\times \frac{1}{4E_p^Q E_p^D} \left(\frac{1}{(P_0 - p_0) - E_p^Q + i\epsilon} - \frac{1}{(P_0 - p_0) + E_p^Q - i\epsilon} \right) \times$$

$$\times \left(\frac{1}{p_0 - E_p^D + i\epsilon} - \frac{1}{p_0 + E_p^D - i\epsilon} \right) .$$

Now, we will evaluate the scalar and vector contribution separately to obtain the related imaginary parts. The real parts of the integral, necessary for the inverse nucleon propagator, are given by a principal value integration already introduced in the chapters before.

Evaluation of $J_s(P)$

The scalar part, in accordance with equation (F.32), is given by

$$J_s(P_0, \vec{P} = 0) = -ig_{Dqq}^2 M \int \frac{\mathrm{d}^4 p}{(2\pi)^4}$$

$$\times \frac{1}{4E_p^D E_p^Q} \left(\frac{1}{(P_0 - p_0) - E_p^Q + i\epsilon} - \frac{1}{(P_0 - p_0) + E_p^Q - i\epsilon} \right)$$

$$\times \left(\frac{1}{p_0 - E_p^D + i\epsilon} - \frac{1}{p_0 + E_p^D - i\epsilon'} \right) , \tag{F.34}$$

and is equal to the definition of I_2' in appendix D.13 up to the pre-factors of the integral. Hence, we not repeat the discussion and refer to appendix D.1.1 instead. The final result for the imaginary is given by

$$\mathrm{Im}J_s(P_0) = g_{Dqq}^2 M \frac{1}{16\pi} \sqrt{\frac{\left((M + m_{sad})^2 - P_0^2\right)\left((M - m_{sad})^2 - P_0^2\right)}{P_0^4}} \Theta(P_0^2 - (M + m_{sad})^2) .$$
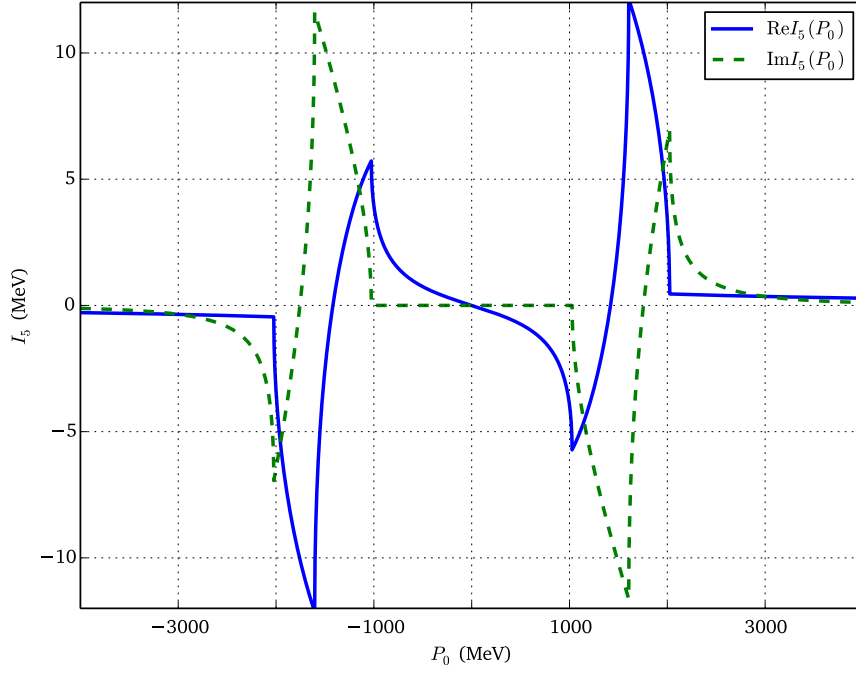$$\tag{F.35}$$

Figure F.3. Real and imaginary part of the integral I_5.

Evaluation of $J_v(P)$

For the vector contribution a similar discussion as for the integral I_2' leads to

$$J_v(P_0) = -g_{Dqq}^2 \int \frac{\mathrm{d}^3 p}{(2\pi)^3} \frac{1}{4E_p^D E_p^Q} \left(\frac{P_0 + E_p^D}{P_0 + E_p^D + E_p^Q - i\epsilon} - \frac{P_0 + E_p^D}{P_0 - E_p^D - E_p^Q + i\epsilon} - 1 \right) \tag{F.36}$$

$$= g_{Dqq}^2 \int \frac{\mathrm{d}^3 p}{(2\pi)^3} \frac{1}{2E_p^D} \left(\frac{P_0}{P_0^2 - (E_p^D + E_p^Q)^2 + i\epsilon} \right) \tag{F.37}$$

$$= g_{Dqq}^2 \frac{1}{4\pi^2} \int \mathrm{d}p \frac{p^2}{2E_p^D} \left(\frac{P_0}{P_0^2 - (E_p^D + E_p^Q)^2 + i\epsilon} \right) , \tag{F.38}$$

after performing the p_0 integration with the residue theorem. To obtain the imaginary part of the upper expression, we can use the identity given in (D.17) again. This yields

$$\mathrm{Im} J_v(P_0) = g_{Dqq}^2 \frac{1}{32\pi} \frac{(m_{sad}^2 - M^2 - P_0^2)}{P_0^3} \times \tag{F.39}$$

$$\times \sqrt{[(m_{sad} + M)^2 - P_0^2][(m_{sad} - M)^2 - P_0^2]} \Theta(P_0^2 - (m_{sad} + M)^2) .$$

In figure F.3 the real and imaginary part of $J_v(P_0)/g_{Dqq}^2 =: I_5(P_0)$ is shown.

F.5.1. Medium version of the baryon polarisation loop

The baryon polarisation loop within the Matsubara formalism is given by

$$-\frac{\Pi^B(i\nu + \mu + \mu_D, \vec{P} = 0)}{g_{Dqq}^2}$$

$$= T \sum_{\{i\omega\}} \int \frac{d^3p}{(2\pi)^2} \left((i\nu - i\omega + \mu)\gamma_0 + M\mathbb{1}\right) \frac{1}{(i\nu - i\omega + \mu)^2 - (E_p^Q)^2} \frac{1}{(i\omega + \mu_D)^2 - (E_p^D)^2}.$$

(F.40)

As in the previous chapters $i\nu$ and $i\omega$ are related to a fermionic and bosonic Matsubara frequency, respectively. The emerging chemical potential $\mu_D = 2\mu$ denotes the diquark chemical potential. Again, we can identify the two integral J_s and J_v, but now in their medium version. Both contribution will be discussed separately.

Medium version of $J_s(P_0)$

The scalar contribution of the polarisation loop reads

$$-\frac{J_s(P_0, \mu, \mu_D, T)}{g_{Dqq}^2} = MT \sum_{\{i\omega\}} \int \frac{d^3p}{(2\pi)^3} \frac{1}{(i\nu - i\omega + \mu)^2 - (E_p^Q)^2} \frac{1}{(i\omega + \mu_D)^2 - (E_p^D)^2}.$$

(F.41)

Performing the residue theorem backwards with the Bose-Einstein distribution introduced in section C.1 to evalute the sum over the Matsubara frequencies leads to

$$L_4(P_0, \mu, \mu_D, T) := -\frac{J_s(P_0)}{g_{Dqq}^2}$$

(F.42)

$$= M \int \frac{d^3p}{(2\pi)^3} \oint_C \frac{dz}{2i\pi} n_B(z) \frac{1}{(i\nu - z + \mu)^2 - (E_p^Q)^2} \frac{1}{(i\omega + \mu_D)^2 - (E_p^D)^2}.$$

(F.43)

Again, the contour C can be deformed to run clockwise around the four poles

$$z_{1\pm} = \pm E_p^D - \mu_D$$

(F.44)

$$z_{2\pm} = i\nu \pm E_p^Q + \mu,$$

(F.45)

which leads, after performing the Residue theorem and taking into account some of the relations in section C.1, to

$$
\begin{aligned}
L_4(P_0, \mu, \mu_D, T) = -M \int \frac{d^3 p}{(2\pi)^3} \frac{1}{4E_p^D E_p^Q} \Bigg(& \frac{1}{i\nu + \mu + \mu_D - s_p} - \frac{1}{i\nu + \mu + \mu_D + s_p} \\
& - n_B(E_p^D + \mu_D) \left(\frac{1}{i\nu + \mu + \mu_D + d_p} - \frac{1}{i\nu + \mu + \mu_D + s_p} \right) \\
& + n_B(E_p^D - \mu_D) \left(\frac{1}{i\nu + \mu + \mu_D - s_p} - \frac{1}{i\nu + \mu + \mu_D - d_p} \right) \\
& + n_F(E_p^Q - \mu) \left(\frac{1}{i\nu + \mu + \mu_D + d_p} - \frac{1}{i\nu + \mu + \mu_D - s_p} \right) \\
& + n_F(E_p^Q + \mu) \left(\frac{1}{i\nu + \mu + \mu_D + s_p} - \frac{1}{i\nu + \mu + \mu_D - d_p} \right) \Bigg).
\end{aligned}
$$

(F.46)

We can immediately identify the vacuum contribution

$$
L_4^{\text{vac}}(P_0, \mu, \mu_D, T) := -M \int \frac{d^3 p}{(2\pi)^3} \left(\frac{1}{4E_p^D E_p^Q} \left(\frac{1}{i\nu + \mu + \mu_D - s_p} - \frac{1}{i\nu + \mu + \mu_D + s_p} \right) \right)
$$

(F.47)

and medium part

$$
\begin{aligned}
L_4^{\text{med}}(P_0, \mu, \mu_D, T) := -M \int \frac{d^3 p}{(2\pi)^3} \frac{1}{4E_p^D E_p^Q} \Bigg(& \frac{1}{i\nu + \mu + \mu_D - s_p} - \frac{1}{i\nu + \mu + \mu_D + s_p} \\
& - n_B(E_p^D + \mu_D) \left(\frac{1}{i\nu + \mu + \mu_D + d_p} - \frac{1}{i\nu + \mu + \mu_D + s_p} \right) \\
& + n_B(E_p^D - \mu_D) \left(\frac{1}{i\nu + \mu + \mu_D - s_p} - \frac{1}{i\nu + \mu + \mu_D - d_p} \right) \\
& + n_F(E_p^Q - \mu) \left(\frac{1}{i\nu + \mu + \mu_D + d_p} - \frac{1}{i\nu + \mu + \mu_D - s_p} \right) \\
& + n_F(E_p^Q + \mu) \left(\frac{1}{i\nu + \mu + \mu_D + s_p} - \frac{1}{i\nu + \mu + \mu_D - d_p} \right) \Bigg).
\end{aligned}
$$

(F.48)

At $\mu = \mu_D = 0$ the vacuum contribution is equal to (F.34).

Moreover, we note that for $\mu_D = 2\mu$ the baryon polarisation loop depends on 3μ. Compared to the diquarks we expect this result in some way since a baryon is a bound state of three quarks. Hence, it should feel three times the chemical potential of a quark.

The vacuum part can be calculated with the analytical continuation $i\nu \mapsto P_0$, and the

123

standard techniques provided in the previous section of the appendix. The medium part, meanwhile, can be analysed with the same continuation. After a straightforward calculation we can separate a fermionic and a bonsonic contribution. For the fermionic part we find

$$L_4^{\text{med,F}}(P_0, \mu, \mu_D, T) := M \sum_{\pm} \int \frac{\mathrm{d}^3 p}{(2\pi)^3} \frac{1}{2E_p^Q} n_F(E_p^Q \pm \mu) \frac{1}{(P_0 + \mu + \mu_D \pm E_p^Q)^2 - (E_p^Q)^2},$$
(F.49)

while the bosonic contribution reads

$$L_4^{\text{med,B}}(P_0, \mu, \mu_D, T) := \sum_{\pm} \pm M \int \frac{\mathrm{d}^3 p}{(2\pi)^3} \frac{1}{2E_p^D} n_B(E_p^D \pm \mu_D) \frac{1}{(P_0 + \mu + \mu_D \pm E_p^Q)^2 - (E_p^Q)^2}.$$
(F.50)

Since both integrals only depend on $\vec{p}^2$ we can use spherical coordinates and using analogous techniques as in the previous discussions of similar integrals. Therefore, we make another replacement $P_0 \mapsto P_0 + i\epsilon$ in order to obtain the retarded version of the upper integrals. Then, it follows that the imaginary parts are given by

$$\mathrm{Im}L_4^{\text{med,F}}(\tilde{P}, \mu, T) = \sum_{\pm} \text{sign}(\tilde{P} \pm \tilde{E}) \frac{M}{8\pi|\tilde{P}|} \sqrt{(\tilde{E})^2 - M^2} \times$$
$$\times n_F(\pm\tilde{E} \pm \mu)\Theta(\pm\tilde{E} - M),$$
(F.51)

$$\mathrm{Im}L_4^{\text{med,B}}(\tilde{P}, \mu_D, T) = \sum_{\pm} \pm\text{sign}(P_0 \pm \tilde{E}) \frac{M}{8\pi|\tilde{P}|} \sqrt{(\tilde{E})^2 - m_{sad}^2} \times$$
$$\times n_B(\mp\tilde{E} \pm \mu_D)\Theta(\mp\tilde{E} - m_{sad}),$$
(F.52)

with

$$\tilde{E} := \frac{m_{sad}^2 - M^2 - \tilde{P}^2}{2\tilde{P}}$$
(F.53)

and

$$\tilde{P} := P_0 + \mu + \mu_D$$
(F.54)

Medium version of $J_v(P_0)$

The vector contribution $J_v(P_0)$ is given by

$$-\frac{J_v(P_0, \mu, \mu_D, T)}{g_{Dqq}^2} = T \sum_{\{i\omega\}} \int \frac{\mathrm{d}^3 p}{(2\pi)^3} \frac{i\nu - i\omega + \mu}{(i\nu - i\omega + \mu)^2 - (E_p^Q)^2} \frac{1}{(i\omega + \mu_D)^2 - (E_p^D)^2}.$$
(F.55)

The steps to evaluate this expression, is analogous to the one on the previous discussion. Hence, we only will give important results within the calculations. Therefore, it is convenient to define the integral $L_5(P_0, \mu, \mu_D, T)$ as follow

$$
\begin{aligned}
L_5(P_0, \mu, \mu_D, T) := & -\int \frac{\mathrm{d}^3 p}{(2\pi)^3} \frac{1}{4E_p^D E_p^Q} \left(-\left(\frac{E_p^D + +\mu + \mu_D P_0}{P_0 + \mu + \mu_D + s_p} - \frac{E_p^Q}{P_0 + \mu + \mu_D - s_p} - 1 \right) \right. \\
& + n_B(E_p^D + \mu_D)(P_0 + \mu + \mu_D + E_p^D) \left(\frac{1}{P_0 + \mu + \mu_D + d_p} - \frac{1}{P_0 + \mu + \mu_D + s_p} \right) \\
& + n_B(E_p^D - \mu_D)(P_0 + \mu + \mu_D - E_p^D) \left(\frac{1}{P_0 + \mu + \mu_D - s_p} - \frac{1}{P_0 + \mu + \mu_D - d_p} \right) \\
& + n_F(E_p^Q - \mu)E_p^Q \left(\frac{1}{P_0 + \mu + \mu_D + d_p} - \frac{1}{P_0 + \mu + \mu_D - s_p} \right) \\
& \left. + n_F(E_p^Q + \mu)E_p^Q \left(\frac{1}{P_0 + \mu + \mu_D + s_p} - \frac{1}{P_0 + \mu + \mu_D - d_p} \right) \right),
\end{aligned}
$$

(F.56)

with $s_p := E_p^D + E_p^Q$ and $d_p := E_p^D - E_p^Q$. We already performed the continuation $iv \mapsto P_0$. Note that the first term represents the vacuum contribution for $\mu = \mu_D = 0$, and is equal to equation (F.36). It can be evaluated as shown in the corresponding section, but in consideration of the chemical potentials. Again, we obtain a medium part

$$
\begin{aligned}
& L_5^{\mathrm{med}}(P_0, \mu, \mu_D, T) := \\
& -\frac{\mathrm{d}^3 p}{(2\pi)^3} \frac{1}{4E_p^D E_p^Q} \left(+ n_B(E_p^D + \mu_D)(P_0 + \mu + \mu_D + E_p^D) \left(\frac{1}{(P_0 + \mu + \mu_D + E_p^D)^2 - (E_p^Q)^2} \right) \right. \\
& + n_B(E_p^D - \mu_D)(P_0 + \mu + \mu_D - E_p^D) \left(\frac{1}{(P_0 + \mu + \mu_D - E_p^D)^2 - (E_p^Q)^2} \right) \\
& - n_F(E_p^Q - \mu)2E_p^D E_p^Q \left(\frac{1}{(P_0 + \mu + \mu_D - E_p^Q)^2 - (E_p^D)^2} \right) \\
& \left. + n_F(E_p^Q + \mu)2E_p^D E_p^Q \left(\frac{1}{(P_0 + \mu + \mu_D + E_p^Q)^2 - (E_p^D)^2} \right) \right)
\end{aligned}
$$

(F.57)

which can be separated into a fermionic and bosonic contribution as well. Both contributions only depend on $\vec{p}^2$ and are given by

$$
L_5^{\mathrm{med,F}}(P_0, \mu, \mu_D, T) := \sum_{\pm} \pm \frac{1}{2} \int \frac{\mathrm{d}^3 p}{(2\pi)^3} n_F(E_p^Q \mp \mu) \frac{1}{(P_0 + \mu + \mu_D \mp E_p^Q)^2 - (E_p^D)^2},
$$

(F.58)

$$L_5^{\mathrm{med,B}}(P_0,\mu,\mu_D,T) :=$$

$$-\sum_{\pm}\int\frac{\mathrm{d}^3p}{(2\pi)^3}\frac{1}{2E_p^D}n_B(E_p^D\mp\mu_D)(P_0+\mu+\mu_D\pm E_p^D)\frac{1}{(P_0+\mu+\mu_D\pm E_p^D)^2-(E_p^Q)^2}\,.$$

$$(\mathrm{F.59})$$

The corresponding imaginary parts, after expressing $P_0\mapsto P_0+i\epsilon$ to obtain the retarded version of the integrals and using (D.17), read

$$\mathrm{Im}L_5^{\mathrm{med,F}}(P_0,\mu,\mu_D,T):=\sum_{\pm}\frac{1}{16\pi|\tilde{P}|}\mathrm{sign}(\tilde{P}\pm\tilde{E})\tilde{E}n_F(\pm\tilde{E}\mp\mu)\times$$

$$\times\sqrt{\tilde{E}^2-M^2}\Theta(\pm\tilde{E}-M)\qquad(\mathrm{F.60})$$

and

$$\mathrm{Im}L_5^{\mathrm{med,B}}(P_0,\mu,\mu_D,T):=\sum_{\pm}\mp\frac{1}{16\pi|\tilde{P}|}\mathrm{sign}(\tilde{P}\mp\tilde{E})(\tilde{P}\mp\tilde{E})n_B(\mp\tilde{E}\pm\mu_D)\times$$

$$\times\sqrt{\tilde{E}^2-M^2}\Theta(\mp\tilde{E}-M)\,.\qquad(\mathrm{F.61})$$

with the definitions (F.53), (F.54) for $\tilde{E}$ and $\tilde{P}$, respectively.

Again the real part of expression (F.51), (F.52), (F.60) and (F.61) can be obtained with a principal value integration under virtue of relation (D.19).

.

References

[1] M. Gell-Mann. A Schematic Model of Baryons and Mesons. *Phys. Lett.*, 8:214–215, 1964.

[2] H. Fritzsch, M. Gell-Mann, and H. Leutwyler. Advantages of the Color Octet Gluon Picture. *Phys. Lett.*, B47:365–368, 1973.

[3] K. G. Wilson. Confinement of quarks. *Phys. Rev. D*, 10:2445–2459, 1974.

[4] D. J. Gross and F. Wilczek. Ultraviolet behavior of non-abelian gauge theories. *Phys. Rev. Lett.*, 30:1343–1346, 1973.

[5] H. D. Politzer. Reliable Perturbative Results for Strong Interactions? *Phys. Rev. Lett.*, 30:1346–1349, 1973.

[6] J. Greensite. The Confinement problem in lattice gauge theory. *Prog. Part. Nucl. Phys.*, 51:1, 2003.

[7] A. Andronic. An overview of the experimental study of quark-gluon matter in high-energy nucleus-nucleus collisions. *Int. J. Mod. Phys.*, A29:1430047, 2014.

[8] F. Karsch. Lattice QCD at high temperature and density. *Lect. Notes Phys.*, 583:209–249, 2002.

[9] Y. Nambu and G. Jona-Lasinio. Dynamical model of elementary particles based on an analogy with superconductivity. i. *Phys. Rev.*, 122:345–358, 1961.

[10] Y. Nambu and G. Jona-Lasinio. Dynamical model of elementary particles based on an analogy with superconductivity. ii. *Phys. Rev.*, 124:246–254, 1961.

[11] H. Kleinert. On the Hadronization of Quark Theories. In *14th International School of Subnuclear Physics: Understanding the Fundamental Constitutents of Matter Erice, Italy, July 23-August 8, 1976*, page 289, 1976.

[12] M. K. Volkov. Meson Lagrangians in a Superconductor Quark Model. *Annals Phys.*, 157:282–303, 1984.

[13] T. Hatsuda and T. Kunihiro. Possible critical phenomena associated with the chiral symmetry breaking. *Phys. Lett.*, B145:7–10, 1984.

[14] M. Buballa. NJL-model analysis of dense quark matter. *Phys. Rept.*, (407):205–376, 2005.

[15] P. Braun-Munzinger and J. Wambach. The Phase Diagram of Strongly-Interacting Matter. *Rev. Mod. Phys.*, 81:1031–1050, 2009.

[16] S.P. Klevansky. The Nambu–Jona-Lasinio model of quantum chromodynamics. *Rev. Mod. Phys.*, (64(3)):649–708, 1992.

[17] S. Möller. *Pion-Pion Scattering and Shear Viscosity in the Nambu–Jona-Lasinio Model*. Master-Thesis, Technische Universität Darmstadt, 2012.

[18] M. Fromm, J. Langelage, S. Lottini, M. Neuman, and O. Philipsen. Onset Transition to Cold Nuclear Matter from Lattice QCD with Heavy Quarks. *Phys. Rev. Lett.*, 110(12):122001, 2013.

[19] J. Beringer et al. Review of Particle Physics. *Phys. Rev. D*, 86:010001, 2012.

[20] C. Burgess and G. Moore. *The Standard Model: A Primer*. Cambridge books online. Cambridge University Press, 2007.

[21] M. E. Peskin and D. V. Schroeder. *An Introduction To Quantum Field Theory*. Westview Press, New York, 1995.

[22] M. L. Goldberger and S. B. Treiman. Decay of the pi meson. *Phys. Rev.*, 110:1178–1184, 1958.

[23] K. Heckmann. *Transport coefficients of strongly interacting matter*. PhD thesis, Technische Universität, Darmstadt, 2011.

[24] G. Ripka. *Quarks bound by chiral fields: The quark-structure of the vacuum and of light mesons and baryons*. 1997.

[25] J. M. Torres-Rincon, B. Sintes, and J. Aichelin. Flavor dependence of baryon melting temperature in effective models of QCD. *Phys. Rev.*, C91(6):065206, 2015.

[26] D. Ebert, K. G. Klimenko, and V. L. Yudichev. Pion, sigma-meson and diquarks in the 2SC phase of dense cold quark matter. *Phys. Rev.*, C72:015201, 2005.

[27] D. Nowakowski. *Inhomogeneous phases and color superconductivity in the NJL model*. Master-Thesis, Technische Universität Darmstadt, 2012.

[28] E. Blanquier. *The Polyakov, Nambu and Jona-Lasinio model and its applications to describe the sub-nuclear particles*. PhD thesis, 2015.

[29] R. Alkofer and L. von Smekal. The Infrared behavior of QCD Green's functions: Confinement dynamical symmetry breaking, and hadrons as relativistic bound states. *Phys. Rept.*, 353:281, 2001.

[30] N. Ishii, W. Bentz, and K. Yazaki. Baryons in the NJL model as solutions of the relativistic Faddeev equation. *Nucl. Phys.*, A587:617–656, 1995.

[31] H. Reinhardt. Hadronization of Quark Flavor Dynamics. *Phys. Lett.*, B244:316–326, 1990.

[32] S. Huang and J. Tjon. Nucleon solution of the Faddeev equation in the Nambu-Jona-Lasinio model. *Phys. Rev.*, C49:1702–1708, 1994.

[33] R. Alkofer and H. Reinhardt. *Chiral quark dynamics*. Lecture Notes in Physics Monographs. Springer, Berlin, 1995.

[34] R. Alkofer A. Buck and H. Reinhardt. Baryons as bound states of diquarks and quarks in the Nambu–Jona-Lasinio model. *Phys. Lett.*, B268:29–35, 1992.

[35] D. Blaschke, A. Dubinin, and D. Zablocki. NJL model approach to diquarks and baryons in quark matter. In *Proceedings, 22nd International Baldin Seminar on High Energy Physics Problems, Relativistic Nuclear Physics and Quantum Chromodynamics, (ISHEPP 2014): Dubna, Russia, September 15-20, 2014*, 2015.

[36] R. de L. Kronig. On the Theory of Dispersion of X-Rays. *J. Opt. Soc. Am.*, 12(6):547–557, 1926.

[37] H. A. Kramers. La diffusion de la lumière par les atomes. *Atti Cong. Intern. Fisici, (Transactions of Volta Centenary Congress) Como*, 2:545–557, 1927.

[38] D. Griffiths. *Introduction to Elementary Particles*. Wiley, New York, second edition, 2008.

[39] U. Vogl and W. Weise. The Nambu and Jona-Lasinio Model: Its Implications of Hadrons and Nuclei. *Progress in Particle and Nuclear Physics*, (27):195–272, 1991.

[40] O. Bohr. *Nichtperturbative Behandlung des linearen $SU(3)_L \otimes SU(3)_R$-σ-Modells*. Diplomarbeit, Technische Universität Darmstadt, 1997.

[41] W. Pauli and F. Villars. On the invariant regularization in relativistic quantum theory. *Reviews of Modern Physics*, 21(3):434, 1949.

[42] V. Koch. Aspects of chiral symmetry. *International Journal of Modern Physics E*, 6(02):203–249, 1997.

[43] M. Oertel. *Investigation of meson loop effects in the Nambu-Jona-Lasinio model*. PhD-Thesis, Technische Universität Darmstadt, 2000. (arXiv:hep-ph/0012224).

[44] U. Vogl, M. F.M. Lutz, S. Klimt, and W. Weise. Generalized SU(3) Nambu-Jona-Lasinio Model. Part 2. From Current to Constituent Quarks. *Nucl.Phys.*, A516:469–495, 1990.

[45] M. Shifman. Understanding Confinement in QCD: Elements of a Big Picture. *Int. J. Mod. Phys.*, A25:4015–4031, 2010.

[46] G. Hellstern and C. Weiss. Baryon form-factors in a diquark - quark bound state description. *Phys. Lett.*, B351:64–69, 1995.

[47] F. Wilczek. Diquarks as inspiration and as objects. In *Deserfest: A celebration of the life and works of Stanley Deser. Proceedings, Meeting, Ann Arbor, USA, April 3-5, 2004*, pages 322–338, 2004.

[48] E. Meggiolaro and C. Wetterich. Evolution equations for the effective four quark interactions in QCD. *Nucl. Phys.*, B606:337–356, 2001.

[49] R. Alkofer, S. Ahlig, C. S. Fischer, M. Oettel, and H. Reinhardt. Octet and decuplet baryons in a confining and covariant diquark - quark model. *Nucl. Phys.*, A663:683–686, 2000.

[50] M. Oettel. *Baryons as relativistic bound states of quark and diquark*. PhD thesis, Tubingen U., 2000.